

OVERVIEW OF THE REACTIVITY OF ORGANICS IN SUPERHEATED WATER: GEOCHEMICAL AND TECHNOLOGY IMPLICATIONS

Michael Siskin,* and Alan R. Katritzky†

*Exxon Research and Engineering Company, Corporate Research Laboratories,
Clinton Township, Route 22 East, Annandale, NJ 08801

†Center for Heterocyclic Compounds, Department of Chemistry, University of Florida, P.O. Box
117200, Gainesville, FL 32611

Keywords: aquathermolysis, kerogen, cleavage chemistry.

ABSTRACT

The reactivity of organic molecules in hot water is a field of chemistry developing from studies aimed at understanding how organic matter (kerogen) forms in natural environments and then breaks down into energy source materials. In natural systems where kerogens are depolymerized, water is ubiquitous and hot and usually contains salt and minerals. Reactions such as cleavages and hydrolyses in these media are facilitated by changes in the chemical and physical properties of water as temperature increases. These changes make water more compatible with the reactions of organics. We will present a brief geochemical background, discuss chemical and physical properties of water, key features of known kerogen structural models and the aqueous chemistry of cleavage and hydrolysis reactions involved in kerogen depolymerization. Based on the understanding of the roles of water as a solvent, reagent and catalyst, potential applications in areas such as plastics recycling and synthesis of chemicals will be described.

INTRODUCTION

This article describes an emerging area of chemistry: the reactivity of organic compounds in superheated water. We begin with a brief geochemical background and then discuss the implications of the aqueous chemistry to understanding the formation of oil from the solid, insoluble, organic material (kerogen) in resources such as shale and coal. Finally, we point out potential implications to more technological areas such as plastics recycling.

Common organic molecules that were previously considered unreactive in liquid water undergo many chemical reactions when the temperature is increased to 250-350 °C; these reactions were previously expected only in the presence of strong acid or base. For example, ethers and esters, which are unreactive to heat alone, undergo facile cleavage and hydrolysis, respectively, in water at 250-350 °C.¹ Ethers and esters are major cross-links in several oil shale kerogens and are illustrated in a portion of the detailed structural model of a Rundle Ramsay Crossing Type I kerogen in Figure 1. Analogously, polyethylene terephthalate polymers (found in plastic soft drink bottles) can be hydrolyzed quantitatively back to their starting materials in superheated water in less than an hour.² Other polyesters, and also polyamides (like nylon), are equally susceptible to hydrolysis. A major analogy to such polymer degradation reactions in nature is catagenesis: the process by which solid petroleum source rock kerogens, which are cross-linked macromolecular structures, are converted into liquid petroleum. Natural catagenesis takes place at temperatures below 200 °C over millions of years in aqueous environments at pressures of about 600 atmospheres. Because of the relatively low temperatures, it has been hypothesized that some of the chemistry by which petroleum is formed is catalyzed by clay minerals in the formations.³ Recent studies in our laboratories have made it clear that two additional factors can affect and catalyze the kerogen depolymerization chemistry that leads to petroleum formation. One factor is that simple aqueous chemistry generates water-soluble products that are acidic or basic, or have redox properties. The other factor involves the salts present in sea water or aqueous environments.^{4,5}

High temperature water under autogenic pressure provides a significantly more favorable reaction medium for ionic reactions of non-polar organic compounds than does water up to its boiling temperature (Table 1). At 300 °C, water exhibits a density and polarity similar to those of acetone at room temperature.⁶ The dielectric constant of water drops rapidly with temperature, and at 300 °C has fallen from 80 (at 20 °C) to 2⁷ and its solubility parameter decreases from 23.4 to 14.5 cal/cm.⁸ This means that, as the water temperature is increased, the solubility of organic compounds increases much more than expected for the natural effect of temperature. Furthermore, the negative logarithmic ionic product of water at 250 °C is 11, and of deuterium oxide is 12, as compared to 14 and 15, respectively, at 20 °C.⁹ This means that water becomes both a stronger acid and a stronger base as the temperature increases. Therefore, in addition to the natural increase in kinetic rates with temperature, both acid and base catalysis by water are enhanced at higher temperatures.

Table 1. Chemical/Physical Properties of Superheated Water Become More Compatible to Reaction with Organics at High Temperature

T (°C)	Density (g/cm ³)	Dielectric Constant	Solubility Parameter (cal/cm ³) ^{1/2}	-logKw	Vapor Pressure (psi)
25	0.997	78.85	23.4	13.99	23.8
150	0.917	43.89	20.6	11.64	69.0
200	0.863	34.59	19.0	11.30	225.5
250	0.799	26.75	17.0	11.20	576.6
300	0.713	19.66	14.5	11.30	1245.9
350	0.572	12.61	10.3	-----	2397.8

Geochemical Background

Jurg and Eisma¹⁰ reacted samples of behenic acid (*n*-C₂₁H₄₃COOH) with the acidic clay mineral, montmorillonite, in sealed tubes in the presence and absence of water at 200 °C for 89 and 760 h. They found significant hydrocarbon formation only in the presence of the clay catalyst. The ratios of iso- to normal-butane (1:40) and iso- to normal-pentane (1:40) were raised significantly in the presence of water (1:1) in both cases, indicating that the water induces carbocation chemistry. The proportion of saturated hydrocarbons increased with time at the expense of unsaturated hydrocarbons, suggesting alkylation and/or hydrogenation reactions. Among the higher molecular weight hydrocarbons (C₁₄-C₃₄), there was a strong predominance (55-60%) of C₂₁H₄₄, the direct decarboxylation product of behenic acid.

Johns¹¹ studied kinetically the decarboxylation of behenic acid using a series of clays under anhydrous conditions. Arrhenius plots of the data show large decreases in activation energy (from 58.4 to 24.7 kcal/mol) for decarboxylation in the clay-catalyzed reactions compared to the reaction without clay catalysis. The effects of these catalysts were shown dramatically, by calculating the time required for 90% decarboxylation at 60 °C, which ranged from 2.9 x 10²⁰ years for the thermal conversion to only 0.03 year (11 days) when nontronite, an iron-containing clay, was present. Johns points out that the catalytic activity measured in these laboratory studies surpasses that of the natural shale kerogen systems, a finding partially explained by the sharp decrease in clay acidity with increasing water content.

Frenkel and Heller-Kalai¹² demonstrated that the main reaction of the low molecular weight terpene, limonene (VII), in the presence of montmorillonites, is conversion to the aromatic hydrocarbon *p*-cymene (VIII) and to *p*-menthane (IX) and *p*-menthene (X), demonstrating that kerogens could be converted by surface-active materials in sediments to low molecular weight aromatic compounds of the type found in petroleum. A subsequent study by Goldstein¹³ showed that geraniol (VI), a biologically synthesized unsaturated alcohol, undergoes stepwise catalytic conversion in the presence of water, clays, and other sediments at <100 °C initially to form polymeric materials. These polymeric materials were converted into the more thermodynamically stable phenyl, naphthyl, and higher condensed aromatic products. This model system study nicely demonstrates that clay, limestone, and other sediments catalyze a wide variety of reactions in closed, water-containing systems of varying pH (3.9-9.7).

In addition, several other studies have considered the reaction of resource materials (kerogens) in hot water as an alternative to anhydrous pyrolysis at higher temperature. Simulation of petroleum formation required hydrous conditions because water is ubiquitous in sediments. Winters et al.¹⁴ demonstrated that the characteristic low olefin (high saturates) content of natural petroleum oils could be produced by hydrous pyrolysis of Woodford (Devonian), Phosphoria (Permian), and Kimmeridge (Jurassic) source rock shales at 330 °C. Thus, hydrous pyrolysis in a closed system appeared to be a more realistic reaction system than anhydrous pyrolysis in an open system which, by contrast, generates large amounts of olefins. This work is complemented by that of Tannenbaum and Kaplan¹⁵ who carried out a comparative study in which low molecular weight hydrocarbons were generated from Green River oil shale kerogen by both hydrous and anhydrous pyrolysis. At 300 °C, production of initial C₂-C₆ olefins was comparable in both systems, but under aqueous conditions, their concentrations then started to decrease with time (also observed by Jurg and Eisma¹⁰). This high reactivity of the olefins may explain why olefins were not previously observed under hydrous conditions.

The hydrous pyrolysis¹⁶ of a benzene-methanol extracted Messel shale at 330 °C for 3 days in the presence of D₂O gave saturated hydrocarbon products multiply (1-14) substituted by deuterium. Heating the saturated hydrocarbon docosane (C₂₂H₄₆) with a sample of solvent-extracted shale in an excess of D₂O showed only minor deuteration of the re-isolated docosane (80%). This result suggested that simple hydrogen exchange on saturated molecules can be ruled out as a major pathway. However, under similar conditions in the aqueous system, the olefin 1-octadecene was completely reduced to octadecane (60%) with simultaneous significant deuterium incorporation. Hoering applied similar treatment to a kerogen- 2-ethylheptadecanoic

acid mixture and found that the acid decarboxylated to 2-methylheptadecane in 10% yield, while facile deuterium exchange took place at hydrogen atoms adjacent to (α -to) oxygenated functional groups. In other studies, Hoering and Abelson¹⁷ showed that deuterated hydrocarbons are generated from kerogen heated in D₂O at 100 °C and then dried and pyrolyzed in an inert atmosphere. They proposed that olefins, or olefin intermediates generated during pyrolysis, exchanged with the D₂O. Alexander et al.¹⁸ found considerable exchange of isotopic hydrogen between naphthalenes and the acidic clay surfaces, at 23 °C, or in aqueous slurries at 70 °C.

Eglington et al.¹⁹ carried out the hydrous pyrolysis of a Kimmeridge kerogen (Type II) at 280 or 330 °C for 72 h in the presence of clay or carbonate minerals. They found that more organic-soluble pyrolyzate was formed when calcium carbonate was the inorganic phase, which suggests significant base catalyzed cleavage of cross-links.

Graff and Brandes²⁰ found that a steam pretreatment of an Illinois bituminous coal (Type III kerogen) between 320 and 360 °C dramatically improved the yield of liquids upon subsequent conversion or solvent extraction. The steam-modified coal contains twice the hydroxyl groups of the raw coal. This leads to the conclusion that steam reacts with the ether linkages in coal, forming hydroxyl groups, and thereby substantially reducing an important covalent cross-link in the coal structure.²⁰ These conclusions are consistent with model compound studies on ether reactivity in hot water.^{1,20,21}

Aqueous Cleavage/Hydrolysis Reactions

1. Neutral Reactions

Rapid and clean ring cleavage of the cyclic aromatic ether 2,5-dimethylfuran in pure deuterium oxide at 250 °C yielded 2,5-hexanedione quantitatively and irreversibly within 30 min.²² the 2,5-hexanedione product undergoes no ring closure at this temperature in 1 h. These reaction conditions are in contrast to those reported in a mechanistic study of this reaction, in which a 0.1M DCl solution at 70 °C was required to cleave the ring.²³ Dibenzofuran¹ and 2-hydroxydibenzofuran²⁴ proved to be stable to aquathermolysis even at 460 °C.

Acetals and ketals are highly reactive to neutral aquathermolysis, undergoing in nearly all cases 100% hydrolysis within 30 min at 205-250 °C without side or secondary reactions.²² Greater than 90% deprotection of cyclopentanone ethylene ketal and 1,4-cyclohexanedione bis(ethylene ketal) was achieved at 250 °C. Equal reactivities to pure water were determined for benzaldehyde and tolualdehyde diethyl acetals at 186 and 250 °C resulting, during 30 min reaction, in 91-94% and 100% conversion, respectively. Hydrolysis of benzaldehyde diethyl acetal went to completion overnight at room temperature but decreased to 33% in the presence of basic barium oxide at 80 °C over 45 min. At 254 °C, quantitative hydrolysis of this acetal in aqueous KOH at acetal:base molar ratios as low as 1:0.25 (72.5 mM in KOH) was followed by a Cannizzaro disproportionation, as indicated by the formation of benzyl alcohol, benzoic acid, and, via subsequent decarboxylation of the acid, small amounts of benzene. Formation of Cannizzaro products of benzaldehyde in the presence of a much weaker base, pyridine, was reported previously.²⁵ Tsao and Houser suggested the possibility of a Cannizzaro reaction of this aldehyde catalyzed by ammonia in supercritical water, but, product distributions indicate the involvement of radical pathways.²⁶

Diacetone-D-glucose (0.31 M) and 1,6-anhydro- β -D-glucose (0.30M) were converted quantitatively at 205 °C to predominantly D-glucose and traces of another glucose isomer.¹⁶ Under the same conditions in the presence of 1 equivalent of KOH (0.29 M), 1,6-anhydro- β -D-glucose was unreactive and only the exocyclic, 5,6-acetone moiety of diacetone-D-glucose was cleaved. Cellulose is rapidly converted to soluble species with relatively high glucose yield in pure water near its critical temperature.²⁷ In a semi-batch or flow reactor, 100% conversion of cellulose was achieved in 1 h or less (15 sec at 400 °C). Parallel thermal transformations of the glucose product take place to form fructose, 1,6-anhydro D-glucose, erythrose, glycolaldehyde, glyceraldehyde, dehydroxyacetone, pyruvaldehyde, and acids.

2. Other Cleavage Reactions

The thermally stable ester, methyl 1-naphthoate is quantitatively hydrolyzed after 2 h and 5.5 day treatments at 343 and 250 °C, respectively.¹ Naphthoic acid is the major product at 250 °C, but its decarboxylation led predominantly to the formation of naphthalene during a 2 h conversion at 343°C; a reaction catalyzed by the generated carbonic acid. Examinations of methyl benzoate and its 4-chloro, 4-methyl, and 4-methoxy derivatives revealed up to 50% hydrolysis within 30 min at 250°C,²² but no evidence of decarboxylation. Partial cleavage of the *p*-methoxy group is assumed to be caused by the increased acidity of the medium resulting from carboxylic acid formation, since no ether cleavage was observed for α -ethyl-4-methoxybenzyl alcohol, in neutral water under otherwise more extreme conditions (277 °C, 75 min). Aliphatic 1,1-dicarboxylic acids are more reactive and Brill followed the decarboxylation of 1.07 M malonic acid to CO₂ and H₂O and the slower decarboxylation of monosodium malonate to CO₂ and acetate ion at 120-230 °C and 275 bar.²⁸ In a reaction typical of β -keto esters, ethyl

acetoacetate underwent complete conversion to acetone, ethanol, and CO₂ (not analyzed) in 30 min at 250°C.²² Under similar conditions, *tert*-butyl acetate decomposed to a bright red, highly insoluble mixture of unidentified products resulting from polymerization of isobutylene;¹³ but methyl trimethylacetate was unreactive.

Cyclohexyl-*x*-phenyl compounds, characteristic of structures found in Type II Kimmeridge shales, with oxygen, sulfur, and nitrogen links were shown to be relatively unreactive thermally but readily cleaved in water at 250 °C to form methylcyclopentene together with phenol, thiophenol, or aniline, respectively (Eq 5).²¹

Ionic reactions of these types are enhanced in 10% NaCl (acting as a weak acid) and in the presence of an acidic clay, but are depressed by basic calcium carbonate. This evidence supports an acid-catalyzed carbocation mechanism for this system in water at high temperature. Although an acyclic diaryl ether (diphenyl ether) and a cyclic diaryl ether (dibenzofuran) were unreactive under both aqueous and thermal conditions, an activated diaryl ether (4-phenoxyphenol) was cleaved in water to form phenol (Eq 6).¹ Penninger and Kolmschate treated 2-methoxynaphthalene with supercritical water at 390 °C for 1.5 h to give 2-naphthol and methanol as main reaction products.²⁹ Benzyl aryl ethers were also much more susceptible to cleavage under aqueous than thermal conditions at 250 °C. Klein reported that phenethyl phenyl ether formed phenol and styrene as the primary products after 1 h at 400 °C and dibenzyl ether yielded benzyl alcohol, toluene, and benzaldehyde after treatment in water at 374 °C for 1 h.³⁰

The thermally stable diaryl ether 1-phenoxy-naphthalene is cleaved in water at 315 °C after three days to phenol and 1-naphthol (95% conversion) and is thus significantly more reactive than diphenyl ether.³¹ In aqueous sodium formate reduction of the 1-naphthol to naphthalene and dihydronaphthalenes occurs. 9-Phenoxyphenanthrene similarly yields phenol and 9-hydroxyphenanthrene (Eq 8) and is more reactive than its 1-phenoxy isomer.³² Interestingly, the rate of hydrolysis of such diaryl ethers is affected dramatically by additives such as NaCl, LiCl, KBr, and Na₂SO₄.³³ The conversion of 1-phenoxy-naphthalene in water alone at 315 °C after 72 hours was 94.6%; on reaction of this substrate with a 1% aqueous solution of each of the above salts, the conversion was reduced to 7.4%, 4.8%, 3.8%, and 0%, respectively. These results strongly suggest that at high temperatures, alkali metal halides and sodium sulfate behave as salts of strong bases and weak acids and reduce the hydrogen ion activity of the solutions, in agreement with previous indications.³³

Hydrogen Exchange Reactions

When the ring cleavage reaction of 2,5-dimethylfuran was conducted in deuterium oxide,³⁴ extensive deuteration of the methyl and methylene groups in the product, 2,5-hexanedione, was observed; the same result was detected by ¹H and ¹³C NMR when this dione was the initial reagent. Thus, it became evident that this medium was suitable for ¹H/²H exchange.²² These exchange reactions afforded an additional means to study organic transformations in a reaction environment undergoing minimal changes; for example, no products are formed that have significantly different properties or reactivities from those of the initial reagents. Also, no changes occur in reaction mechanisms, volume, vapor pressure, or the dielectric or dissociation constants of deuterium oxide because of the formation of ionic products and potential catalysts or co-solvents.

Deuterium oxide treatment of methyl (300 °C, 93 h), isopropyl, and neopentyl alcohol (200 °C, 30 min and 300 °C, 60 min, respectively) did not induce any exchange of C-H hydrogens; the same negative results were obtained in experiments with ethylene glycol (300 °C, 60 min) and pentaerythritol (250 °C, 60 min).²² Hydrogen exchange was achieved rapidly and nearly quantitatively in the α and α' (where applicable) positions of ketone carbonyl groups. Table 2 lists the extents and sites of deuteration observed in selected ketones. In all cases, the operating enol-keto tautomerism led exclusively to hydrogen exchange; no aldol products were observed.

Table 2. Hydrogen/Deuterium Exchange in Ketones

Compound	% D (position)	Reaction Conditions	
		°C	Min
Pinacolone ^a	100 (α CH ₃)	277	60
Acetone	97 (α , α' CH ₃)	200	60
Cyclopentanone ^b	100 (α , α' CH ₂)	225	30
1,4-cyclohexanedione	100 (α , α' CH ₂)	225	30
Acetophenone	>88 (α CH ₃)	250	60
Deoxybenzoin ^c	99 (α CH ₂)	250	30

a Exchange observed in the rearrangement product of pinacol.

b Exchange observed in the hydrolysis product of the corresponding ethylene ketal.

c PhCH₂COPh.

Nearly quantitative exchange by reaction with only 0.016M sodium deuteroxide solution for 10 min at 400 °C and ~300 bar pressure occurred for molecules having pK_a's up to approximately 43, while longer heating time and more concentrated base solutions allow deuteration of still more weakly acid compounds having pK_a's up to 50.³⁵

Technological Applications

Chemical reactions carried out in hot water have the potential to provide a cleaner, safer environment than reactions in hydrocarbon solvent media. In addition, water acting as a catalyst or reagent could minimize, or possibly eliminate, the need for catalyst synthesis, recycle, regeneration, and disposal. Such application to the recycle of condensation polymers including plastics, synthetic fibers, and polycarbonates is attractive.^{2,36} Another potential application is the use of hot water treatment to upgrade low-value by-products. A demonstrated example occurs in the hydration of propylene with sulfuric acid to form isopropyl alcohol with thermally stable diisopropyl ether as a by-product. Hydrous cleavage of this by-product ether at 315 °C for 30 min readily forms essentially equimolar amounts of the desired product (isopropyl alcohol) and recyclable propylene.³⁷ Di-*sec*-butyl ether, a by-product in the hydration of butylene to *sec*-butyl alcohol in the methyl ethyl ketone (MEK) process, can similarly be converted to the alcohol in hot water³⁷ (Eqs 9 and 10). The aldol condensation by-product of MEK production, a C₈-unsaturated ketone, is quantitatively reversed to MEK by hydration followed by retro-aldol cleavage.³⁸

CONCLUSIONS

This article describes the reactivity of organic molecules in superheated water. Emphasis was placed on the geochemical perspective because, outside of biological processes, where aqueous chemistry predominates and is catalyzed by enzymes, kerogen formation and its subsequent depolymerization into petroleum is the major arena in nature where aqueous chemistry is observed. In this chemistry, water participates as catalyst, reactant, and solvent. While the geochemical aspects serve as a foundation for understanding the aqueous chemistry, the implications for a wide variety of other organic chemical transformations and technological applications are potentially large and just beginning to emerge. The unique ability of water to carry out condensation, cleavage, and hydrolysis reactions and provide an opportunity (not accessible thermally) to effect selective ionic chemistry, is largely due to changes in the chemical and physical properties of water, which become more compatible with the reactions of organics as the temperature is increased. Therefore, its solvent properties at 250-350 °C approach that of polar organic solvents at room temperature. It can act as an acidic or basic catalyst and its reactivity can often be reinforced by autocatalysis from water soluble reaction products generated. Additional positive aspects of the use of aqueous chemistry are its simplicity, low cost, and favorable environmental impact.

REFERENCES

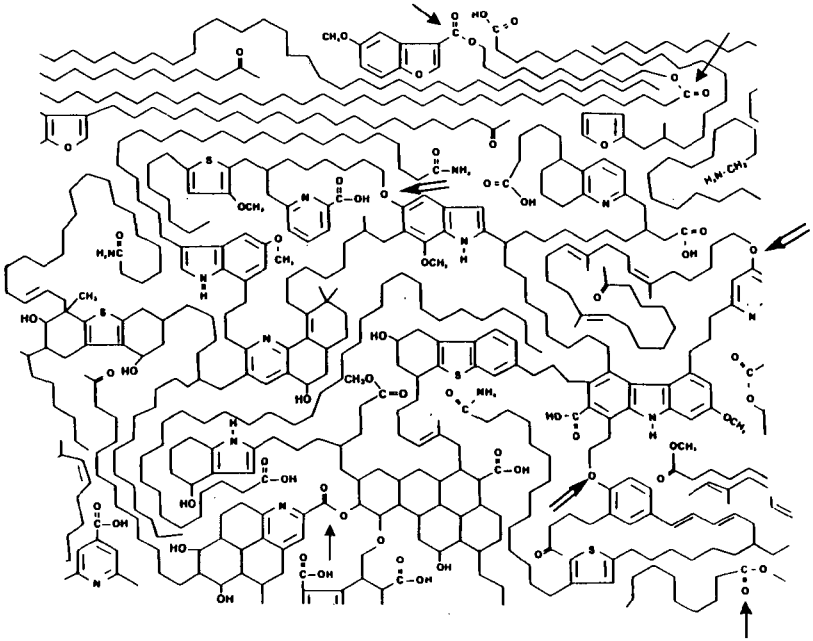
1. Siskin, M.; Brons, G.; Vaughn, S. N.; Katritzky, A. R.; Balasubramanian, M. *Energy Fuels* 1990, 4, 488.
2. Mandoki, J. W. *U.S. Patent* 4 1986, 605, 762.
3. Grim, R. E. *Am. Assoc. Pet. Geol. Bull.* 1974, 31, 1491.
4. Siskin, M.; Brons, G.; Katritzky, A. R.; Balasubramanian, M. *Energy Fuels* 1990, 4, 475.
5. Katritzky, A. R.; Lapucha, A. R.; Murugan, R.; Luxem, F. J.; Siskin, M.; Brons, G. *Energy Fuels* 1990, 4, 493.

REFERENCES (Cont'd.)

6. Pitzer, K. S. *Proc. Natl. Acad. Sci. U.S.A.* **1983**, *80*, 4574.
7. Akerlof, G. C.; Oshry, H. I. *J. Am. Chem. Soc.* **1950**, *72*, 2844. Franck, E. U. *J. Chem. Thermodyn.* **1987**, *19*, 225.
8. Calculated from the specific internal energy of vaporization in Steam Tables by J. H. Keenan, F. G. Hayes, P. G. Hill, J. G. Moore (Wiley Interscience, 1969)
9. Franck, E. U. *J. Chem. Thermodyn.* **1987**, *19*, 225. Akerlof, G. C.; Oshry, H. I. *J. Am. Chem. Soc.* **1950**, *72*, 2844. See also Perrin, D. D. *Ionization Constants of Inorganic Acids and Bases in Aqueous Solutions*, 2nd Ed.; IUPAC Data Series 29; Pergamon, New York, 1982.
10. Jurg, J. W.; Eisma, E. *Science* **1964**, *144*, 1451.
11. Johns, W. D. *Dev. Sedimentol.* **1982**, *35*, 655.
12. Frenkel, M.; Heler-Kalai, L. *Org. Geochem.* **1977**, *1*, 3.
13. Goldstein, T. P. *AAPG Bull.* **1983**, *67*, 152.
14. Winters, J. C.; Williams, J. A.; Lewan, M. D. *Adv. in Org. Geochem.* **1981**, 524.
15. Tannenbaum, E.; Kaplan, I. R. *Nature* **1985**, *317*, 708.
16. Hoering, T. C. *Org. Geochem.* **1984**, *5*, 267.
17. Hoering, T. C.; Abelson, P. H. *Carnegie Inst. Wash. Yearbook* **1963**, *62*, 229 and Hoering, T. C. *Carnegie Inst. Wash. Yearbook* **1968**, *67*, 199.
18. Alexander, R.; Kagi, R. I.; Larcher, A. V. *Geochim. Cosmochim. Acta* **1982**, *46*, 219.
19. Eglington, T. I.; Rowland, S. J.; Curtis, C. D.; Douglas, A. G. *Adv. Org. Geochem.* **1985**, *10*, 1041 and 2589.
20. Brandes, S. D.; Graff, R. A. *Energy Fuels* **1987**, *1*, 84; Brandes, S. D.; Graff, R. A.; Gorbaty, M. L.; Siskin, M. *Energy Fuels* **1989**, *3*, 494.
21. Siskin, M.; Brons, G.; Katritzky, A. R.; Murugan, R. *Energy Fuels* **1990**, *4*, 482.
22. Kuhlmann, B.; Arnett, E. M.; Siskin, M. *J. Org. Chem.* **1994**, *59*, 3098.
23. Kankaanpera, A.; Kleemola, S. *Acta Chem. Scand.* **1969**, *23*, 3607.
24. Siskin, M.; Katritzky, A. R.; Balasubramanian, M. *Fuel* **1995**, *74*, 1509.
25. Katritzky, A. R.; Balasubramanian, M.; Siskin, M. *Energy Fuels* **1990**, *4*, 499.
26. Tsao, C. C.; Houser, T. J. *Prepr. Pap.-Am. Chem. Soc., Div. Fuel Chem.* **1990**, *35*(2), 442.
27. Adschiri, T.; Hirose, R. M.; Arai, K. *J. Chem. Eng. Japan* **1993**, *26*, 676.
28. Maiella, P. G.; Brill, T. B. *J. Phys. Chem.* **1996**, *100*, 14352.
29. Penninger, J. M. L.; Kolmschate, J. M. M. *Supercritical Fluid Science and Technology* eds. Johnston, K. P. and Penninger, J. M. L. *ACS Symp. Series #406*, ACS, Wash. DC **1989**, 245; Penninger, J. M. L. *Fuel* **1988**, *67*, 490.
30. Townsend, S. H.; Abraham, M. A.; Hubbert, G. L.; Klein, M. T.; Paspek, S. C. *Ind. Eng. Chem. Res.* **1988**, *27*, 143.
31. Siskin, M.; Katritzky, A. R.; Balasubramanian, M. *Energy Fuels* **1991**, *5*, 770.
32. Siskin, M.; Katritzky, A. R.; Balasubramanian, M. *Fuel* **1993**, *72*, 1435.
33. Katritzky, A. R.; Balasubramanian, M.; Siskin, M. *J. Chem. Soc., Chem. Commun.* **1992**, 1233.
34. The ion product of D₂O is approximately 1 order of magnitude larger than that of H₂O at equal temperature; e.g. at 250 °C, -log K(H₂O) = 11 and -log K(D₂O) = 12. See: Perrin, D. D. *Ionization Constants of Inorganic Acids and Bases in Aqueous Solutions*, 2nd ed.; IUPAC Data Series 29; Pergamon: New York, 1982.
35. Yao, Y.; Evilia, R. F. *J. Amer. Chem. Soc.* **1994**, *116*, 11229.
36. Kinstle, J. F.; Forshey, L. D.; Valle, R.; Campbell, R. R. *Polym. Prepr. (Am. Chem. Soc., Div. Polym. Chem.)* **1983**, *24* 446. Campbell, G. A.; Meluch, W. C. *Environ. Sci. Technol.* **1976** *10*, 182.
37. Siskin, M.; Brons, G.; Vaughn, S. N.; Saleh, R. Y. *U.S. Patent 5,043,486*, **August 27, 1991**.
38. Dolfini, J. E.; Glinka, J. *U.S. Patent 4,709,098*, **November 24, 1987**.

Figure 1

**EXAMPLE OF KEY CLEAVABLE LINKAGES IN RESOURCES ...
... RUNDLE RAMSAY CROSSING OIL SHALE KEROGEN**



STRUCTURE-REACTIVITY RELATIONSHIPS FOR ORGANICS IN SUB- AND SUPERCRITICAL AQUEOUS MEDIA: DEVELOPMENT OF A KNOWLEDGE BASE.

Alan R. Katritzky^a, Michael Siskin^b and Daniel A. Nichols^a

^aCenter for Heterocyclic Compounds, Department of Chemistry, University of Florida, P. O. Box 117200, Gainesville, FL 32611

^bExxon Research and Engineering Co., Corporate Research Labs, Rt. 22E, Clinton Twp., Annandale, NJ 08801

Abstract: The products and reactions of diverse classes of organics with superheated water have been analyzed quantitatively by GCMS supplemented by QSPR-derived response factors.

Reaction types to be discussed include: (i) heterolytic carbon-heteroatom bond cleavages and formations catalyzed by water acting as an acid or base, (ii) oxidation-reductions and disproportionations, and (iii) heterolytic carbon-carbon bond formations and cleavages. The results (a) assist the rationalization of aspects of the diagenesis and catagenesis chemistries of kerogens, (b) help in the formulation of superior preparative procedures in which pure water is selected as a solvent, reagent, or catalyst and in special circumstances if it is optimal to add traces of specific reagents, and (c) offer potential solutions for chemical weapons disposal.

Keywords: water, supercritical, organic reactivity

The work carried out at the University of Florida was intended to complement the more applied studies underway at Exxon (see preceding paper) and to help build a knowledge base concerning the reactions undergone by carbon skeletons and typical functional groups found in naturally occurring feedstocks in superheated water. A supplemental objective was to explore the potential of aquathermolysis for chemical weapons disposal. A summary of the work has been published in *Accounts of Chemical Research*¹ and a more detailed overview is in preparation for *Chemical Reviews*.

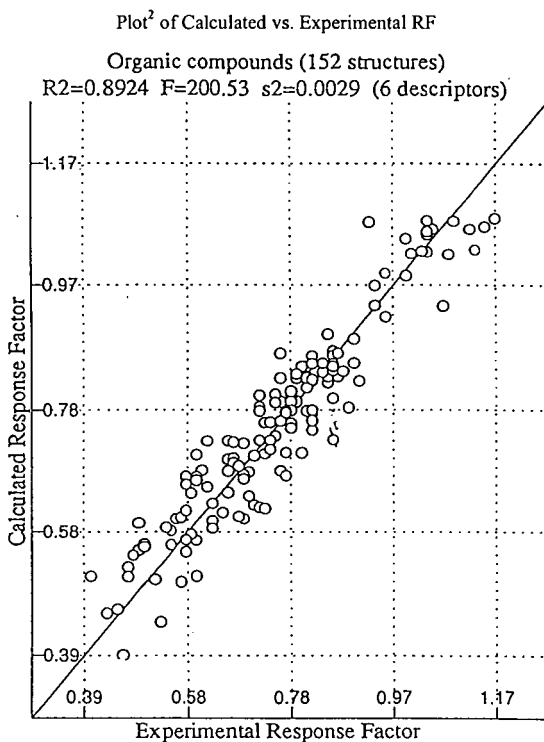
The methodology adopted was to heat known quantities of compounds in water (or water containing definite amounts of such additives as phosphoric acid, sodium hydroxide or formic acid) in small stainless steel bombs. Reactions were analyzed by GC/MS. From the fragmentation pattern and knowledge of the chemistry of the compounds in question at lower temperatures it was usually possible to deduce the structures of the products. This allowed a qualitative analysis. To turn from a qualitative into a quantitative analysis, it was necessary to know the response factors for all the products in the GC flame ionization detector. As it was impractical to measure these, a supplementary investigation was carried out and a quantitative structure property relationship established between chemical structures of a training set of 152 diverse compounds and their flame ionization response factors². It was found possible to correlate response factors with an R^2 value of 0.89 using six theoretical descriptors as shown in the Plot.

Heterolytic carbon-heteroatom bond cleavages and formations were found to be readily catalyzed by water acting as an acid or a base. Oxidation-reductions and disproportionations were also found to be common. Heterolytic carbon-carbon bond formations occurred frequently and sometimes such cleavage reactions were also uncovered.

Thus, benzyl alcohol undergoes a wide variety of condensations to give benzyl benzyl alcohols and polybenzylated benzyl alcohols. Its hydroxy group can also be reduced into a methyl or oxidized into an aldehyde, and further transformations of both of these types of products occur to give a highly complex reaction palette, but one that is completely rationalizable in terms of expected chemical transformations. This research indicated that thermolysis of benzyl alcohol is in effect an aquathermolysis reaction significantly influenced by the water produced during the reaction; however, normal aquathermolysis reaction produces higher quantities of disproportionation products and less dibenzyl ether³.

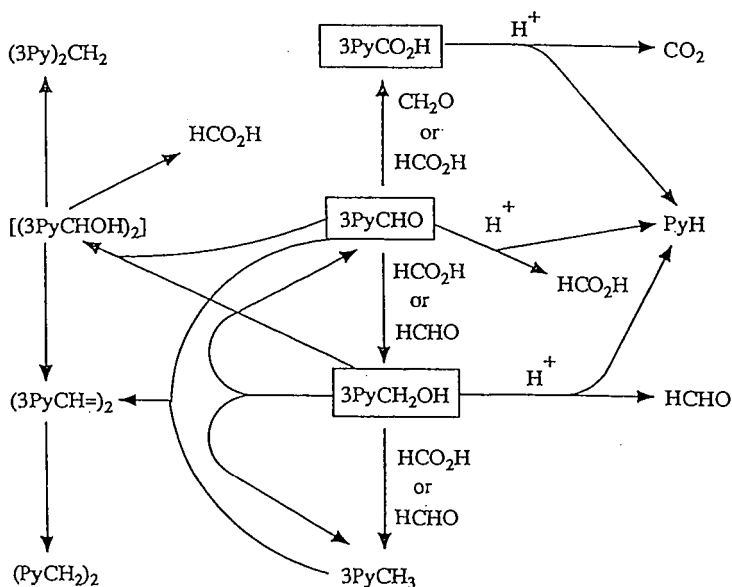
The behavior of hydroxymethyl, aldehyde and carboxyl groups attached to a pyridine ring were studied, and it was found that eventually all these compound types were converted into the parent pyridine together with the corresponding methyl pyridine by disproportionation and substituent cleavage reactions^{4,5}. The overall reaction pathways for pyridines substituted with a carboxyl, aldehyde or hydroxymethyl group in the 3-position⁴ as shown in Scheme 1. The patterns for the corresponding 2-⁶ and 4-⁵ substituted pyridines are still more complex.

In a system simulating water/carbon monoxide, it was found for a series of alkylpyridines that the ring can be cleaved by heating at 350 °C with 50% formic acid ($\text{HCOOH} \rightarrow \text{H}_2\text{O}/\text{CO}$). The products are a series of *N*-substituted piperidines where the *N*-substituent is derived from the fragmentation and C-C bond cleavage at the 3,4 positions of the pyridine ring of a second molecule of the starting pyridine⁷. This process shows considerable similarity to the formation of pyridines from one, two and three carbon building units in commercially well-known catalytic synthetic procedures.



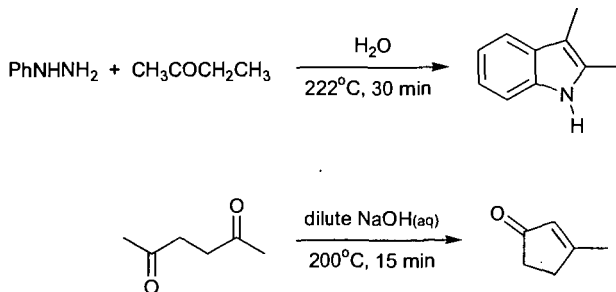
The applications of superheated water as a solvent for superior preparative procedures has been explored particularly by Strauss and his co-workers⁸. As depicted in Scheme 2, such

Scheme 1: Overall Reaction Pathways for 3-Substituted Pyridines⁶



reactions in pure water and in water containing traces of acid or base can have rate enhancements far exceeding those expected for such dilute systems. This is well illustrated by the one step Fisher indole synthesis of 2,3-dimethylindole from phenylhydrazine and butanone in neutral water at 222 °C in 67% yield in 30 minutes⁹. Additionally, although 2,5-hexanedione in neutral water failed to undergo ring closure at 250 °C in 1 hour¹⁰, Strauss found that 3-methylcyclopent-2-enone was formed in 81% yield within 15 minutes at 200 °C from the intramolecular aldol condensation in 0.05% aqueous sodium hydroxide⁸.

Scheme 2: Application of Superheated Water to Preparative Procedures^{8,9}



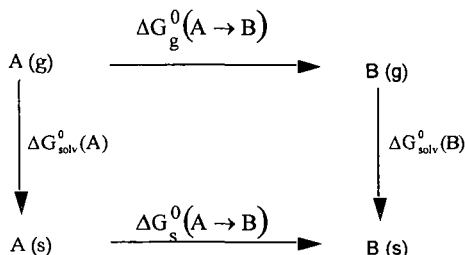
References

- 1 Katritzky, A. R.; Allin, S. M.; Siskin, M. *Acc. Chem. Res.* **1996**, *29*, 399.
- 2 Katritzky, A. R.; Ignatchenko, E. S.; Barcock, R. A.; Lobanov, V. S.; Karelson, M. *Anal. Chem.* **1994**, *66*, 1799.
- 3 Katritzky, A. R.; Balasubramanian, M.; Siskin, M. *Energy Fuels* **1990**, *4*, 499.
- 4 Katritzky, A. R.; Lapucha, A. R.; Murugan, R.; Luxum, F. J.; Siskin, M.; Brons, G. *Energy Fuels* **1990**, *4*, 493.
- 5 Katritzky, A. R.; Lapucha, A. R.; Siskin, M. *Energy Fuels* **1990**, *4*, 510.
- 6 Katritzky, A. R.; Lapucha, A. R.; Siskin, M. *Energy Fuels* **1990**, *4*, 506.
- 7 Siskin, M.; Katritzky, A. R.; Balasubramanian, M.; Ferrughelli, D. T.; Brons, G.; Singhal, G. H. *Tetrahedron Lett.* **1993**, *34*, 4739.
- 8 An, J. Y.; Bagnell, L.; Cablewski, T.; Strauss, C. R.; Trainor, R. W. *J. Org. Chem.* **1997**, *62*, 2505.
- 9 Strauss, C. R.; Trainor, R. W. *Aust. J. Chem.* **1995**, *48*, 1665.
- 10 Kuhlmann, B.; Arnett, E. M.; Siskin, M. *J. Org. Chem.* **1994**, *59*, 3098.

QUANTUM MOLECULAR MODELING OF REACTIONS IN WATER: A DIELECTRIC CONTINUUM APPROACH

Thanh N. Truong
Henry Eyring Center for Theoretical Chemistry
Department of Chemistry, University of Utah
Salt Lake City, UT 84112.

The dielectric continuum solvation approach provides a simple methodology for inclusion of solvent effects directly into the matrix elements of the solute Hamiltonian. This allows that computational procedures for studying reactions in the gas phase such as optimizing transition state structure and determining reaction path, etc. can also be used for reaction in solution. However, direct application of such procedures is not correct. From a thermodynamic cycle, we proposed a rigorous methodology for modeling free energy profiles of reactions in solution within the frame work of the dielectric continuum solvation approach.¹ Let us consider an A → B reaction. The standard free energies of reaction in the gas phase and in solution are denoted as ΔG_g^0 and ΔG_s^0 , respectively. Associating with the reactant A and product B are free energies of solvation denoted as ΔG_{solv}^0 . From the thermodynamic cycle given below



the standard free energy of the reaction in solution can be written as

$$\Delta G_s^0 = \Delta G_g^0 + \left\{ \Delta G_{\text{solv}}^0(\text{B}) - \Delta G_{\text{solv}}^0(\text{A}) \right\}, \quad (1)$$

where the gas-phase free energy is given by

$$\Delta G_g^0 = \Delta E - RT \ln \left(\frac{Q^{\text{B}}}{Q^{\text{A}}} \right). \quad (2)$$

Here ΔE is the reaction energy; R is the Boltzmann constant; T is the temperature; Q^{A} and Q^{B} are the total partition functions evaluated with the zero of energy set at the bottom of each respective potential well.

This expression can be generalized for the free energy profile of reaction in solution. In particular, the standard free energy at a point $\mathbf{R}(s)$ along the reaction coordinate s relative to that of the reactant A is expressed as

$$\Delta G_s^0(s) = \Delta G_s^0(\text{A} \rightarrow \mathbf{R}(s)) = V_{\text{MEP}}(s) - RT \ln \left(\frac{Q(\mathbf{R}(s))}{Q^{\text{A}}} \right) + \Delta G_{\text{solv}}^0(\mathbf{R}(s)) - \Delta G_{\text{solv}}^0(\text{A}) \quad (3)$$

where $V_{\text{MEP}}(s)$ is the gas-phase potential energy along the reaction coordinate s with the zero of energy set at the reactant. Eq. (3) indicates that *in order to obtain accurate free energy profile for reaction in solution, one requires to have not only accurate free energy of solvation but also*

accurate gas-phase free energy profile. In calculations of free energies of activation of many reactions in solution, previous studies have focused mostly on the solvation free energy contributions and often overlooked errors in the calculated gas-phase free energy profile.

The central issue here is how to define the reaction coordinate s . Adopting the reaction path Hamiltonian formalism, the reaction coordinate s for reactions in solution is defined as the distance along the minimum free energy path on the free energy surface. However, following the reaction path on the solution-phase free energy surface, as defined in Eq. (3), is almost an impossible task. The major difficulty arises from the necessity to perform normal mode analysis at every point on the gas-phase potential surface in order to calculate vibrational partition functions. To circumvent this problem, an assumption is made that the gas-phase Born-Oppenheimer potential energy surface $E(\mathbf{R})$ has similar topology to the gas-phase free energy surface along the reaction coordinate. In this case, a pseudo-free energy surface $G^*(\mathbf{R})$ in the solute nuclear coordinates \mathbf{R} is related to $E(\mathbf{R})$ by the following expression

$$G^*(\mathbf{R}) = E(\mathbf{R}) + \Delta C_{\text{solv}}(\mathbf{R}). \quad (4)$$

The pseudo-free energy surface defined above allows one to utilize advanced computational methods that have been well developed for following reaction paths in the gas phase. Analogous to the gas phase, the reaction coordinate s in solution is defined as the distance along the minimum free energy path (MFEP) which is the steepest descent path from the transition state toward both the reactant(s) and product(s) on the pseudo-free energy surface $G^*(\mathbf{R})$. To obtain free energy profile of reaction in solution the gas-phase $-RT \ln \left(\frac{Q(s)}{Q^A} \right)$ term is added to the pseudo-free energy profile $\Delta G^*(s)$. In summary, the procedure for calculating free energy profiles of reaction in solution involves three steps: 1) select the appropriate level of theory and basis set that can give accurate gas-phase free energy surface; 2) Determine the transition state and calculate the minimum free energy path on the pseudo-free energy surface defined above; 3) Add contributions from the gas-phase solute internal degrees of freedom along this MFEP. These contributions were mistakenly omitted in previous dielectric continuum calculations of free energies of activation including our own first study of solvent effects on reaction profile of the $\text{S}_\text{N}2 \text{ Cl}^- + \text{CH}_3\text{Cl}$ reaction.²

We will discuss advantages and disadvantages of the above methodology in details through applications to several important organic reactions.^{1,3,4}

References

- (1) Truong, T. N.; Truong, T.-T. T.; Stefanovich, E. V. *J. Chem. Phys.* **1997**, *107*, 1881.
- (2) Truong, T. N.; Stefanovich, E. V. *J. Phys. Chem.* **1995**, *99*, 14700.
- (3) Truong, T. N. *J. Phys. Chem. B* **1998**, in press.
- (4) Truong, T. N. *Int. Rev. Phys. Chem.* **1998**, in press.

TRANSITIONS IN THE SOLVATION STRUCTURE ABOUT IONS IN SUPERCRITICAL WATER AND THEIR EFFECTS ON REACTIVITY

John L. Fulton, Markus M. Hoffmann, John G. Darab
Pacific Northwest National Laboratory,
P.O. Box 999 MS P8-19
Richland, WA, 99352.

ABSTRACT

We have determined the molecular structure about ions in water under hydrothermal conditions using X-ray absorption fine structure spectroscopy (XAFS). We report a large decrease in the extent of ion hydration in Ni^{2+} , Sr^{2+} , Rb^+ , and Br^- solutions and the formation of contact-ion pairs in aqueous nickel bromide at temperatures exceeding 325°C. The results demonstrate the large changes in the solvation dynamics that occur in the transition from ambient to supercritical conditions. Such fundamental structural information on the speciation in aqueous solutions under hydrothermal conditions is scarce but needed for an understanding of both inorganic and organic reactions in a supercritical-water solvent. Such an understanding will further the development of new hydrothermal technologies such as organic synthesis or waste destruction processes.

INTRODUCTION

It is well known that ionic species start to associate with their respective counter ions in water at high temperatures. For solutions containing ionic species at moderate concentrations, the onset of this phenomena occurs at temperatures above about 325°C where the breakdown of the water hydrogen-bonding network¹ leads to a dielectric constant (low-frequency) that is dramatically lower than for ambient conditions. The low value of the dielectric constant means that the electrostatic interactions between charged species is no longer effectively screened. A detailed description of the ion-pairing phenomena was first made available through theoretical and simulation work^{2,3}. Some experimental evidence^{4,5} of the existence of ion-pairing was also derived from electronic and Raman spectroscopy but yielded little direct structural information. This XAFS technique⁶⁻⁹ gives the short-range structure of the first several solvation shells about the ion. Therefore, for the first time, we can measure the detailed structural transitions that occur under hydrothermal conditions. We have previously reported observation of significant dehydration occurring under supercritical water conditions for mono- and di-valent cations¹⁰⁻¹² (Sr^{2+} and Rb^+) and for a monovalent anion (Br^-).¹³ More recently we have explored NiBr_2 hydration and ion pairing in moderately dilute systems.¹⁴ Seward et al.¹⁵ have also reported XAFS studies of the hydration and ion-pairing of Ag^+ in subcritical water solutions at their vapor pressure. In this paper, we explore a Ni^{2+} system in which the Br^- concentration is greatly increased through the addition of NaBr . This promotes the formation of the more highly coordinated NiBr_6 species.

Although this presentation will deal with association of inorganic ions in supercritical water ($T_c = 375^\circ\text{C}$), the results are important to systems that also contain organic species. The structural transition that occurs for these inorganic species will also have their analogous transition for organic ionic species. Thus, the existence of ion pairs is an important consideration for manipulating reaction pathways and reaction rates in supercritical water. For instance, ion-pair formation may enhance the reactivity of charged organic molecules if it involves the association of two ionic reactant species (oppositely charged) or it involves an ionic reactant species with an ionic catalytic species. The reactivity may be reduced in those instances where an ionic reactant is sequestered by ion-pair formation with a non-reactive ionic species. Similar mechanisms of enhanced or reduced reaction rates would also affect pathways that involve ionic transition-state species. Finally, the regioselectivity may also be influenced for charged or very polar reactants since the reactants can assume a strongly-bound spatial orientation in an ion-pair structure. It is in this light, that we explore the detailed nature of ion pairing under hydrothermal conditions.

EXPERIMENTAL

In XAFS, the x-ray energy is tuned to the region bounding the electron absorption (in this case the K-edge). The ejected photoelectrons are back-scattered by atoms in the nearest solvation shells giving rise to oscillations in the XAFS spectra on the high energy side of the edge. The Fourier transformation of these *k*-space spectra gives a real-space distribution plot that is closely

related to a radial distribution function. XAFS is a short-range technique, that gives structural information out to one or two solvent shells from the central scattering atom. This is the region of critical importance for understanding ion hydration in a water environment. XAFS spectra were acquired at the insertion device beamline (PNC-CAT) at the Advance Photon Source (Argonne National Laboratory) and at beamline X-19A of the National Synchrotron Light Source (NSLS) at the Brookhaven National Laboratory. A schematic of the high-temperature, high-pressure XAFS equipment and of the data transformation methods are depicted in Figure 1. The details of the experimental techniques^{11-13,16,17} are given elsewhere.

The methods for data collection, background correction and data transformation are well-established^{9,18,19}. The analysis of the $\chi(k)$ function was based upon the standard XAFS relationship

$$\chi(k) = \frac{F(k)S_0^2N}{kR^2} e^{-2k^2\sigma^2} e^{-2R/\lambda(k)} \sin(2kR + \delta(k) - \frac{4}{3}k^3C_3) \quad (1)$$

Where $F(k)$, $\delta(k)$, and $\lambda(k)$ are the amplitude, phase and mean-free path factor, respectively, that are derived from the theoretical standard FEFF.²⁰ Detailed description of fitting methods for these parameters can be found elsewhere.¹⁴ The remaining terms in Equation 1 are N , the coordination number of the shell, R , the shell distance, σ^2 , the Debye-Waller factor which represents the mean-square variation in R due to both static and thermal disorder, and finally C_3 , the anharmonicity of the pair-distribution. These terms, which contain the quantitative structural information, were found using the FEFFIT^{21,22} analysis program that employs a non-linear, least-squares fit to the theoretical standards calculated by FEFF.²⁰

DISCUSSION AND CONCLUSIONS

Figure 2 is a radial structure plot for Ni^{2+} . The figure relates the probability of finding a water molecule or a Br^- at some distance from the central Ni^{2+} ion. Under ambient conditions the Ni^{2+} is octahedrally coordinated with 6 water molecules. As the temperature of the solution is increased, the number of water molecules in the first solvation shell decreases and we observe the appearance of a new peak at about 2.1 Å due to the Br^- counterion. In all the systems that have been studied in detail thus far, the decrease in the extent of hydration occurs concurrent with the formation of the contact ion pairs. This may be primarily a size-exclusion effect or may be in part due to the reduction in the local electric field due to the presence of the counterions.

Table 1 relates the change in the extent of hydration upon going from ambient to a supercritical state for a variety of different cations and an anion. Again there are dramatic reductions in the extent of hydration upon reaching supercritical conditions for these ionic species.

Table 2 reports the detailed structural parameters for a NiBr_2 contact ion pair. The results are derived from a global-model fit to two independent XAFS measurements at both the Ni and Br absorption edges. Thus, a very high degree of confidence is obtained for the NiBr_n ion-pair structural parameters. In this system, the concentration of the Br^- was increased to 6 times the Ni^{2+} concentration in order to favor the formation of Ni^{2+} species with a high degree of ion pairing. The results strongly suggest that there is a transition from octahedral Ni^{2+} coordination at room temperature to tetrahedral coordination at elevated temperatures. The average number of Br^- ions in contact with a Ni^{2+} ion is 3.3. Since electrostatically neutral species are strongly favored in this solvent, the likely species may include dimers $(\text{NiBr}_4\text{Ni}(\text{H}_2\text{O})_n)^0$ or species that also include Na^+ association such as $(\text{NiBr}_3\text{Na}(\text{H}_2\text{O})_n)^0$.

In conclusion, a great deal of structural information is available from XAFS about a wide range of supercritical water systems. Information from these studies will aid in the development of structurally-appropriate models of reaction rates and pathways under hydrothermal conditions.

ACKNOWLEDGMENTS

This research was supported by the Director, Office of Energy Research, Office of Basic Energy Sciences, Chemical Sciences Division of the U. S. Department of Energy, under contract DE-AC06-76RLO 1830.

REFERENCES

- Hoffmann, M. M.; Conradi, M. S. *J. Am. Chem. Soc.* **1997**, *119* 3811-3817.
- Chialvo, A. A.; Cummings, P. T.; Cochran, H. D.; Simonson, J. M.; Mesmer, R. E. *J.*

- Chem. Phys.* **1995**, 1039379-9387.
- Oelkers, E. H.; Helgeson, H. C. *Science* **1993**, 261888-891.
 - Susak, N. J.; Crerar, D. A. *Geochim. Cosmochim. Acta* **1985**, 49555-564.
 - Spohn, P. D.; Brill, T. B. *J. Phys. Chem.* **1989**, 936224-6231.
 - Sayers, D. E.; Stern, E. A.; Lytle, F. W. *Phys. Rev. Lett.* **1971**, 271204.
 - Lee, P. A.; Citrin, P. H.; Eisenberger, P.; Kincaid, B. M. *Rev. Modern Physics* **1981**, 53769-806.
 - Lytle, F. W. In *Applications of Synchrotron Radiation*; Winick, H.; Xian, D.; Ye, M.; Huang, T., Eds.; Gordon and Breach: New York, 1989; pp 135-223.
 - Teo, B. K. *EXAFS: Basic Principles and Data Analysis*; Springer-Verlag: New York, 1986.
 - Palmer, B. J.; Pfund, D. M.; Fulton, J. L. *J. Phys. Chem.* **1996**, 10013393-13398.
 - Fulton, J. L.; Pfund, D. M.; Wallen, S. L.; Newville, M.; Stern, E. A.; Ma, Y. *J. Chem. Phys.* **1996**, 1052161-2166.
 - Pfund, D. M.; Darab, J. G.; Fulton, J. L.; Ma, Y. *J. Phys. Chem.* **1994**, 9813102-13107.
 - Wallen, S. L.; Palmer, B. J.; Pfund, D. M.; Fulton, J. L.; Newville, M.; Ma, Y.; Stern, E. A. *J. Phys. Chem. A* **1997**, 1019632-9640.
 - Wallen, S. L.; Palmer, B. J.; Fulton, J. L. *J. Chem. Phys.* **1998**, 1084039-4046.
 - Seward, T. M.; Henderson, C. M. B.; Charnock, J. M.; Dobson, B. R. *Geochim. Cosmochim. Acta* **1996**, 602273-2282.
 - Fulton, J. L.; Pfund, D. M.; Ma, Y. *Rev. Sci. Instrum.* **1996**, 67(CD-ROM Issue)1-5.
 - Hoffmann, M. M.; Darab, J. G.; Heald, S. M.; Yonker, C. R.; Fulton, J. L. *Chemical Geology* **1999**, Submitted.
 - Stern, E. A.; Heald, S. In *Handbook of Synchrotron Radiation*; Eastman, D. E.; Farge, Y.; Koch, E. E., Eds.; North Holland: Amsterdam, 1983.
 - X-Ray Absorption: Principles, Applications, Techniques of EXAFS, SEXAFS and XANES*; Koningsberger, D. C.; Prins, R., Eds.; John Wiley & Sons: New York, 1988.
 - Zabinsky, S. I.; Rehr, J. J.; Ankudinov, A.; Albers, R. C.; Eller, M. J. *Phys. Rev. B* **1995**, 522995-3009.
 - Newville, M.; Ravel, R.; Haskel, D.; Rehr, J. J.; Stern, E. A.; Yacoby, Y. *Physica B* **1995**, 208 & 209154-156.
 - Stern, E. A.; Newville, M.; Ravel, B.; Yacoby, Y.; Haskel, D. *Physica B* **1995**, 208 & 209117-120.

FIGURES AND TABLES

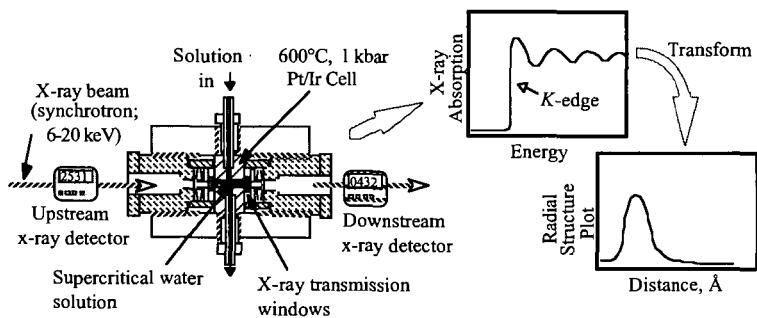


Figure 1. Schematic of the supercritical water XAFS cell and the data analysis technique.

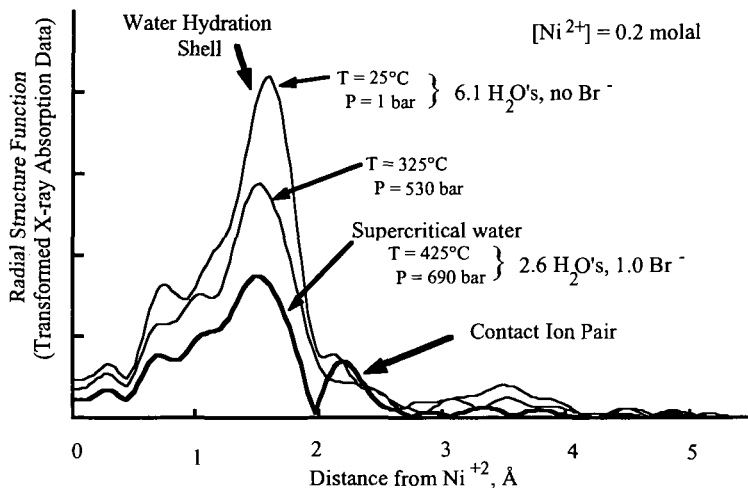


Figure 2. Radial structure around Ni^{2+} ions in supercritical water and the evolution of the Br^- contact ion pair. Distances are not corrected in this figure for the XAFS phase shift but the corrected distances are reported in the following tables.

Table 1. De-hydration of cations/anions in SC Water $[\text{M}^{n+}] = 0.2 \text{ m}$

Ion	Ambient		Supercritical			
	Number of nearest waters	Distance of nearest waters	Temp. °C	Number of nearest waters	Distance of nearest waters	% De-hydration
Rb^{1+}	5.6	2.93 Å	425	3.6	--	36%
Br^{1-}	7.1	3.35 Å	425	2.8	3.39 Å	60%
Sr^{2+}	7.3	2.60 Å	385	3.6	--	51%
Ni^{2+}	6.1	2.06 Å	425	2.6	2.095 Å	57%

Table 2. Hydration and contact-ion pair structure of Ni^{2+} in ambient, subcritical and supercritical water from Ni and Br XAFS measurements. $[\text{NiBr}_2] = 0.2 \text{ molal}$, $[\text{NaBr}] = 0.8 \text{ molal}$.

°C	Density, g/cm^3	Ni^{2+} Hydration / Br^{1-} Hydration ^a			$\text{NiBr}_n^{(2-n)}$ Structure		
		Number $\text{H}_2\text{O}'\text{s}$	Distance $\text{H}_2\text{O}'\text{s}$, Å	σ^2 , $\times 10^{-3} \text{ \AA}^2$	Number Br^{1-}s	Distance Br^{1-}s , Å	σ^2 , $\times 10^{-3} \text{ \AA}^2$
25	1.05	5.9/7.1	2.062/3.36	5.9/28	0.0	--	--
325	0.81	^b ---/4.6	^b -----/3.29	^b ---/28	1.1	2.55	11
425	0.65	1.0/4.3	2.091/3.31	3.2/43	3.3	2.405	12

^a Error associated with nearest neighbor numbers is approximately ± 0.3 , error associated with distance is approximately $\pm 0.05 \text{ \AA}$, and error associated with σ^2 is ± 0.003

^b The Ni XAFS was not measured for this concentration.

HYDROTHERMAL DECARBOXYLATION OF RCO_2H STUDIED BY REAL-TIME VIBRATIONAL SPECTROSCOPY

T. B. Brill, A. J. Belsky and P. G. Maiella
Department of Chemistry
University of Delaware
Newark, DE 19716

Water at high pressure and high temperature (the hydrothermal environment) is wide spread in the Earth's crust. On the ocean floor the high density of water leads to hot water "black smoker" vents which were first discovered in 1979 on the deep-sea Pacific rift zones.¹ Mineral-laden fluid H_2O flows at temperatures of about 350°C under pressures determined by hydrostatics, e.g. 270 atm at a depth of 2500 meters.^{2,3} At these conditions, H_2O maintains a single fluid phase. A large amount of organic chemical synthesis occurs in the shear layer where the hot vent water interfaces with the cooler sea water.⁴ These unusual conditions thermodynamically drive alterations of relatively simple, but universally important molecules such as H_2 , CO , CO_2 , H_2S , NH_3 , CH_4 and H_2O , to synthesize larger molecules,⁵⁻⁷ such as various carboxylic acids,^{6,8,10} amino acids,⁶ aldehydes¹¹ and metal carboxylate complexes¹². Feeding on the resulting organic compounds, a complex ecosystem ranging from single cell species to large invertebrates develops in the vicinity of these vents¹³⁻¹⁵ and, thus, the synthesis of small organic molecules in the hydrothermal regime is thought to have contributed to the origin of life.^{14,16,17}

Underlying these fascinating and profound issues is a series of basic questions in thermodynamics and kinetics. A large body of measurements and analyses in the references cited above particularly support the notion that thermodynamics is the main driving force for the synthesis of small organic molecules in the hydrothermal environment. On the other hand, it appears that, by comparison, relatively few kinetic considerations have been incorporated into reactions of small organic and inorganic molecules under conditions particular to hydrothermal vents. Instead, most hydrothermal and supercritical water kinetic measurements and analyses have been driven by biomass conversion¹⁸⁻²¹ and waste stream remediation technologies.²²

Hydrothermal vents involve transient phenomena in which temperature gradients exist in the shear layer and where turbulent mixing occurs. As such, kinetic phenomena are likely to be very important factors. The vast majority of kinetic and mechanistic studies of alterations of organic compounds in the hydrothermal medium are based on analysis of products after cooling a tube reactor that was heated in the batch mode or by post-reaction analysis of products from a flow reactor. Comparatively fewer kinetic and mechanism data have been obtained spectroscopically during the reaction, especially in the flow mode.²³⁻³⁴ This method, however, provides an unprecedented level of detail about hydrothermal chemical reactions.

The focus of this talk is on recent work dealing with the kinetics and mechanism of decarboxylation of carboxylic acids in real-time at hydrothermal conditions.^{30,33,34} Such studies augment previous work on kinetics conducted by other experimental methods.^{10,35}

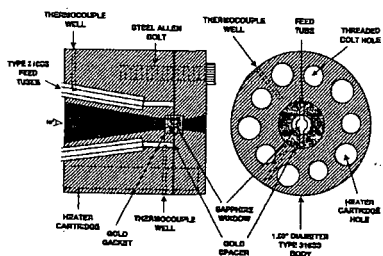


Fig. 1. The flow cell used for real-time IR at hydrothermal conditions.

The experimental methods used in this work are described elsewhere in detail.^{25,27,32} The short-path length IR flow cell is shown in Fig. 1 and is connected to a flow control apparatus that precisely maintains the temperature ($\pm 1^\circ\text{C}$), pressure (± 1 atm) and flow rate (0.01 - 1 ml/min). The resulting residence times in kinetic regime studied are 1-60 sec. These devices enabled a variety of kinetic and mechanistic details to be uncovered that would be opaque in the batch mode where determinations are made at longer times and by post-reaction analyses.

Wall-Assisted Decarboxylation. The clearest evidence that the reactor surface could assist or catalyze the decarboxylation reaction was obtained with formic acid, HCO_2H .³³ Figure 2 shows the rate of formation of CO_2 from a 1.00 M HCO_2H solution as a single phase at 310°C . Two batches of 316 stainless steel (SS) gave somewhat different results but, at least initially, not much different from 90/10 Pt/Ir. Titanium gave a much slower rate of CO_2 formation. These results strongly suggest that the reactor wall can affect the rate of decarboxylation of HCO_2H .

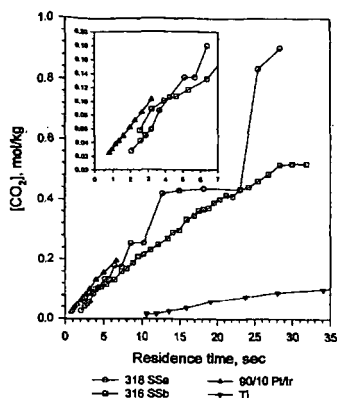


Fig. 2. The concentration of CO_2 from decomposition of $1.00 \text{ M HCO}_2\text{H}$ at 310°C and 275 atm as a function of residence time in four types of cell materials.

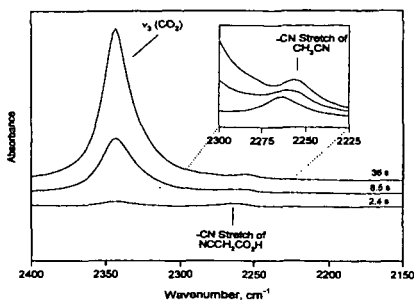


Fig. 3. A time series of IR spectra for $1.00 \text{ M NCCH}_2\text{CO}_2\text{H}$ at 220°C under 275 atm in the 316 SS flowcell. Conversion by reaction (1) is indicated.

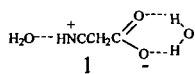
Homogeneous Phase Decarboxylations. The mechanisms of hydrothermal reactions of organic compounds in H_2O solution can be expected to depend on the functional groups attached to the reactive site. This subject has not been investigated previously and was established by the use of the SS and Ti cells in Fig. 1 and with another higher volume cell by Raman spectroscopy.^{30,34} Derivatives of acetic acid were used for this work RCO_2H ($\text{R} = \text{CCl}_3^-$, CF_3^- , CF_3CH_2^- , $\text{HOC}(\text{O})\text{CH}_2-\text{NH}_2\text{C}(\text{O})\text{CH}_2-$, NCCH_2- , and $\text{CH}_3\text{C}(\text{O})-$). All of these substituents are electron-withdrawing which accelerates the decarboxylation reaction. Relatively small effects were induced by the material of construction (SS or Ti) of the cell. The R group on the other hand exerted a pronounced effect on the rate of decarboxylation, which is described at least initially by reaction 1. Figure 3 illustrates



reaction 1 when $\text{R} = \text{NCCH}_2-$ in which the reactant $-\text{CN}$ stretch, product $-\text{CN}$ stretch (CH_3CN), and CO_2 can all be spectrally observed simultaneously. The spectral absorbance can be integrated to obtain the concentrations at all times. Figure 4 is a first-order rate plot for the decarboxylation of $\text{NCCH}_2\text{CO}_2\text{H}$ at 275 atm and the temperatures shown. These data can, of course, be expressed in the Arrhenius form.³⁴ When kinetic constants of this type are determined for all of the substituted acetic acids, the rates or Arrhenius parameters failed to correlate with common linear free energy relations, such as the electronic Hammett or Taft parameters.³⁶ On the other hand, the use of the expanded Taft equation 2 produced useful results. Equation 2 expresses the steric, E_s , and electronic, σ^* , substituent parameters weighted by the adjustable variables ρ and δ in terms of the rate constants, k , normalized to that of acetic acid, k_0 , measured at the same conditions. Figure 5 shows that these categories of compounds separate. The line shown represents the fit for $\rho = 1.5$ and $\delta = -3.6$. The

$$\ln(k/k_0) = \delta E_s + \rho \sigma^* \quad (2)$$

larger absolute value of δ indicates that the steric effect of R is somewhat more important in the rate than the electronic effect. This finding is consistent with structure 1 in which H_2O polarizes the carboxylate group, rather than structure 2 in which H_2O acts as a nucleophile, because the steric bulk of R should impede the reaction in the latter case.



Another category of compounds in Fig. 5 arises when $\text{R} = \text{HOC}(\text{O})\text{CH}_2-$ and $\text{NH}_2\text{C}(\text{O})\text{CH}_2-$. These compounds react faster than expected and probably do so as a result of their ability to form the cyclic transition state structure 3. This structure facilitates the unimolecular pathway of decarboxylation. When $\text{R} = \text{CF}_3-$, Fig. 5 shows the rate of decarboxylation is slower than expected from the substituent effect. The CF_3- group impedes the process probably because the hyperconjugative interaction shown in structure 4 strengthens the C-C bond.

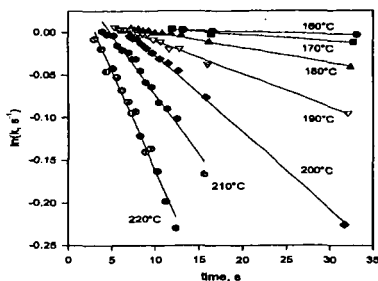


Fig. 4. First-order rate plot of decarboxylation of $\text{NCCH}_2\text{CO}_2\text{H}$ at 275 atm.

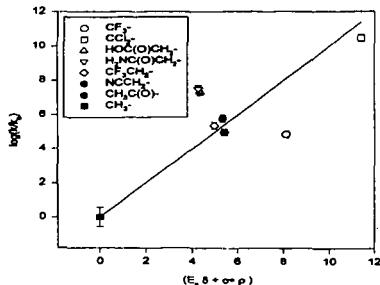
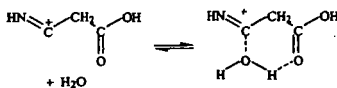
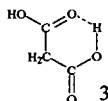


Fig. 5. A Taft plot for decarboxylation of RCO_2H at 200°C and 275 atm.



5

The Effect of pH. Strecker synthesis is believed to provide easy access to α -amino and α -hydroxyl carboxylic acids in the early life forming process.³⁷ In this reaction, NH_3 and HCN react with aldehydes and ketones to form the α -amino and α -hydroxy organonitriles that react with H_2O to form the carboxylic acid. Our study of $\text{NCCH}_2\text{CO}_2\text{H}$ ³⁴ decarboxylation raised a question about the conditions by which H_2O reacts with the $-\text{CN}$ group. To this end, the kinetics of decomposition of $\text{NCCH}_2\text{CO}_2\text{H}$ in 0.3-1.0N HCl was conducted at 150-260°C under 275 atm pressure. The mechanism worked out is shown in Fig. 6. Channel A occurs in the absence of acid as is discussed above. Channels B, C and D are opened by the presence of HCl and channel A does not occur. Hence, the presence of acid makes the $-\text{CN}$ group more reactive than the $-\text{CO}_2\text{H}$ group while the reverse is true in neutral solution. The probable reason is that the $-\text{CN}$ group is protonated by acid which facilitates nucleophilic attack by H_2O as shown in structure 5.

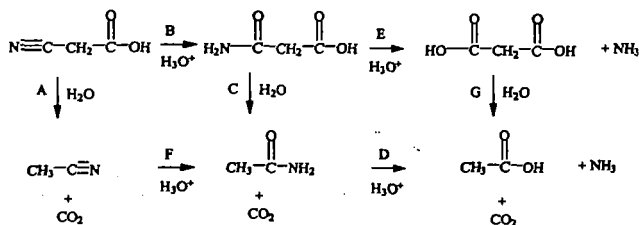


Fig. 6. The pathway of decarboxylation and deamination of $\text{NCCH}_2\text{CO}_2\text{H}$ determined in the hydrothermal regime.

In conclusion, real-time IR and Raman spectroscopy during hydrothermal reactions provides experimentally-based, mechanistic details about hydrothermal reactions under conditions of interest in geothermal vents and in waste steam remediation. Several different types of molecule-dependent decarboxylation mechanisms are uncovered for the seemingly simple reaction 1. In some cases H_2O appears to play a key role whereas in others it does not.

Acknowledgments. We are grateful to the Army Research Office for support of this work on DAAG55-98-1-0253 and to the NSF for support on CHE-9807370.

References

1. RISE Project Group (Spiess, F. N. et al.) *Science*, **207**, 1421 (1980).
2. Rona, P. A.; Bostrom, K.; Laubier, L.; Smith, K. L., Eds. *Hydrothermal Processes at Sea Floor Spreading Centers*, Plenum, NY (1984).
3. Haymon, R. M. and Macdonald, K. C. *Am. Sci.* **73**, 441 (1985).
4. Shock, E. L. *Origins of Life and Evolution of the Biosphere* **22**, 67 (1992).
5. Shock, E. L. *Origins of Life and Evolution of the Biosphere* **20**, 331 (1990).
6. Shock, E. L. *Geochim. Cosmochim. Acta* **54**, 1175 (1990).
7. Shock, E. L. and Helgeson, H. C. *Geochim. Cosmochim. Acta* **54**, 915 (1990).
8. Lundegard, P. D. and Kharaka, Y. K. In *Chemical Modeling of Aqueous Systems II* (ed. D. C. Melchior and R. L. Bassett); *Amer. Chem. Soc. Symp. Series* **416**, 169 (1990).
9. Shock, E. L. *Geochim. Cosmochim. Acta* **57**, 3341 (1993).
10. Pittman, E. D. and Lewan, M. D., Eds. *Organic Acids in Geological Processes*, Springer-Verlag, Berlin, 1994.
11. Schulte, M. D. and Shock, E. L. *Geochim. Cosmochim. Acta* **57**, 3735 (1993).
12. Shock, E. L. and Koretsky, C. M. *Geochim. Cosmochim. Acta* **59**, 1497 (1995).
13. Felbeck, H. and Somero, G. N. *TIBS*, **201** (1982).
14. Brock, T. D. *Science* **23**, 132 (1985).
15. Lutz, R. A.; Shank, T. M.; Fornari, D. J.; Haymon, R. M.; Lilley, M. D.; Von Damm, K. L.; Desbruyeres, D. *Nature* **371**, 663 (1994).
16. Wächtershäuser, G. *Prog. Biophys. Molec. Biol.* **57**, 75 (1992).
17. Huber, C. and Wächtershäuser, G. *Science* **276**, 245 (1997).
18. Katritzky, A. R.; Allin, S. M.; Siskin, M. *Accs. Chem. Res.* **29**, 399 (1996).
19. Mishra, V.; Mahajani, V. V.; Joshi, J. B. *Ind. Eng. Chem. Res.* **34**, 2 (1995).
20. Savage, P. E.; Gopalan, S.; Mizan, T. I.; Martino, C. J.; Brock, E. E. *AIChE J.* **41**, 1723 (1995).
21. Ding, Z. Y.; Frisch, M. A.; Li, L.; Gloyna, E. F. *Ind. Eng. Chem. Res.* **35**, 3257 (1996).
22. Tester, J. W.; Holgate, H. R.; Armellini, F. J.; Webley, P. A.; Killilea, W. R.; Hong, G. T.; Barner, H. E. In *Emerging Technology in Hazardous Waste Management III*; Tedder, D. W., Pohland, F. G., Eds., *ACS Symposium Series 517*; American Chemical Society: Washington, D.C., 1993, pp. 35-75.
23. Masten, D. A.; Foy, B. R.; Harradine, D. M.; Dyer, R. B. *J. Phys. Chem.* **97**, 7557 (1993).
24. Ryan, E. T.; Xiang, T.; Johnston, K. P.; Fox, M. A. *J. Phys. Chem.* **100**, 9395 (1996).
25. Kieke, M. L.; Schoppelrei, J. W.; Brill, T. B. *J. Phys. Chem.* **100**, 7455 (1996).
26. Schoppelrei, J. W.; Kieke, M. L.; Brill, T. B. *J. Phys. Chem.* **100**, 7463 (1996).
27. Schoppelrei, J. W.; Kieke, M. L.; Wang, X.; Klein, M. T.; Brill, T. B. *J. Phys. Chem.* **100**, 14343 (1996).
28. Schoppelrei, J. W. and Brill, T. B. *J. Phys. Chem.* **101A**, 2297 (1997).
29. Schoppelrei, J. W. and Brill, T. B. *J. Phys. Chem.* **101A**, 8593 (1997).
30. Maiella, P. G. and Brill, T. B. *J. Phys. Chem.* **100**, 14352 (1996).
31. Maiella, P. G. and Brill, T. B. *Inorg. Chem.* **37**, 454 (1998).
32. Belsky, A. J. and Brill, T. B. *J. Phys. Chem.*, **102A**, 14509 (1998).
33. Maiella, P. G. and Brill, T. B. *J. Phys. Chem.*, **102A**, 5886 (1998).
34. Belsky, A. J. and Brill, T. B. *J. Phys. Chem.*, submitted.
35. Bell, J. L. S.; Palmer, D. A.; Barnes, H. L.; Drummond, S. E. *Geochim. Cosmochim. Acta* **58**, 4155 (1994).
36. Unger, S. H. and Hansch, C. *Prog. Phys. Org. Chem.* **12**, 91 (1976).
37. Cronin, J. R. and Chang, S. *The Chemistry of Life's Origin*, J. M. Greenberg and V. Pirronella, eds., Kluwer Academic Publ. Dordrecht, The Netherlands, 1993, p. 209.

REACTIVITY OF MONOCYCLIC AROMATIC COMPOUNDS UNDER HYDROTHERMAL CONDITIONS

T. M. McCollom and J. S. Seewald
Woods Hole Oceanographic Institution
MS #4
Woods Hole, MA 02540
e-mail: tmccollom@whoi.edu

INTRODUCTION

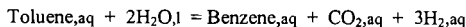
In recent years, there has been an increasing awareness among geochemists that aqueous reactions may play a significant role in the thermal maturation of organic matter in geologic environments (1,2). There are several ways in which water may enhance the reactivity of organic compounds, including serving as a solvent for reactions or participating directly as a reactant in the process. Understanding the role of aqueous reactions in the maturation of organic matter can be substantially improved by examining the reactivity of individual model compounds in laboratory experiments. We will present results from experimental studies on the hydrothermal reactivity of monocyclic aromatic compounds (MAC; benzene, toluene, phenol, cresols, etc.). These compounds are particularly suitable for such studies because MAC have relatively high aqueous solubilities and represent a significant fraction of the organic matter found in geologic environments.

EXPERIMENTAL

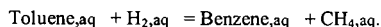
The experiments were conducted in a flexible-cell hydrothermal apparatus (3) using a gold reaction cell with titanium fittings. The reaction cell was equipped with a valve that allowed subsamples to be taken during the course of the experiment, so that the progress of the reactions could be followed over time. Experiments were carried out at either 300° or 330°C and 350 bars. Aqueous solutions of the compound to be studied were either loaded in the cell before heating or injected through the valve after an equilibration period. Assemblages of iron oxide and sulfide minerals were also included within the reaction cell. The intent of including these minerals is two-fold: first, to buffer the oxidation state of the system, and, second, to provide potential catalytic surfaces similar to those typically found in geologic environments. Mineral assemblages used in the experiments included pyrite-pyrrhotite-magnetite (PPM), hematite-magnetite-pyrite (HMP) and hematite-magnetite (HM).

RESULTS AND DISCUSSION

The principal reaction products from heating aqueous solutions of toluene were benzene and CO₂ (Figure 1). Other identified reaction products included phenol, benzoic acid, and cresols. Trace amounts of methane and other hydrocarbons were also observed, but these compounds appeared to derive from small amounts of organic matter in the minerals and not from toluene. Benzene and CO₂ were produced in a one-to-one ratio, suggesting that the formation of benzene from toluene proceeded by an oxidative decarboxylation reaction pathway:



rather than by demethylation:

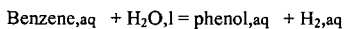


Benzoic acid appears to be an intermediate product of this reaction.

Aqueous solutions of benzoic acid decomposed rapidly during heating to benzene and CO₂ (plus minor phenol and toluene; Figure 2). Production of benzene from benzoic acid was much more rapid than the production from toluene, indicating that the formation of benzoic acid is the rate-limiting step in the reaction pathway from toluene to benzene.

None of the experiments conducted to date have shown any evidence for the decomposition of the aromatic ring from MAC. In all cases, the aromatic moiety from the original compound can be accounted for among the reaction products and remaining reactant. Thus, it appears that the aromatic ring is highly persistent under hydrothermal conditions, and reactions are limited to transformations among MAC with different substituent groups on the aromatic ring.

Comparisons of the relative concentrations of reaction products with predicted equilibrium ratios based on the thermodynamic properties of individual compounds indicates that reactions among several MAC compounds may rapidly approach equilibrium. For instance, equilibrium ratios of benzene to phenol predicted for the reaction



agree closely with the measured ratios in the experiments (Figure 3), suggesting that this reaction equilibrates very rapidly at the experimental temperatures. Consequently, it appears that the relative concentrations of benzene and phenol were controlled by chemical equilibrium between the compounds as the experiments progressed (note that this is strictly a *metastable* equilibrium, since both compounds should decompose almost completely to a mixture of CO₂ and methane as stable thermodynamic equilibrium of the system is approached). The possibility that other pairs of MAC compounds (e.g. toluene/cresols, toluene/benzene) may also reach equilibrium proportions is being investigated in ongoing experiments.

CONCLUSIONS

The experimental results demonstrate that monocyclic aromatic compounds readily undergo reactions in aqueous solutions at elevated temperatures, and indicate that these reactions mostly involve transformations among MAC with different substituent groups. The reactivity of MAC implies that similar reactions may play a large role in controlling the relative proportions of these compounds in geologic environments such as petroleum reservoirs and hydrothermal systems. Furthermore, the results suggest that the relative proportions of benzene and phenol (and perhaps other MAC) may be controlled by metastable equilibrium reactions taking place in the aqueous phase and involving water as a reactant. Since these reactions involve oxidation/reduction, the relative amounts of benzene and phenol in geologic environments should reflect the oxidation state of the system.

REFERENCES

- (1) Lewan, M. D., *Geochim. Cosmochim. Acta*, **61**, 3691-3723 (1997).
- (2) Helgeson, H. C., Knox, A. M., Owens, C. E., and Shock, E. L., *Geochim. Cosmochim. Acta*, **57**, 3295-3339 (1993).
- (3) Seyfried, W. E., Jr., Janecky, D. R., and Berndt, M. E., in *Hydrothermal Experimental Techniques*, Edited by Ulmer, G. C. and Barnes, H. L., John Wiley and Sons, pp. 216-239 (1987).
- (4) Johnson, J.W., Oelkers, E.H., Helgeson, H.C., *Comput. Geosci.* **18**, 899-947 (1992).
- (5) Dale J. D., Shock, E. L., MacLeod G., Aplin A. C. and Larter S.R. *Geochim. Cosmochim. Acta*, **61**, 4017-4024 (1997).
- (6) Shock, E.L., Helgeson, H.C., and Sverjensky, D.A., *Geochim. Cosmochim. Acta*, **53**, 2157-2183 (1989).
- (7) Shock, E.L. and Helgeson, H.C., *Geochim. Cosmochim. Acta*, **54**, 915-945 (1990).

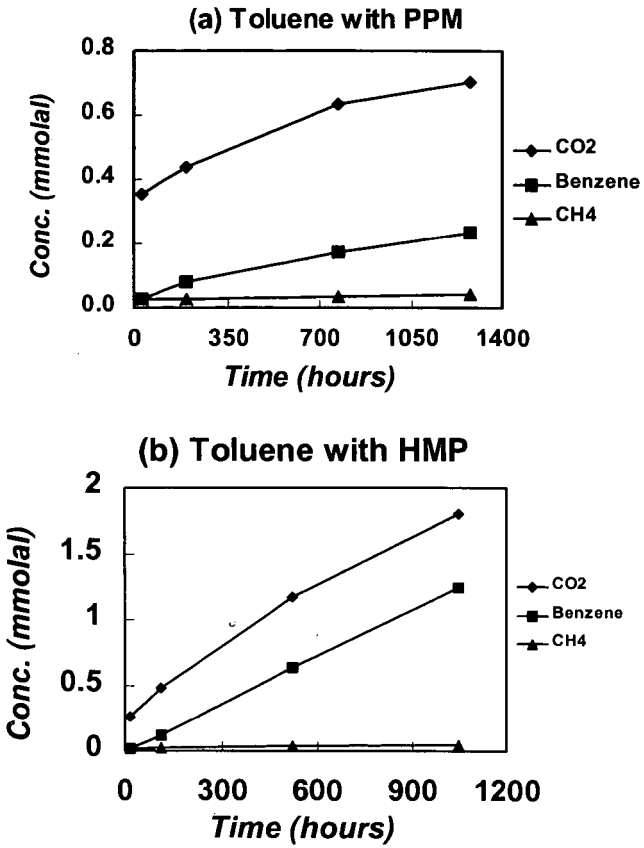


Figure 1. Selected reaction products from heating aqueous solutions of toluene at 330°C in the presence of the mineral assemblages (a) PPM and (b) HMP.

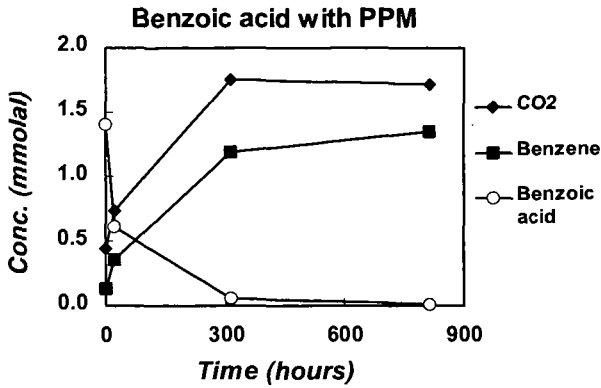


Figure 2. Selected reaction products from heating an aqueous solution of benzoic acid at 330°C in the presence of the mineral assemblage PPM.

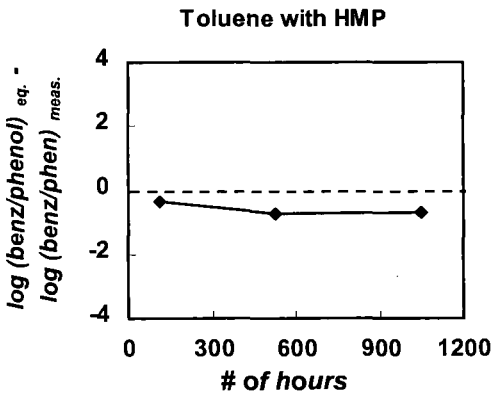


Figure 3. Difference between the predicted equilibrium ratio for benzene to phenol and the measured ratio for reaction products following heating of an aqueous solution of toluene at 330°C in the presence of the mineral assemblage HMP. Note that ratios are given on a log scale. Equilibrium ratios calculated using SUPCRT (4) with thermodynamic data from references 5,6 and 7.

High Pressure Hydrothermal Chemistry of Citric Acid and Related Acids

George D. Cody, Jennifer G. Blank, Jay Brandes, Robert Hazen, and Hatten Yoder, Jr.,

Geophysical Laboratory
Carnegie Institution of Washington
5251 Broad Branch Road, NW
Washington, DC 2001

Abstract High pressure hydrothermal reactions were run using sealed gold tube reactors and an internally heated high pressure apparatus. The reaction conditions varied from 150 to 350° C and from 0.5 to 5.0 Kb. The effects of pressure on a wide range of reactions was clearly evident and in some cases counter intuitive. Although high pressure clearly favored hydration reactions, decarboxylation reactions were greatly accelerated. In the system pyruvic acid - water, the chemistry was dominated by Aldol and Diels-Alder cycloaddition chemistry leading to a broad array of functionalized aromatic molecules which exhibited micellar qualities. The system citric acid - water yielded an interesting reaction network characterized by a number of isomeric equilibria. The effects of pressure operated on displacing the various equilibria towards specific isomers. The effects of pH on the citric acid chemistry also had significant control on metastable equilibria. These results are being integrated into a larger study of the feasibility of biochemistry emerging from the intrinsic organic chemistry associated with hydrothermal vents.

Experimental

All reactions were run in sealed (welded) gold tube reactors. Pressure and temperatures of interest were obtained using an internally heated high pressure apparatus. Following reaction, samples were quenched. Each sample was weighed before and after reaction to ensure sample integrity. Samples tubes were immersed in vials of BF₃/propanol, a known quantity of pentadecane was added as a standard, and heated at 90 °C for 1 hr. to esterify products. The derivitized products were extracted in dichloromethane, dried over NaSO₄, and analyzed with gas chromatography with mass spectrometric detection.

Results and Discussion

In order to better understand the potential for organic synthesis and the feasibility of biochemical reactions under extremes of pressure and temperature characteristic of deep sea hydrothermal vents we have begun to explore the high pressure aqueous chemistry of a number of potentially relevant biochemicals. In particular we have sought to address the question of whether metabolism recapitulate biogenesis, i.e. we are focusing on establishing whether the various metastable equilibria among the principal components of the tricarboxylic acid cycle favor anabolic synthesis at high pressures and temperatures. The results presented below involve high-pressure hydrothermal experiments probing the reactions and stability of pyruvic acid and citric acid, respectively, in CO₂ - H₂ bearing aqueous fluids in the temperature range of 150-350 °C and 0.5 to 5.0 Kbar. At this stage our principal focus is in identifying the effect of pressure on reaction selectivity in systems that exhibit multi-channel reactions. Towards this end, we have focused on two relatively simple systems in order to gain fundamental information on the kinetics of reactions that typify biological processes, albeit under strictly abiotic conditions. The data derived will provide a foundation for subsequent work on the potential for abiotic synthesis of classically bio-organic compounds at extremes of temperature and pressure, conditions that typify deep ocean hydrothermal vents.

In the pyruvic acid system we set out to determine whether pressure would favor the synthesis of oxaloacetic acid through an electrophilic addition of CO₂ at elevated temperatures. Thus far, have not revealed any evidence for the synthesis of oxaloacetic acid. Other interesting reactions, however, are operative within this pressure and

temperature regime. We observe substantial product yields from three reaction channels operating in series and parallel. One of these channels yields appreciable quantities of the five carbon diacid, methyl succinic acid, that forms through a cascade of reactions moving (evidently) through a number of intermediates. There is evidence that this reaction may be concerted (Figure 1). The reaction pathway is superficially similar to the citric acid cycle with the exception of the initial step; i.e. the initial step involves the formation of an Aldol condensation product rather than an electrophilic addition reaction.

A second reaction channel involves the straightforward de-carboxylation of pyruvic acid and is not particularly interesting beyond helping to establish the limits of pyruvic acid stability. On the other hand, the third reaction channel produces a very interesting and complex suite of compounds with amphiphilic qualities (Figure 2). This particular reaction channel operates, in general, through sequential Aldol condensations, Diels-Alder cyclo-additions, decarboxylations, dehydrations, dehydrogenations, and/or hydro-genations. Significant and systematic pressure and temperature induced changes in the distribution of molecules within this suite are observed.

In general, we observe that pyruvic acid is destabilized with increases in temperature and pressure, leading to the formation of the aforementioned products. Clearly evident are pressure effects manifested in the yields of methyl succinic acid and within the amphiphilic suite of compounds.

The system citric acid in CO_2 - H_2 bearing aqueous fluids is equally interesting. As would be expected, the principal reactions involve mono, double, and triple decarboxylations; with and without dehydration, as well as hydrogenation (Figure 3). The product distributions exhibit strong temperature and pressure selectivity (Figure 4). In general the citric system under the range of conditions explored exhibits catabolic chemistry. This is due, principally the apparent irreversibility of acid catalyzed decarboxylations. Surprisingly, pressure enhances the kinetics of these reactions, thus greatly accelerates the catabolic evolution of the system. The citric acid system, does however, serve as a useful and relatively simple system to explore the role of pressure in essentially pure ionic aqueous organic chemistry.

Acknowledgements

Support from NASA is gratefully acknowledged.

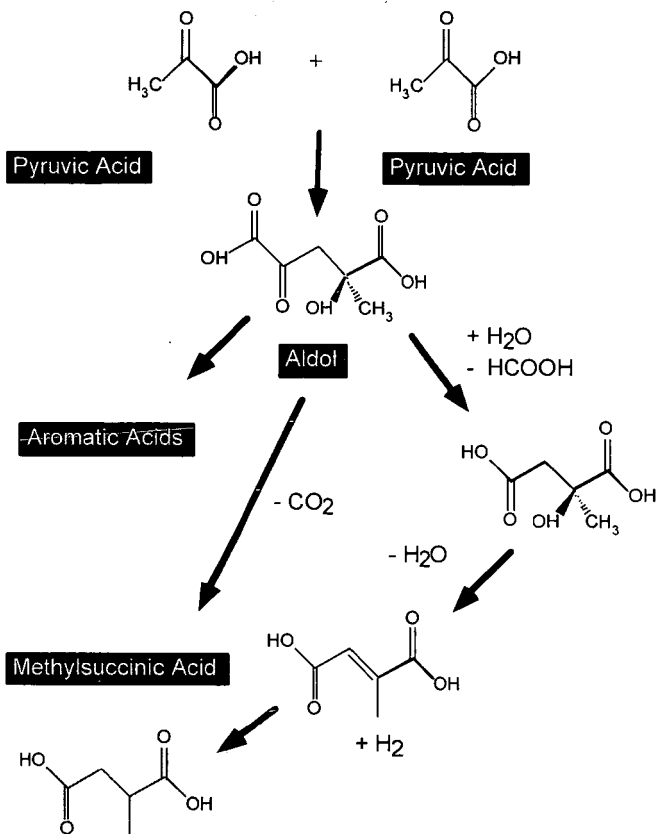


Figure 1: Reaction pathway through which pyruvic acid forms methyl succinic acid. The lack of observation of any of the intermediates suggests a concerted reaction.

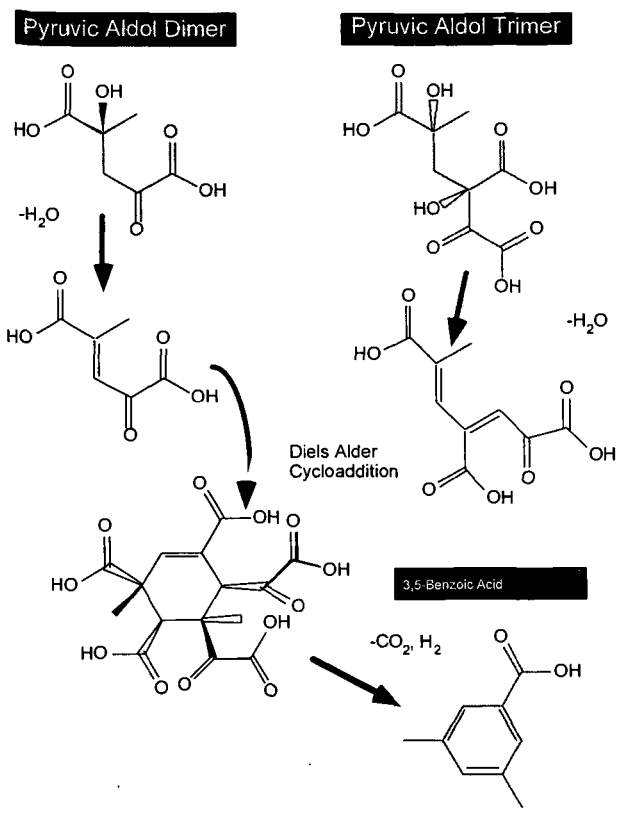


Figure 2: An example of one of many anabolic reactions exploited by pyruvic acid at elevated pressures and temperatures.

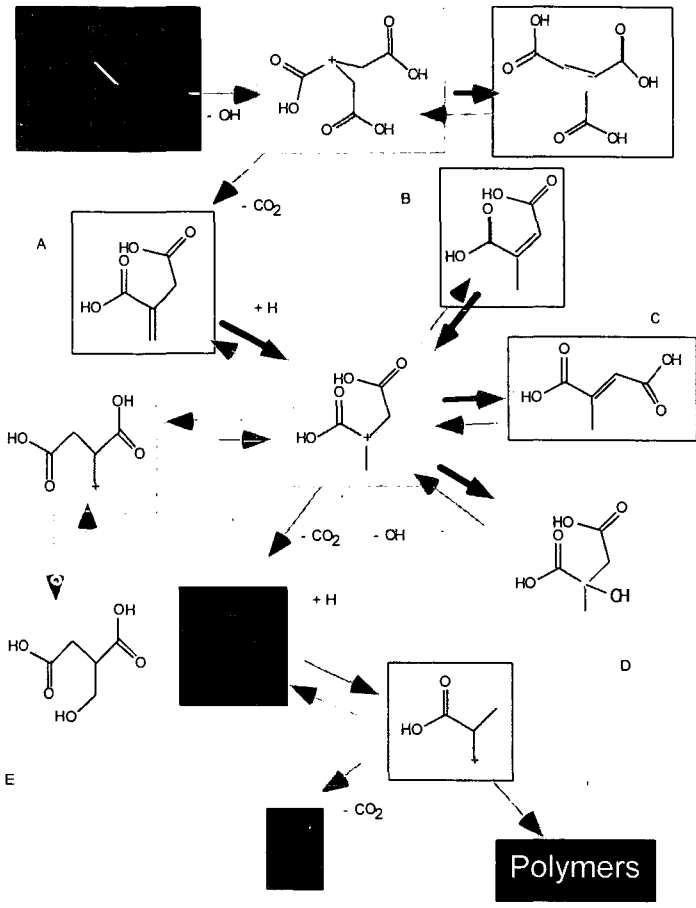


Figure 3: A schematic of the reaction network operational in the system citric acid + water at elevated temperatures and pressures.

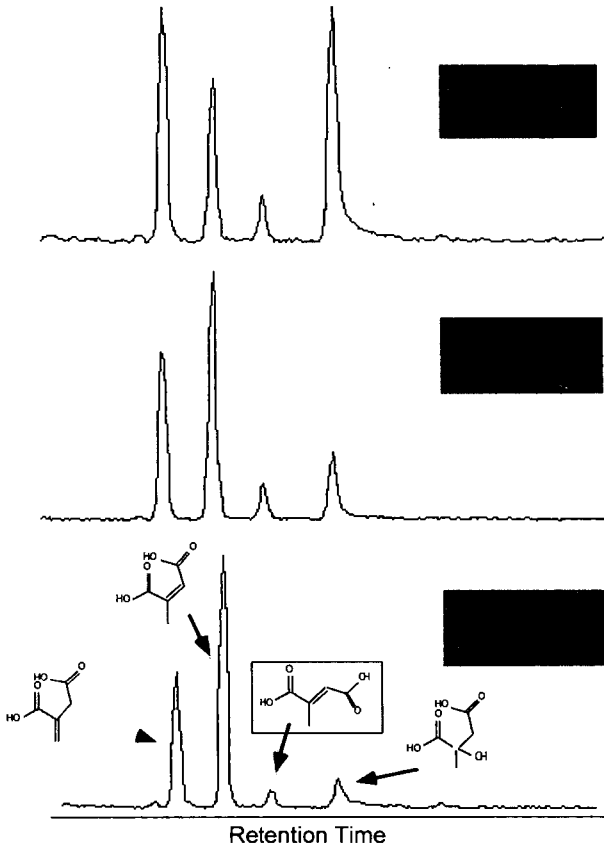


Figure 4: An example of the effect of pressure on displacing the isomeric equilibria within the system citric acid + water. Not surprisingly pressure greatly favors hydrated species.

REACTIONS OF MODEL COMPOUNDS OF PHENOL RESIN IN SUB- AND SUPER-CRITICAL WATER

H. Tagaya, K. Katoh, M. Karasu, J. Kadokawa and K. Chiba
Department of Materials Science and Engineering, Yamagata University
4-3-16 Jonan, Yonezawa, Yamagata, 992-8510 Japan

Key words: Supercritical Water, Chemical Recycling of Polymer, Phenol Resin

INTRODUCTION

The critical temperature and pressure of water at supercritical conditions are 647.2K and 22.1 MPa, respectively. The dielectric constant, ion product, and viscosity of the water at the critical point are 6, 10-12(Kw:(mol)²), and 0.002, respectively. Under supercritical conditions, water, organic compounds and gases are completely miscible. Furthermore, it is pointed out that the supercritical water is emerging as a medium which could provide the optimum conditions for a variety of chemical reactions among them the destruction of hazardous waste.

In recent years, the amounts of waste plastics increase and it becomes a serious problem because of lack of landfill field. The chemical recycling of waste plastics into their monomers has been gaining greater attention as a means of obtaining valuable products from waste plastics. The plastics are classified into thermoplastic resin and thermosetting resin. In the case of thermoplastic resin such as polyesters and polyamide, chemical recycling process has been reported. However, chemical recycling process for thermosetting resin wastes such as phenol resin waste has not been yet reported. Recently, we have communicated our findings on chemical recycling process for thermosetting resin wastes such as phenol resin waste (1-3). We have been studying on decomposition of polymeric compounds such as cellulose in water at supercritical conditions. In this study to obtain information of the role of water on chemical reaction of phenol resin waste, we have tried the decomposition reaction of model compounds of phenol resin such as p- and o-bis(hydroxyphenyl)methane, and various prepolymers.

EXPERIMENTAL

Decomposition reaction in water was carried out in 10 ml tubing bomb reactor. The reactants such as p- and o-bis(hydroxyphenyl)methanes were commercially available in a purity of 98% or higher and were used without further purification. 0.1g of model compound and 1 - 4 ml of water were introduced in the reactor. The reaction temperatures were 523 to 703K and reaction times were 0.25 to 1h. Reaction products were extracted by ether. The organic phase was concentrated using an evaporator. It was dissolved with organic solvent after adding a standard. The reaction products were identified by GC/MS and quantified by GC with a flame ionization detector (FID). In the case of GC/MS, the oven temperature was held at 333K for 3 min at initial stage. After then the oven temperature increased from 333K to 493K at a rate of 10K/min. The final temperature was maintained for an additional 6 min. In the case of GC the oven initial temperature was 403K and the oven temperature increased 503K at a rate of 10 K/min. The final temperature was maintained for an additional 6 min. Basic compound such as NH₄OH, NaOH, KOH, Na₂CO₃ was added.

RESULTS AND DISCUSSION

Decomposition reaction of model compounds in supercritical water

It is well known that thermal cleavage of methylene bond is not easy. However, we have found that methylene bond was cleaved in the reaction of phenol resin model compound with supercritical water. In the reaction of p-bis(hydroxyphenyl)methane, it was decomposed to their monomers such as phenol, p-cresol, o-cresol and 2,4-dimethylphenol. To obtain information on the reaction mechanism of decomposition reaction in water, p-bis(hydroxyphenyl)methane (compound 1), o-bis(hydroxyphenyl)methane (compound 2), diphenylmethane (compound 3), di-p-tolylmethane (compound 4), dibenzyl (compound 5) were reacted at 573 to 703K for 1h. However, model compounds 3, 4 and 5 were scarcely decomposed even by the reaction at 703K for 1 h. Compounds 1 and 2 easily decomposed in the reaction with supercritical water. It was considered that the presence of hydroxyl groups was essential for the decomposition reaction. We have tried to add phenol in the reaction of compound 3, however, no acceleration of decomposition reaction was observed. It indicates that the reactant

itself should possess hydroxyl groups. Model compound 1 decomposed into monomers such as phenol, p-cresol, o-cresol, and 2,4-dimethylphenol at 703K. Also, we have confirmed the productions of benzaldehyde and p-dihydroxybenzene by the reaction at 573K for 0.25h, although the yields of them were small. They were unstable at high temperature and the presence of them were not confirmed by the reactions at over 623K. The results suggested the direct participation of water as a reactant in the decomposition. Model compound 2 decomposed into their monomers such as phenol, p-cresol, o-cresol and so on. The production of xanthene was also confirmed. Phenol and cresol were main products. Xanthene was undesirable dehydrated product of compound 2. Even in the neat reaction at 703K for 0.25h, the yield of xanthene reached 20.2% although the yield of phenol was only 7.4%. Although conversion of compounds 1 and 2 reached more than 70% at 703K for 1h, the yield of identified products was less than 50%, indicating the presence of unidentified products. We confirmed the presence of trimer of phenol by the GC/MS analysis of water soluble products although we could not quantify. It indicated the presence of condensation reactions.

The effect of hydrogen donor, tetralin on the decomposition reaction

If the decomposition reaction proceeded via radical intermediates, the addition of hydrogen donor should be effective to avoid the condensation reaction. Therefore, hydrogen donor, tetrahydronaphthalene(tetralin), was added to the reaction of compounds 1 and 2 with water. The addition of tetralin for the decomposition reaction of compound 2 was effective. Although the yields of phenol and xanthene were 10.3% and 18.4% at 703K for 0.5h, they became 32.9% and 2.0% by the addition of tetralin. Xanthene was stable in supercritical water.

The addition of tetralin was effective to prevent the production of xanthene. However, the addition of tetralin was not effective for the decomposition reaction of compound 1. Position of hydroxyl groups was important for the decomposition reaction.

The effect of the addition of acid and alkali salt

The addition of hydrogen donor was not effective for the decomposition reaction of compound 1 indicating that radical reaction was not so important. If the ionic decomposition reactions occurred, the addition of acid or alkali salts might be effective to avoid the condensation reaction. The addition of acid was not effective for the reaction of compounds 1 and 2. However, the addition of alkali salts was effective and the yields of reaction products increased on the reactions of compounds 1 and 2. The addition of Na_2CO_3 or NaHCO_3 was more effective than the addition of NH_4OH , NaOH , KOH or K_2CO_3 . In the case of the compound 2, the yields reached more than 60% at 703K for 0.5h and yield of xanthene decreased by the addition of Na_2CO_3 . These results indicated that the reaction proceeded via the ionic processes. It was considered that both ionic radical reactions occurred in the decomposition reaction of compound 2. Even by the addition of small amounts of Na_2CO_3 or NaHCO_3 , a total yield of phenol and cresol reached 50% at 673K for 0.25h when additive/model compound ratio was 0.02. For the yields of phenol in the decomposition reactions, 0.1% was the best among these concentrations.

The effect of the addition of NaCl

To obtain information on the mechanism of the effects of alkali salt addition, neutral salt, NaCl was added. The yield of phenol in the reaction of compound 1 increased from 7.0% to 11.0% at 703K for 0.25h by the addition of NaCl. It is well known that the addition of NaCl increased the density of water at near supercritical region. The increment of the yield was not large. It indicates that the role of Na_2CO_3 was not only to increase water density.

The effect of water density

Decomposition reactions were carried out by varying the injection amounts of water from 1 ml, 2 ml to 4 ml. A yield of products increased for the decomposition reactions of compounds 1 and 2 and yield of xanthene decreased with an increase of injection amounts of water. In the reaction in 4 ml of water, a yield of products also increased by the addition of Na_2CO_3 although the increment of the yield by the addition was small. The large effect of water on the decomposition reaction indicated that the density was important factor for the decomposition of compounds 1 and 2 in these reaction conditions.

Decomposition reaction of prepolymer of phenol resin

Seven prepolymers whose molecular weights were 247-923 were reacted with supercritical water at 703K for 0.5h. Prepolymers were kindly provided by Dainippon Ink & Chemicals Co., Ltd, and their exact compositions were unknown. Main decomposition products from prepolymers A and C were phenol and p-isopropylphenol. It indicated that prepolymers A and C were isopropylphenol resins. Also the main decomposition products from prepolymers F and G were o-cresol, p-cresol and 2,4-dimethylphenol. It indicated that they were cresol resins.

Based on the model compound studies, decomposition reactions of prepolymers were carried out by adding 1wt% Na₂CO₃ for prepolymer. The yields fairly increased in the case of isopropylphenol resins, prepolymers A and C, and yields of phenol reached 48.9% and 58.0%. The total yields of identified products reached more than 90%. Certainly, reactivities of prepolymers were larger than those of compounds 1 and 2.

Conclusions

In this study we have clarified that water is excellent solvent for the decomposition reaction of phenol resin containing methylene bridges. The addition of tetralin was effective for the decomposition reaction of bis(o-hydroxyphenyl)methane. The yields of products increased and yield of xanthene decreased by the addition of tetralin. The addition of alkali salts was effective for the decomposition reactions of bis(p-hydroxyphenyl)methane and bis(o-hydroxyphenyl)methane. The significant increment of the yield was observed by the addition. It was suggested that the density was important factor for the decomposition of phenol resin model compounds such as bis(o-hydroxyphenyl)methane and bis(p-hydroxyphenyl)methane in these reaction conditions. Acceleration mechanism of alkali salts addition for the reaction was not clear, however, effective decomposition of model compounds and prepolymers of phenol resin was attained by the reaction with supercritical water, especially in the conditions adding alkali salt.

REFERENCES

1. H. Tagaya, Y. Suzuki, J. Kadokawa, M. Karasu, K. Chiba, Chem. Lett., 1997, 47.
2. H. Tagaya, Y. Suzuki, T. Asou, J. Kadokawa, K. Chiba, Chem. Lett., 1998, 937.
3. H. Tagaya, K. Kato, J. Kadokawa, K. Chiba, Polym. Degra. Stab., in press.

EXPERIMENTAL INVESTIGATION OF ORGANIC COMPOUND STABILITY UNDER HYDROTHERMAL CONDITIONS

Mitchell D. Schulte

NASA Ames Research Center
Mail Stop 239-4
Moffett Field, CA 94035

Keywords: hydrothermal, organic compounds, experimental

ABSTRACT

Hydrothermal systems are the most likely locations on the early Earth for the emergence of life due to the abundant chemical energy inherent in the characteristic disequilibrium of these environments. Hydrothermal conditions are theoretically favorable for the formation and stability of organic compounds; we are investigating this hypothesis experimentally. Initial experiments with amino acids at 250°C and 250-350 bars have yielded ammonia, carbon dioxide and carboxylic acids as the main reaction products. While the amino acids decomposed rapidly, the ratios of the products remained constant during the course of the experiments, in agreement with field and experimental observations of other metastable organic states, as well as with calculated organic compound metastability. Further experiments are currently underway and the results will be presented.

INTRODUCTION

Hydrothermal systems are the most likely locations on the early Earth for the emergence of life (1-3). Because of the disequilibrium inherent in such dynamic, mixing environments, abundant chemical energy would have been available for formation of the building blocks of life. In addition, theoretical and experimental studies suggest that organic compounds in these conditions would reach metastable states, due to kinetic barriers to the formation of stable equilibrium products CO₂ and methane (4-7). The speciation of organic carbon in metastable states is highly dependent on the oxidation state, pH, temperature, pressure and bulk composition of the system. The goal of our research is to investigate experimentally the effects of a number external variables on the formation, transformation, and stability of organic compounds at hydrothermal conditions. We have begun work to attempt to control the oxidation state of simulated hydrothermal systems by using buffers composed of mineral powders and gas mixtures. We are also beginning to test the stability of organic compounds under these conditions. The experiments are being performed using a hydrothermal bomb apparatus at the U.S. Geological Survey in Menlo Park, CA (Figure 1) and a supercritical water oxidizer (SCWO; Figure 2) at NASA Ames Research Center in Moffett Field, CA.

EXPERIMENTAL

Initial experiments have been performed using the hydrothermal bomb set-up to test amino acid stability at 250°C and 250-350 bars. In order to attempt to control the oxidation state inside the experimental cells, we added mineral powders to sample cells, along with distilled, deionized water. Two different mineral assemblages were used in two different experiments; pyrite-pyrrhotite-magnetite (PPM) and iron-iron oxide (FeFeO). The cells were then sealed, heated, and pressurized. The bomb assemblies were rocked to ensure continual contact between the solution and fresh mineral surfaces, and the buffers were allowed to equilibrate over a period of weeks. Amino acids were then added to the reaction vessels, and the system was sampled at regular intervals.

The set-up available at NASA Ames Research Center for this work consists of a supercritical water oxidizer, or SCWO, previously used to oxidize waste organic matter to CO₂ and H₂O. Work is currently underway to restore the SCWO to operational status. A schematic diagram of the SCWO is shown in Figure 2.

Because the SCWO is a flow-through apparatus, we can simulate the dynamic mixing environment characteristic of hydrothermal systems. Solutions of differing compositions and temperatures can be combined to investigate the potential for organic compound synthesis or stability. The oxidation state will be controlled using gas mixtures, allowing evaluation of the catalytic effect of minerals which will be added to the reaction vessel.

PRELIMINARY RESULTS

In the experiments conducted using the hydrothermal bombs, the amino acids decomposed rapidly, but yielded ammonia, carbon dioxide and carboxylic acids as the main reaction products. The ratios of the products remained constant during the course of the experiments, in agreement with field and experimental observations of other metastable organic states^{4,6}, as well as with calculated organic compound metastability. Further experiments of this type are currently underway and the results will be presented, along with some preliminary results from our initial SCWO experiments.

ACKNOWLEDGMENTS

I would like to thank Sherwood Chang, James Bischoff, Robert Rosenbauer, Dahlia Chazan, Jennifer Blank and Kathy Cummins for their help with the U.S.G.S. experiments, and Maher Tliemat, Suresh Pisharody, John Fisher and Sherwood Chang for their efforts in setting up the SCWO at NASA Ames. Cindy Lerner and Sandra Pizzarello were instrumental in helping me obtain GC-MS analyses of amino acids. Thanks to George Cody and Mike Lewan for inviting me to contribute to this symposium.

REFERENCES

- (1) Baross, J. A.; Hoffman, S. E. *Orig. Life and Evol. Biosphere*. 1985, 15, 327- 345.
- (2) Corliss, J. B.; Baross, J. A.; Hoffman, S. E. *Oceanologica Acta*. 1981, No. Sp, 59- 69.
- (3) Holm, N. G. *Orig. Life and Evol. Biosphere*. 1992, 22, 5-14.
- (4) Shock, E. L. *Geology*. 1988, 16, 886-890.
- (5) Shock, E. L. *Orig. Life and Evol. Biosphere*. 1992, 22, 67-107.
- (6) Seewald, J. S. *Nature*. 1994, 370, 285-287.
- (7) Shock, E. L.; Schulte, M. D. *J. Geophys. Res.* 1998, in press.

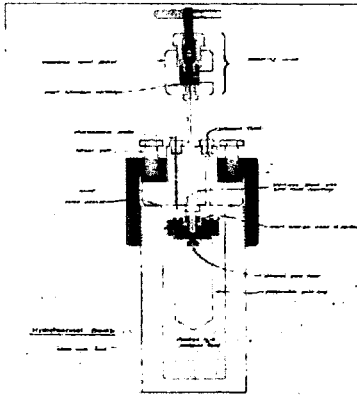


Figure 1. Schematic diagram of the hydrothermal bomb apparatus used for organic compound stability experiments.

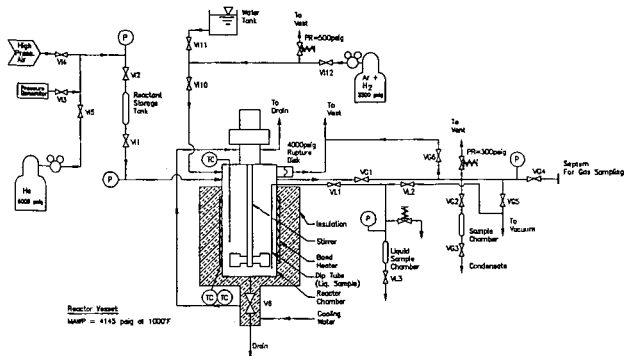


Figure 2. Schematic diagram of the supercritical water oxidizer (SCWO) used for organic compound stability experiments.

THE ROLE OF WATER DURING DECOMPOSITION OF OIL AT ELEVATED TEMPERATURES: CONSTRAINTS FROM REDOX BUFFERED LABORATORY EXPERIMENTS

Jeffrey S. Seewald¹ and Peter J. Saccocia²

¹Woods Hole Oceanographic Institution, MS#4, Woods Hole, MA 02543

²Bridgewater State College, Bridgewater, MA 02325

Keywords: Petroleum Geochemistry, Natural Gas, Hydrous Pyrolysis

INTRODUCTION

Oil and natural gas coexist with water and minerals in sedimentary basins. There is increasing evidence that inorganic chemical processes play a critical role in regulating organic reactions responsible for the generation of oil and its decomposition to form natural gas. In particular, water has been implicated as both a solvent and reactant during organic reactions at elevated temperatures and pressures (1,2,3). Moreover, the redox state of subsurface environments and the presence or absence of catalytically active transition metals may influence the absolute amounts and relative distribution of organic alteration products (2,4,5). Understanding the extent to which such processes affect the stability of petroleum at elevated temperatures is essential to predict the timing and location of natural gas formation.

The present study was undertaken to examine the stability of oil in the presence of water at elevated temperatures and pressures. Hydrous pyrolysis experiments have proven to be an effective tool for examining organic-inorganic interactions during oil and natural gas generation. Experimental apparatus utilized during conventional hydrous pyrolysis, however, results in the coexistence of source rocks, liquid water, floating oil, and volatile species occupying the pressure vessel head space at experimental conditions (6). As a result it is not always possible to distinguish whether secondary reactions involve gaseous, aqueous, or oil phase species. The experiments presented here were designed to minimize such uncertainties and allow a comparison of reactions involving oil dissolved in water with reactions taking place within a separate oil phase. Because organic reactions are influenced by their chemical environment, we used naturally occurring mineral assemblages to regulate key chemical variables such as redox, sulfur fugacity, and pH.

EXPERIMENTAL

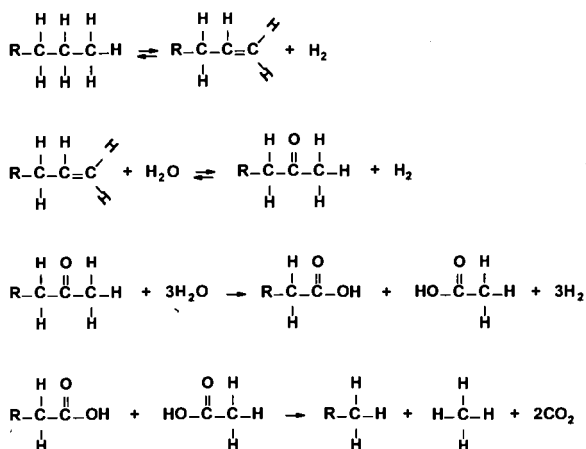
Two experiments examining the decomposition of a medium weight oil from Eugene Island block 330 in the U.S. Gulf Coast were conducted in a flexible-cell hydrothermal apparatus (7) consisting of a flexible gold and titanium reaction cell contained within a stainless steel pressure vessel. This equipment allows external control of pressure at sufficiently high values to preclude the formation of a vapor filled head space during an experiment. A titanium sampling tube connected to the reaction cell allows reaction progress to be monitored as a function of time by periodic extraction of fluid samples. Experiment PPM-AQ was conducted at 350°C and 350 bars and contained 37.2 g an aqueous Na-Mg-Cl solution and 52.9 mg of oil. The relatively small amount of oil in this experiment did not exceed the aqueous solubility of oil at 350°C and 350 bars (8) ensuring all reactions involved aqueous species. In contrast, experiment PPM-OIL was designed to maintain a separate oil phase floating on top of liquid water at experimental conditions. This experiment initially contained 13.3 g of aqueous Na-Mg-Cl solution and 10.7 g of oil. To allow sampling of both the oil and water the flexible-cell hydrothermal apparatus was modified to include two titanium sampling lines at opposite ends of the tubular reaction cell. By orienting the apparatus vertically, the aqueous phase could be sampled through the lower sampling line while the oil was sampled through the upper sampling line. Experiment PPM-OIL was initially conducted at 325°C and 350 bars but after 1130 h of heating the temperature was increased to 350°C.

To regulate redox and sulfur fugacity during the experiments a mineral assemblage containing equal amounts of pyrite, pyrrhotite, and magnetite were added to each experiment. In addition, brucite and amorphous silica were added to PPM-AQ and brucite was added to PPM-OIL to regulate *in situ* pH. Because the densities of the added minerals are greater than water and oil, the minerals resided within the aqueous phase at the bottom of the reaction cell during experiment PPM-OIL. Fluid samples were removed from the experiments at selected times and analyzed for the concentrations of CO₂, H₂, H₂S, inorganic anions and cations, and numerous organic species including C₁-C₆ hydrocarbons, alcohols, aldehydes, ketones, organic acids, and phenols.

RESULTS AND DISCUSSION

Heating of oil in the presence of water and inorganic minerals during both experiments resulted in extensive alteration of the oil and the generation of low molecular weight carbon compounds. In general, generation of dissolved gaseous products proceeded at a faster rate during PPM-AQ relative to PPM-OIL (Fig. 1) and produced dissolved gas containing a substantially higher proportion of CO₂ (Fig. 2). Examination of the dissolved gaseous hydrocarbon fraction reveals a significant enrichment in CH₄ during PPM-AQ relative to PPM-OIL (Fig. 3). Dissolved H₂ concentrations during PPM-AQ were consistent with values predicted for thermodynamic equilibrium between water and the pyrite-pyrrhotite-magnetite mineral assemblage. In contrast, measured H₂ concentrations in the aqueous phase of experiment PPM-OIL were higher than those predicted for equilibrium with a pyrite-pyrrhotite-magnetite mineral assemblage suggesting that the rate of H₂ generating reactions involving carbon compounds in the oil exceeded the rate at which the redox buffer consumed H₂. The higher H₂ concentrations during PPM-OIL in comparison to PPM-AQ indicate redox conditions were considerably more reducing during the PPM-OIL experiment.

Maturation of oil during experiment PPM-AQ also resulted in the continuous generation of substantial amounts of organic acids, ketones, and lesser, but measurable, quantities of alkenes. Production of these compounds is consistent with data from redox buffered experiments examining the stability of individual aqueous hydrocarbons under redox buffered conditions (2,9,10). These experiments have demonstrated the degradation of aqueous *n*-alkanes via a stepwise oxidative processes to produce CO₂ and CH₄. This process can be represented in general as follows:



Reactions in the above scheme that do not involve breaking of C-C bonds are reversible in aqueous solution and may approach a state of redox dependent metastable thermodynamic equilibrium (2,9,10). Under sufficiently reducing conditions the abundance of reaction intermediates decreases, resulting in an overall decrease in the rate of *n*-alkane decomposition. Accordingly, during experiment PPM-OIL, high H₂ produced relatively reducing redox conditions and lower amounts of CO₂ and CH₄ were generated. In the absence of extensive oxidative decomposition during experiment PPM-OIL, it is likely that decomposition of hydrocarbons residing in the oil phase occurred predominantly via thermal cracking to produce a relatively CH₄- and CO₂- poor gas.

The formation of natural gas is conventionally viewed as a two-step process in which kerogen maturation initially produces both oil and gas. Continued heating over geologic time and increasing temperatures associated with progressive burial subsequently results in the decomposition of generated oil to form natural gas. As discussed by Mango *et al.* (5), a purely thermal model for the cracking of *n*-alkanes cannot account for the generation of dry gas at geologically reasonable heating rates. The stepwise oxidation of aqueous *n*-alkanes, however, may represent an alternative mechanism to generate a CH₄-rich gas at relatively low thermal stress. For such a mechanism to be active in natural systems, however, suitable oxidizing agents are required. Likely candidates include sulfate minerals present in evaporites and commonly occurring sedimentary components containing ferric iron, such as pyrite, magnetite, hematite, and a variety of aluminosilicates. In addition to providing a mechanism for the generation of dry-gas at thermal maturities lower than those required for thermal cracking, the absence of a suitable oxidizing agent and/or water could preclude stepwise

oxidation and account for the persistence of oil in a variety of environments at temperatures higher than conventional models predict (11). The results presented here emphasize the fact that time and temperature are not the only variables influencing the stability of petroleum in sedimentary basins.

REFERENCES

- (1) Siskin, M. and Katritzky, A. R., *Science* **254**, 231 (1991).
- (2) Seewald, J. S., *Nature* **370**, 285 (1994).
- (3) Lewan, M. D., *Geochim. Cosmochim. Acta* **61**, 3691 (1997).
- (4) Helgeson, H. C., Knox, A. M., Owens, C. E., and Shock, E. L., *Geochim. Cosmochim. Acta* **57**, 3295 (1993).
- (5) Mango, F. D., Hightower, J. W., and James, A.T., *Nature* **368**, 536 (1994).
- (6) Lewan, M. D., in: *Organic Geochemistry* (eds. M. H. Engel and S. A. Macko.), 419 (1993), Plenum.
- (7) Seyfried, W. E. Jr., Janecky D. R., and Berndt M. E., in: *Experimental Hydrothermal Techniques* (eds. G. C. Ulmer and H. L. Barnes), 216 (1987), John Wiley and Sons.
- (8) Price, L. C., *J. Petrol. Geol.* **4**(2), 195 (1981).
- (9) Seewald, J. S., *Mat. Res. Soc. Symp. Proc.* **432**, 317 (1996).
- (10) Seewald, J. S., unpublished data.
- (11) Price, L. C., *Geochim. Cosmochim. Acta* **57**, 3261 (1993).

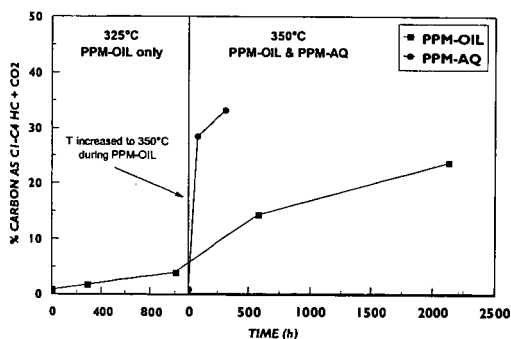


Figure 1. Variations in the percentage of carbon in the total oil as C_1 - C_4 hydrocarbons and CO_2 with time during experiments PPM-OIL and PPM-AQ. Note that only experiment PPM-OIL was initially conducted at 325°C.

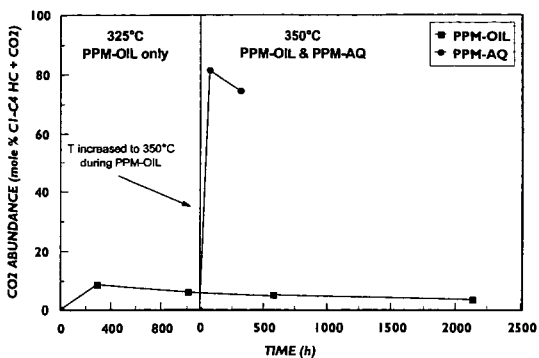


Figure 2. Variations in the relative abundance of CO₂ in the dissolved gas fraction (mole % of C₁-C₄ hydrocarbons and CO₂) as a function of time during experiments PPM-OIL and PPM-AQ. Note that only experiment PPM-OIL was initially conducted at 325°C.

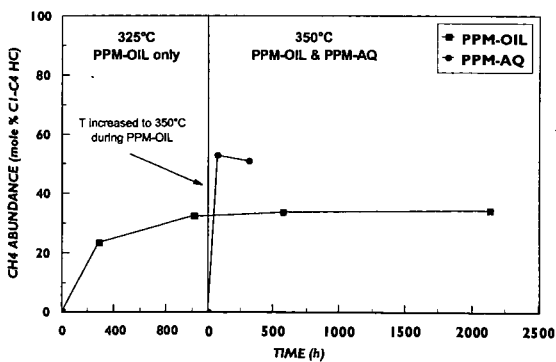


Figure 3. Variations in the relative abundance of CH₄ in the dissolved hydrocarbon gas fraction (mole % of C₁-C₄ hydrocarbons) as a function of time during experiments PPM-OIL and PPM-AQ. Note that only experiment PPM-OIL was initially conducted at 325°C.

RELEASE OF BIOMARKERS FROM SULFUR-RICH KEROGENS DURING HYDROUS PYROLYSIS

Martin P. Koopmans^{1,3}, Jaap S. Sinninghe Damsté¹ and Michael D. Lewan²

¹Netherlands Institute for Sea Research, Department of Marine Biogeochemistry and Toxicology, P.O. Box 59, 1790 AB Den Burg, Netherlands

²U.S. Geological Survey, Box 25046, MS 977, Denver Federal Center, Denver, CO 80225, USA

³Present address: (i) University of Oslo, Department of Geology, P.O. Box 1047 Blindern, 0316 Oslo, Norway, and (ii) Saga Petroleum ASA, P.O. Box 490, 1301 Sandvika, Norway

Keywords: hydrous pyrolysis, generation of biomarkers, S-rich kerogen

INTRODUCTION

Hydrous pyrolysis is an established laboratory technique for the simulation of the natural maturation of kerogen. There has been some debate in the literature whether water plays a purely physical or maybe a chemical role during hydrous pyrolysis (*e.g.* Monthieux *et al.*, 1986; Lewan, 1992). This issue has recently been reviewed by Lewan (1997). Mass balance calculations have shown that CO₂ generated during hydrous pyrolysis derives O from the water added before the experiment (Lewan, 1992). Hydrothermal experiments with ethane and ethene showed that water was a source of H₂ (Seewald, 1994). In addition, experiments with kerogen and heavy water suggested that the deuterated alkanes generated were formed by reaction of alkyl radicals with heavy water-derived D (Hoering, 1984). Thus, the current understanding is that water acts as a source of H to quench thermally generated alkyl radicals, thereby both forming saturated hydrocarbons and inhibiting cross-linking reactions which may lead to the formation of an insoluble pyrobitumen.

The thermal degradation of kerogen has been characterised as a two step process (Lewan, 1992). First, kerogen is partially decomposed to a polar-rich bitumen, which at higher temperatures decomposes to yield free hydrocarbons as thermal stress increases. This sequence was also recognised in a study of a S-rich sample from the Monterey Formation (Baskin and Peters, 1992). However, these observations were based on bulk quantities (*i.e.* kerogen, bitumen, and free hydrocarbons), and a similar sequence based on molecular data using biomarkers has not been clearly established. Here, we describe results of thermal maturation experiments designed to follow the kerogen degradation pathway at a molecular level using a biomarker approach. In addition, we have investigated the role of water by performing experiments in the absence and presence of water.

EXPERIMENTAL

Hydrous and anhydrous pyrolysis experiments (200-360°C; 72 h) were carried out with two sedimentary rocks containing immature sulfur-rich organic matter. Detailed descriptions of the experimental procedures can be found elsewhere (Koopmans *et al.*, 1996, 1998). One sample is a claystone from the Gessoso-solfifera Formation (Upper Miocene, northern Italy), with a TOC content of 2.0 wt.%. Its mineral composition consists of quartz, smectite, illite, chlorite, and dolomite. The other sample is a limestone from the Ghareb Formation (Upper Cretaceous, Jordan), with a TOC content of 19.6 wt.%. Its mineral composition consists almost exclusively of calcite with only minor amounts (<10 wt.%) of quartz and apatite.

RESULTS

The extract of the claystone contains saturated hydrocarbons and organic sulfur compounds (OSC) with mainly normal and isoprenoid alkane skeletons. In addition, the extract comprises a polar fraction which contains molecular aggregates consisting of predominantly isoprenoid and cyclic alkane skeletons linked by S- and O-bonds (Koopmans *et al.*, 1996). The kerogen has been desulfurised and consists mainly of normal, isoprenoid and cyclic alkanes (Schaeffer *et al.*, 1995; Putschew *et al.*, 1998).

Hydrous pyrolysis of the claystone generates large amounts of saturated hydrocarbons and OSC from thermal degradation of the kerogen and the polar fraction (Koopmans *et al.*, 1996). We were able to follow the kerogen thermal degradation pathway at a molecular level by monitoring the speciation of several biomarkers. C₃₇ and C₃₈ alkenones, for example, were present in an S- and O-bound form in the kerogen of the unheated claystone, while their carbon skeletons were absent in the extract. After hydrous pyrolysis at gradually increasing temperatures, these carbon skeletons are first released into the polar fraction, and then as free hydrocarbons, OSC and saturated ketones (Fig. 1; Koopmans *et al.*, 1997).

In order to elucidate the role of water during hydrous pyrolysis, we also conducted experiments in the absence of water (anhydrous pyrolysis). For the claystone, the results are quite dramatic. While hydrous pyrolysis generates large amounts of normal, isoprenoid and cyclic alkanes, anhydrous pyrolysis does not generate these compounds (Fig. 2). For the limestone, normal, isoprenoid and cyclic alkanes are generated in comparable amounts during hydrous and anhydrous pyrolysis, although during anhydrous pyrolysis destruction of alkanes at high temperatures seems to occur at an earlier stage (Fig. 2). In addition, desulfurisation of the polar fraction of the claystone heated at 200°C by anhydrous pyrolysis does not release any biomarkers, in contrast to hydrous pyrolysis. This strongly suggests that anhydrous pyrolysis is not capable of converting S-bound biomarkers in the polar fraction to free biomarkers.

DISCUSSION

Our results suggest that the presence of water and the mineral matrix play an important role in the generation of biomarkers from S-rich kerogens (cf. Fig. 2). Quantitative experimental studies by Huizinga *et al.* (1987a,b) showed that mineral matrix effects on hydrocarbon generation from powdered mixtures of kerogen and minerals were more extreme under anhydrous than hydrous pyrolysis, especially when smectite was the employed mineral. In addition, they found evidence that the combined effect of smectite and a high organic S content leads to increased degradation of bitumen generated from the kerogen. Thus, the combination of smectite and a high organic S content for the claystone in our study may explain the large differences observed between the claystone and the limestone.

The actual mechanism and reactions responsible for smectite inhibiting the generation of biomarkers under anhydrous conditions and not under hydrous conditions remain to be determined. The greater availability of clay mineral interlayers to bitumen under anhydrous pyrolysis may be important, because under anhydrous pyrolysis these interlayers are probably less hydrated than under hydrous pyrolysis. Huizinga *et al.* (1987a) showed that adsorption of the polar constituents of bitumen to smectite was enhanced during anhydrous pyrolysis. For our experiments, this would imply that the polar fraction of the claystone, which contains abundant S-bound biomarkers, would be adsorbed to these clay minerals during anhydrous pyrolysis. Once inside the clay mineral interlayers, the high contact area of mineral surface to organic matter may favor cross-linking reactions that form an insoluble pyrobitumen rather than cracking reactions that form free hydrocarbons. This is supported by our desulfurisation experiments, which showed that S-bound biomarkers in the claystone were destructed during anhydrous at 200°C.

Thus, during anhydrous pyrolysis, the biomarker thermal generation sequence described above, *i.e.* (i) bound moiety in the kerogen, (ii) bound moiety in the polar fraction, (iii) free biomarker, is hindered because no biomarkers are generated from the polar fraction. This explains the differences in the amounts of S-bound biomarkers during hydrous and anhydrous pyrolysis of the claystone, and consequently also the differences in generation of free biomarkers (i) between hydrous and anhydrous pyrolysis of the claystone, and (ii) between anhydrous pyrolysis of the claystone and the limestone.

CONCLUSIONS

Our experiments show that the thermal degradation of kerogen to bitumen to free biomarkers can be monitored on a molecular level. Water is essential in releasing biomarkers from S-rich kerogens, especially when clay minerals are present. The exact chemical role that water plays, however, remains to be determined.

ACKNOWLEDGEMENTS

The Natural Resources Authority of Jordan is gratefully acknowledged for their assistance in helping the authors collect a sample of the Ghareb Formation from the El Lajjun quarry. Analytical assistance was provided by F. Carson, M. Dekker, W.I.C. Rijpstra and Dr W.G. Pool.

REFERENCES

- Baskin, D.K. and Peters, K.E., 1992, Early generation characteristics of a sulfur-rich Monterey kerogen: AAPG Bulletin, v. 76, pp. 1-13.
- Hoering, T.C., 1984, Thermal reactions of kerogen with added water, heavy water and pure organic substances: Organic Geochemistry, v. 5, pp. 267-278.
- Huizinga, B.J., Tannenbaum, E. and Kaplan, I.R., 1987a, The role of minerals in the thermal alteration of organic matter - III. Generation of bitumen in laboratory experiments: Organic Geochemistry, v. 11, pp. 591-604.

- Huizinga, B.J., Tannenbaum, E. and Kaplan, I.R., 1987b, The role of minerals in the thermal alteration of organic matter - IV. Generation of *n*-alkanes, acyclic isoprenoids, and alkenes in laboratory experiments: *Geochimica et Cosmochimica Acta*, v. 51, pp. 1083-1097.
- Koopmans, M.P., de Leeuw, J.W., Lewan, M.D. and Sinninghe Damsté, J.S., 1996, Impact of dia- and catagenesis on sulphur and oxygen sequestration of biomarkers as revealed by artificial maturation of an immature sedimentary rock: *Organic Geochemistry*, v. 25, pp. 391-426.
- Koopmans, M.P., Schaeffer-Reiss, C., de Leeuw, J.W., Lewan, M.D., Maxwell, J.R., Schaeffer, P. and Sinninghe Damsté, J.S., 1997, Sulphur and oxygen sequestration of *n*-C₃₇ and *n*-C₃₈ unsaturated ketones in an immature kerogen and the release of their carbon skeletons during early stages of thermal maturation: *Geochimica et Cosmochimica Acta*, v. 61, pp. 2397-2408.
- Koopmans, M.P., Rijpstra, W.I.C., de Leeuw, J.W., Lewan, M.D. and Sinninghe Damsté, J.S., 1998, Artificial maturation of an immature sulphur- and organic matter-rich limestone from the Ghareb Formation, Jordan: *Organic Geochemistry*, v. 28, pp. 503-521.
- Lewan, M. D., 1992, Water as a source of hydrogen and oxygen in petroleum formation by hydrous pyrolysis: *ACS, Div. Fuel Chemistry Preprints*, v. 37, No. 4, pp. 1643-1649.
- Lewan, M.D., 1997, Experiments on the role of water in petroleum formation: *Geochimica et Cosmochimica Acta*, v. 61, pp. 3691-3723.
- Monthieux, M., Landais, P. and Durand, B., 1986, Comparison between extracts from natural and artificial maturation series of Mahakam delta coals: in Leythaeuser, D. and Rullkötter J., eds., *Advances in Organic Geochemistry 1985*; *Organic Geochemistry*, v. 10, pp. 299-311.
- Putschew, A., Schaeffer-Reiss, C., Schaeffer, P., Koopmans, M.P., de Leeuw, J.W., Lewan, M.D., Sinninghe Damsté, J.S. and Maxwell, J.R., 1998, Abundance and distribution of sulfur- and oxygen-bound components in a sulfur-rich kerogen during simulated maturation by hydrous pyrolysis: *Organic Geochemistry*, in press.
- Schaeffer, P., Harrison, W.N., Keely, B.J. and Maxwell, J.R., 1995, Product distributions from chemical degradation of kerogens from a marl from a Miocene evaporitic sequence (Vena del Gesso, N. Italy): *Organic Geochemistry*, v. 23, pp. 541-554.
- Seewald, J.S., 1994, Evidence for metastable equilibrium between hydrocarbons under hydrothermal conditions: *Nature*, v. 370, pp. 285-287.

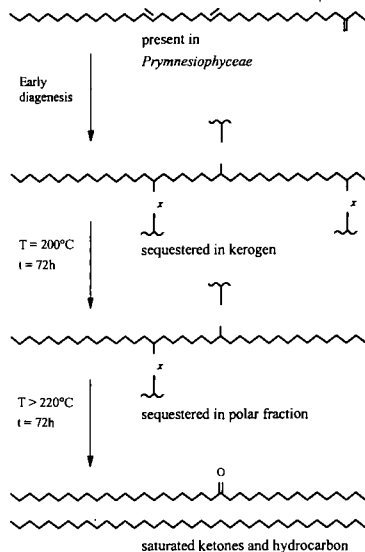


Fig. 1. Biomarker thermal generation sequence for C_{38} alkenone.

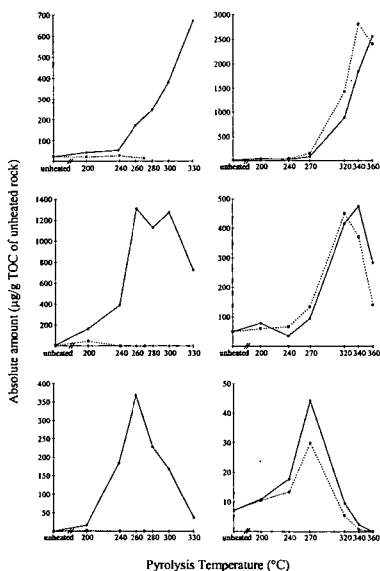


Fig. 2. Generation profiles of (a) octadecane, (b) phytane and (c) (20R)-5 α -24-ethylcholestane for the claystone and (d-f) limestone from hydrous (solid line) and anhydrous pyrolysis (stippled line) for 72 h. Anhydrous pyrolysis of the claystone does not generate biomarkers.

INVESTIGATING THE CONSTITUTION OF MACROMOLECULAR MATERIAL IN METEORITES USING HYDROUS PYROLYSIS

M. A. Sephton, C. T. Pillinger and I. Gilmour

Planetary Sciences Research Institute, Open University, Milton Keynes, MK7 6AA, UK
(m.a.sephton@open.ac.uk)

ABSTRACT

Carbon content analyses of hydrous pyrolysis residues of macromolecular material from the Murchison meteorite reveal that more than 55 % of macromolecular carbon is solubilised by this pyrolysis method. GC-MS analyses indicate that the majority of products are volatile one or two ring aromatic compounds.

Pyrolysis-GC-MS analyses of hydrous and anhydrous pyrolysis residues reveal that the macromolecular material contains a nitrogen-containing moiety. This organic entity is liberated by hydrous pyrolysis. It follows therefore that nitrogen-containing moieties may have been released from the macromolecular material during the aqueous alteration event known to have affected the Murchison meteorite parent body.

INTRODUCTION

Most meteorites are fragments of asteroids propelled into Earth-crossing orbits by relatively recent collisions in the asteroid belt (1). Asteroids, and therefore the meteorites derived from them, have escaped the extensive geological processing experienced on the planets. Due to this quiescent history meteorites contain primitive materials relatively unchanged since their formation of the solar system. The carbonaceous chondrites are especially primitive meteorites and excepting the most volatile elements, have a bulk composition similar to the Sun (2). These meteorites are particularly interesting to the organic cosmochemist as they contain up to several percent carbon which is present as organic matter.

Approximately 25 % of this organic matter is present as solvent-soluble or free molecules while the remaining 75 % is present as a solvent-insoluble macromolecular material (3). The soluble organic matter has been the most intensively studied of the two solubility classes and contains aliphatic hydrocarbons, aromatic hydrocarbons, amides, amines, nitrogen heterocycles, amino acids, carboxylic acids, sulphonic acids, phosphonic acids, alcohols and carbonyl compounds (3).

By comparison, the insoluble macromolecular material has been neglected. Pyrolytic release studies have revealed an empirical formula of $C_{100}H_{48}N_{1.8}O_{12}S_2$ for this organic component in the Murchison meteorite (4). It consists of condensed aromatic cores, connected by aliphatic and ether linkages and with various functional groups attached (5,6). Several techniques have been used to study the macromolecular material including infrared spectroscopy, nuclear magnetic resonance spectroscopy and pyrolysis (5,6).

Pyrolysis thermally dissociates macromolecular material in an inert atmosphere into lower molecular weight moieties. For meteorite research, most analyses of this type have utilised an on-line anhydrous pyrolysis unit directly coupled to a gas chromatograph or mass spectrometer (e.g. 5). Off-line hydrous pyrolysis requires that the heated samples are in contact with liquid water for the duration of the experiment and is used to simulate oil-generation from terrestrial rocks (7). This technique is conventionally performed on several hundred grams of sample (7,8) but has recently been scaled down to accommodate less than two grams of extraterrestrial sample (9).

As hydrous pyrolysis transforms the insoluble macromolecular material into free molecules, an obvious application of this technique is to investigate the relationships between the two organic solubility classes in meteorites. Previous authors have suggested that the free molecules in meteorites cannot be related to the macromolecular material because of the large isotopic differences between these two organic components (10). However isotopic measurements of individual free aromatic hydrocarbons and their structurally identical counterparts, released from the macromolecular material in the Murchison meteorite by hydrous pyrolysis, have revealed that they are related by an extraterrestrial degradative event (11). Whether more polar organic moieties are transferred between solubility classes in the extraterrestrial environment has not previously been established.

Here we report pyrolysis-gas chromatography-mass spectrometry (pyrolysis-GC-MS) and carbon content analyses of meteoritic macromolecular material in the Murchison meteorite both before and after hydrous pyrolysis. This information is used to further understand the yields and nature of the organic moieties liberated by the hydrous pyrolysis procedure. Furthermore, the implications of these analyses to reconstructing the extraterrestrial history of meteoritic organic matter are also considered.

EXPERIMENTAL

Hydrous pyrolysis. Full details of the hydrous pyrolysis method can be found in (9). The insoluble organic material in the Murchison meteorite was isolated by digesting the inorganic matrix with hydrofluoric (HF) and hydrochloric (HCl) acids and by removing any free organic compounds with solvent extraction (11). 136 mg of the HF/HCl residue was placed in a 1ml stainless steel insert and 0.4 ml of high purity water was added. The insert was then purged with nitrogen gas, sealed and placed into a 71 ml stainless steel high pressure reactor

(series 4740, Parr Instrument Co.) which was filled with 20 ml water. The whole arrangement was heated to 320 °C for 72 hours.

Supercritical fluid extraction. Hydrous pyrolysis products were extracted by supercritical fluid extraction (SFE). An initial static extraction with pure CO₂ (99.9995 %, 4000 psi) for 90 mins was followed by a dynamic extraction (4000 psi, 1 ml/min) for 45mins. The extract was collected in diethyl ether cooled to approximately 0 °C. These conditions produced an extract of non-polar compounds dissolved in a few 100 µl of solvent ready for immediate analysis.

Gas chromatography-mass spectrometry. Compound detection and identification was performed by gas chromatography-mass spectrometry (GC-MS) using a Hewlett Packard 5890 gas chromatograph interfaced with a 5971 mass selective detector. Analyses were by on-column injection onto a HP5 capillary column (50 m x 0.2 mm x 0.17 µm). Following a 10 min period at 25 °C the GC oven was programmed from 25 °C to 220 °C at 5 °C min⁻¹ and then from 220 to 300 °C at 10 °C min⁻¹. The final temperature was held for 12 min.

Anhydrous pyrolysis. Samples were prepared for comparisons with the pyrolysis-GC-MS analysis of the hydrous pyrolysis residue. Unheated and hydrously pyrolysed Murchison HF/HCl residue were subjected to off-line anhydrous pyrolysis. Samples were loaded into Pyrex glass tubes followed by the removal of air by purging the tube interior with N₂ gas. These tubes were then sealed and heated at 320 °C for 72 hours.

Pyrolysis-GC-MS. Samples were introduced as dry pellets (typically ca. 1 mg) into a quartz lined pyrojector (S.G.E, Ltd) held at 500 °C. Separation of the flash pyrolysis products was performed using a Hewlett Packard 5890 GC fitted with a Ultra2 capillary column (50 m x 0.2 mm x 0.32 µm). During a run, the GC oven was held at 50 °C for 1 min before a ramp was employed of 10 °C min⁻¹ to 100 °C and 5 °C min⁻¹ to 300 °C where it was held for 14 min. Detection and identification products was performed as for GC-MS.

RESULTS AND DISCUSSION

Fig. 1 shows GC-MS analyses of the hydrous pyrolysate from the Murchison HF/HCl residue. The main pyrolysis products are volatile aromatic and heteroatom-containing aromatic compounds with low molecular weights, suggesting that the majority of aromatic centres within the macromolecular material are small and consist of one or two aromatic rings. Sephton *et al.* (11) calculated a yield of 1.36 % of the high molecular weight starting material based on a solvent extract of the pyrolysate. Table 1 illustrates the carbon contents of the HF/HCl residues before and after the hydrous pyrolysis procedure. The values reveal that the amount of Murchison macromolecular carbon solubilised by hydrous pyrolysis is 55.3 %. Therefore, there is an obvious disagreement between the amount of carbon solubilised by hydrous pyrolysis and the amount of product measured by weighing a solvent extract dried under a stream of N₂. Hence, as indicated by the SFE extract, it appears that the majority of hydrous pyrolysis products from the Murchison macromolecular material are more volatile than the tricyclic PAHs. These volatile products are lost during conventional solvent extraction and evaporation steps, but are retained by SFE.

To investigate the change in the organic constitution of the macromolecular material brought about by the hydrous pyrolysis procedure, unheated Murchison HF/HCl residue and hydrous pyrolysis residue were analysed by pyrolysis-GC-MS (Fig. 2). Analyses of the hydrous pyrolysis residue indicate that some aromatic moieties do remain following the hydrous pyrolysis procedure. Although when compared to the pyrolysis-GC-MS trace for the unheated Murchison HF/HCl residue, it is apparent that much structural diversity has been lost.

To further investigate the nature of the process which liberates organic moieties from the macromolecular material during hydrous pyrolysis, pyrolysis-GC-MS analyses were performed for hydrously pyrolysed residues and samples pyrolysed anhydrously under comparable conditions. One noticeable difference between the two types of pyrolysis is the relative abundance of benzonitrile. This compound is present in small amounts in the unheated Murchison residue, is absent in the hydrously heated sample, but is abundant in the anhydrously heated sample. This suggests that the Murchison macromolecular material contains a substantial amount of organic nitrogen. The host of this organic nitrogen becomes more visible to pyrolysis-GC-MS following off-line anhydrous pyrolysis.

To confirm whether this nitrogen bearing organic component is removed by hydrous pyrolysis or simply hidden by a reaction with water, a hydrous pyrolysis residue was subjected to anhydrous pyrolysis. The residue from this process failed to produce benzonitrile during pyrolysis-GC-MS. Therefore it appears that the Murchison macromolecular material contains a nitrile precursor which is removed from the macromolecular material by hydrous pyrolysis. Nitriles in meteoritic organic matter have attracted some attention in the past due to the possibility that they may be the degradation products of amino acids, although other structures may degrade during pyrolysis to give these compounds. Possible candidates for the nitrile precursor include macromolecularly-bound amides (RCONH₂), imines (R₂CNR) and amino acids (RCH(NH₂)COOH).

Therefore, a nitrogen-containing moiety is transferred from the insoluble macromolecular material to soluble organic molecules by hydrous pyrolysis. These observations suggest that a CM macromolecule may release nitrogen-bearing organic compounds during aqueous alteration. As the Murchison macromolecule has already been subjected to pre-terrestrial aqueous alteration (12), it is reasonable to expect that communication of nitrogen containing organic matter between solubility classes occurred on the Murchison meteorite parent body. This suggestion is consistent with previous work which established that aromatic hydrocarbons have been released from the Murchison macromolecular material during a preterrestrial alteration event (11).

CONCLUSIONS

The majority of hydrous pyrolysis products of meteoritic macromolecular material are volatile, consisting of mono or diaromatic organic molecules. This suggests that meteoritic macromolecular material is comprised of one or two ring aromatic cores connected by aliphatic linkages and heteroatomic groups.

Pyrolysis-GC-MS analyses of pyrolysis residues indicate that a nitrogenous organic moiety is present in the Murchison macromolecular material. This organic unit is released by hydrous pyrolysis. Therefore it appears that some low molecular weight nitrogen-containing organic compounds in the Murchison meteorite may have been released from the macromolecular material during the aqueous alteration event that is known to have affected the Murchison parent body. This is further evidence that aqueous alteration on the meteorite parent body can exert a strong control on macromolecular material structure and can lead to interaction between organic solubility classes.

REFERENCES

- (1) G. W. Wetherill and C. R. Chapman, in *Meteorites and the Early Solar System System* (eds. J. F. Kerridge and M. S. Mathews, M.S.) 35 (Univ. Arizona Press, Tucson, 1988).
- (2) R. T. Dodd, *Meteorites: A Petrological Chemical Synthesis*. (Cambridge University Press, London, 1981).
- (3) J. R. Cronin and S. Chang, in *Chemistry of Life's Origins* (ed J. M. Greenburg) 209 (Kluwer, Dordrecht, 1993).
- (4) E. Zinner, in *Meteorites and the Early Solar System System* (eds. J. F. Kerridge and M. S. Mathews, M.S.) 956 (Univ. Arizona Press, Tucson, 1988).
- (5) R. Hayatsu, S. Matsuoka, R. G. Scott, M. H. Studier and E. Anders, *Geochim. Cosmochim. Acta*, 41, 1325 (1977).
- (6) J. R. Cronin, S. Pizzarello and J. S. Fyre, *Geochim. Cosmochim. Acta*, 51, 229 (1987).
- (7) M. D. Lewan, J. C. Winters and J. H. McDonald, *Science*, 203, 897 (1979).
- (8) M. D. Lewan, in *Organic Geochemistry: Principles and Applications* (eds. M. H. Engel and S. A. Macko) 419 (Plenum Press, New York, 1993).
- (9) M. A. Sephton, C. T. Pillinger and I. Gilmour, *Planet. Space Sci.*, in press.
- (10) R. H. Becker and S. Epstein, *Geochim. Cosmochim. Acta*, 34, 257 (1982).
- (11) M. A. Sephton, C. T. Pillinger and I. Gilmour, *Geochim. Cosmochim. Acta*, 62, 1821 (1998).
- (12) M. Zolensky, and H. Y. McSween, Jr. in *Meteorites and the Early Solar System* (eds. Kerridge J.F. and Mathews M.S.) 114 (Univ. Arizona Press, Tucson, 1988).

Table 1

% carbon of Murchison HF/HCl residue before and after hydrous pyrolysis	
Sample	Carbon (%)
Murchison HF/HCl residue	8.5
Hydrous pyrolysis residue	3.8

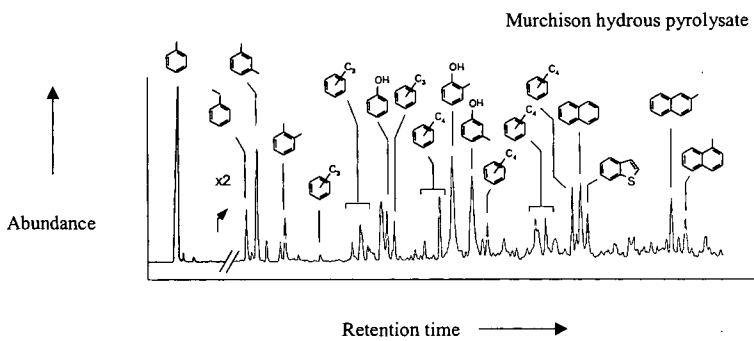


Figure 1. GC-MS analysis of the SFE extract of the hydrously pyrolysed HF/HCl residue from the Murchison meteorite. After Sephton *et al.* (1998).

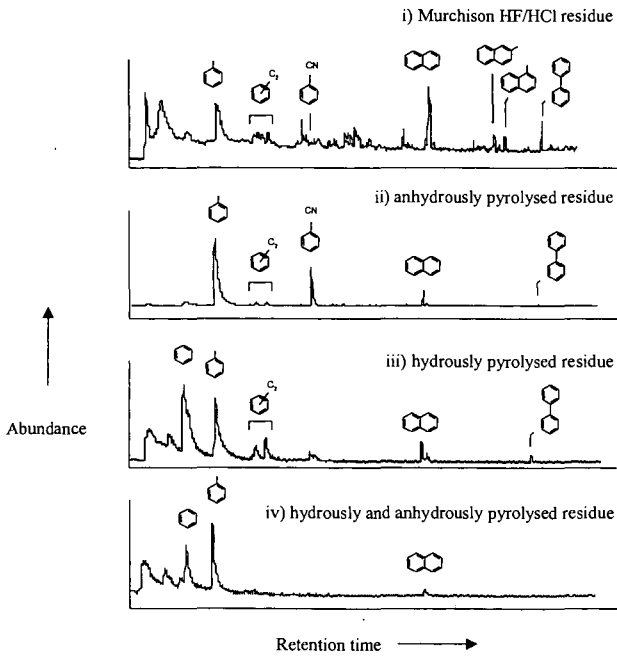


Figure 2. Pyrolysis-GC-MS analyses of i) the unheated Murchison HF/HCl residue, ii) anhydrously pyrolysed residue, iii) hydrously pyrolysed residue, and iv) hydrously and anhydrously pyrolysed residue.

EFFECT OF ACID ADDITION ON THE HYDROTHERMAL DECOMPOSITION OF CHITIN-DERIVED BIOMASS

Kinya Sakanishi¹⁾*, Nobuhide Ikeyama¹⁾, Tsuyoshi Sakaki²⁾, and Masao Shibata²⁾

1) Institute of Advanced Material Study, Kyushu University, Kasuga, Fukuoka 816-8580, JAPAN

TEL 81-92-583-7801 FAX 81-92-583-7797 E-mail: k-saka@asem.kyushu-u.ac.jp

2) Kyushu National Industrial Research Institute, Tosu, Saga 841-0052, JAPAN

ABSTRACT

Hydrothermal decomposition of chitin-derived biomass was carried out using a batch tube reactor or fixed bed flow reactor at 300 - 400 °C for 30 - 120 sec under the pressure of 15 - 30 MPa, in order to clarify the influences of solvation by pressurized water and acid addition on the hydrolysis reactivity. HPLC and TOF-MS analyses of the WS fraction indicated that the decomposition at 300 °C provided oligomer products of 3 to 6 units with a low yield of ca. 5 %. On the other hand, the higher temperature above 350 °C produced the WS fraction with the yield as high as 30 %, however, a large amount of degraded products with UV adsorption was contained in WS, suggesting the ring skeleton of the unit structure as well as the ether linkage between the unit structure should be cleaved under the sub- and supercritical conditions. The addition of acetic acid or formic acid (5 or 10 %) accelerated very much the hydrolysis reaction of chitin to oligomers at the lower temperature of 300 °C, the conversion being increased up to ca. 70 %, although the WS fraction gained its weight by the acid addition. It is pointed out that the control of pH in the acid solution and the dissociation of the aggregate structure in the chitin polymer through the solvation are keys to the enhancement of the hydrothermal decomposition of chitin.

Keywords: Hydrothermal decomposition, acidic hydrolysis, chitin biomass

INTRODUCTION

Chitin, next to cellulose, is one of the major two biomass resources on earth.¹⁻³ Chitin is a natural 1,4-linked polymer which has N-acetyl group at the C-2 position, while the cellulose has hydroxyl group at the same position of the monomer unit. Although chitin and cellulose have the similar skeleton structure, their crystal structure and polymer chain characteristics are completely different depending upon their origins.^{4,5}

Hydrothermal treatments under the sub- or supercritical conditions have been reputed to be efficient for the selective decomposition of biomass.^{6,7} The supercritical water ($T_c = 374$ °C, $P_c = 22$ MPa) accelerates the decomposition of the polymers to produce valuable monomers and clean fuel by shorter reaction times of a few seconds.^{8,9}

In a previous study,¹⁰ it was reported that chitin was much less reactive than cellulose despite their similar unit skeleton structures, probably because their functional groups at C₂ differ (-NHCOCH₃ for chitin; -OH for cellulose), and their structural analyses before and after the hydrothermal treatment indicate that their intra- and intermolecular structures through hydrogen bonds may be the keys to their different hydrothermal reactivities. It was also revealed that the decomposition of chitin under the supercritical water conditions brought about black char materials with increased gas formation, indicating that the ring cleavage of the unit structure should take place above 350 °C, and the supercritical water condition be not favorable probably due to poor solvation of chitin.

In the present study, the effect of acid addition the hydrothermal decomposition reactivity of chitin-derived biomass was examined in order to moderate the reaction conditions for the selective production of chitin oligomers. At the same time, a flow type reactor with the fixed bed of chitin was also designed for the suppression of the secondary decomposition of water soluble fraction.

EXPERIMENTAL

Chitin powder of ca. 100 μ m particle size (deacetylation extent: 38) was supplied by courtesy of Japan Health Summit: JHS Co., Ltd. Acetic acid, formic acid of guaranteed grade and bamboo acid solution supplied from Asia Instrument Co. (extract from the carbonized bamboo) were used as additives for the hydrothermal treatment of chitin.

The reactor used for the hydrothermal reactions was a tube reactor (SUS 316, 9.3 mm i.d. X 83 mm length, 6 mL capacity) equipped with a thermocouple, a valve, and a pressure gauge. 0.5 g of chitin and 3.0 g of distilled water were charged into the reactor, and the atmosphere in the reactor was replaced with nitrogen or carbon dioxide gas. Then, the reactor was sealed after nitrogen gas was pressurized to the prescribed initial pressure.

The reactor was heated in two steps using two salt baths which were heated at 250 °C and the prescribed reaction temperature, respectively. The reactor was preheated at 250 °C for 3 min and subsequently heated in the second bath for the prescribed time while shaking at ca. 250 times a minute. The heating rates at the preheating to 250 °C and to the reaction temperature were ca. 100 °C/min and 600 °C/min. After the prescribed soaking time, the reactor was immediately cooled in a water bath to quench the reaction. The reaction conditions were described by both the heating time in the second heater and the final temperature reached during the reaction period. In the case of hot-water flow reactor with a fixed bed, 1 g of chitin was loaded in the cylindrical bed equipped with 5 μ m ceramic filters at both ends, the atmosphere in the reactor system was replaced with N₂ gas, and pressurized to 5 MPa N₂. The preheated water at the prescribed temperature in salt bath was flowed at 10 ml/min, and the extracted fraction(WS) by pressurized hot water was continuously recovered for sampling.

The liquid and solid contents in the reactor were thoroughly washed with water and filtered using No.4 glass filter. The water in the filtrate was distilled off under vacuum, and the water soluble (WS) fraction was recovered. The filter residue was washed with methanol to recover the methanol soluble (MS) and the insoluble (MI) fractions by the removal of methanol and the drying under vacuum. WS, MS, and MI fractions were weighed and each product yield was calculated based on the dry substrate base. The target product of oligomers was fractionated into WS fraction. MS (water insoluble but methanol soluble) fraction include the larger molecular weight products and degraded products such as aromatic and color compounds which are not able to be analyzed by HPLC. MI(insoluble fraction both in water and methanol) is the mixture of the unreacted substrate and char-like residue. Such characteristics were previously reported.^{6,7}

The WS fraction was analyzed by HPLC equipped with two columns(SEC W12 and SEC W13, Yokogawa Co.) and two detectors of UV(254 nm) and RI(refractive index) in series. HPLC was operated at 40 °C with 0.8 mL/min flow of a mixture of water and acetonitrile(70/30 by volume) as an eluting agent. TOF-MS of WS fraction was measured by MALDI(Matrix-assisted laser desorption ionization) method using Voyager of PerSeptive Biosystems.

RESULTS AND DISCUSSION

Decomposition of chitin in hot pressurized water

The conversion and product distributions in the hydrothermal reactions of chitin by a flow reactor are summarized in Table 1. At 350 °C, WS yields were 24.0 and 29.6 % under the reaction pressures of 7.0 and 18 MPa, respectively, being comparable to those obtained by a batch reactor as previously reported.¹⁰ It is marked that the secondary decomposition of WS was effectively suppressed by the flow reactor because WS was continuously extracted by hot water from the fixed bed reactor. A higher temperature of 400 °C at 25 MPa under the supercritical condition increased the WS yield to 35.5 %, while the recovery was lower because of the higher gas yield. In addition, the WI was converted to the black char above 350 °C, indicating that the retrogressive and coking reactions take place under the severer conditions.

Figure 1 shows the HPLC profiles of the WS fraction produced from chitin under the pressurized hydrothermal conditions. A standard sample of chitin oligomer obtained from JHS Co.Ltd. was also measured for comparison in Figure 1 (a), where monomer to pentamer are clearly shown in the chromatogram. The WS produced at 300 °C contained the oligomer products with 3 to 6 units, although the yield was as low as 5 %. The molecular weights of the oligomers were analyzed by MALDI TOF-MS as illustrated in Figure 2, where the corresponding trimer to hexamer were included in the WS. The WS produced at 350 and 400 °C contained a large amount of the degraded products with the adsorption by UV detector, indicating that the ring cleavage reaction of the unit structure should take place under the sub- and supercritical water conditions. The hydrolysis of chitin under the mild conditions is recommended for the selective production of the oligomers.

Effect of acid addition on the hydrothermal decomposition of chitin

Table 2 summarizes the hydrothermal conversion of chitin by a batch reactor with or without acid addition. The conversion to WS at 300 °C increased very much from 11.4 % in water to 22.0 % in bamboo acid solution(pH: ca. 3). A bamboo acid solution contains acids such as formic acid, acetic acid, and higher carbon acids. A higher temperature of 350 °C did not change the WS conversion with the higher gas yield.

5 % acetic acid aqueous solution significantly increased the WS yield to 55.5 % at 300 °C, and its 10 % solution further increased up to 73.7 % at 300 °C. The addition of 10 % formic acid gave a slightly higher WS yield of 76.3 % compared to that with 10 % acetic acid solution at the same temperature, although the some weight gains were observed with the addition of acetic or formic acid, suggesting some contribution of the addition reaction of the acid to the decomposed ether linkage between the unit structures of chitin.

Figure 3 illustrates the effect of pH on the WS conversion at 300 °C. The WS conversion linearly increased with pH, although it was saturated in the pH range between 1 and 2. The higher conversion is suggested to be related to the acidity of aqueous solution under the subcritical conditions. However, HPLC analyses of WS fractions indicated that the higher acidity may accelerate the ring cleavage of the unit structure and the addition reaction of acid.

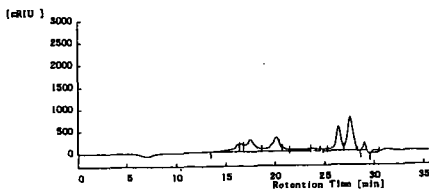
Based on the above results, it is pointed out that the control of pH in the acid solution and the dissociation of the aggregate structure in the chitin polymer through the solvation are keys to the enhancement of the hydrothermal decomposition of chitin.

References

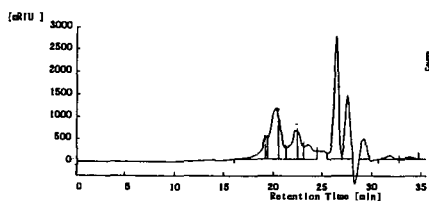
- 1) Muzzarelli, R.A.A., 'Chitin', Pergamon Press, New York (1977).
- 2) Shimahara, K.; Takiguchi, Y.; Ohkouchi, K.; Kitamura, K.; Okada, O. Chitin, Chitosan, and Related Enzymes, Ed.: Zikakis, J.P., Academic Press, Orlando (1984).
- 3) Hoashi, N., Hudson, S.M. Chitin - Healing Power from the Sea. Ed. Morton, R.J. Will Productions, Los Angeles, 1995.
- 4) Atalla, R.H. Conformational Effects in Hydrolysis of Cellulose, Hydrolysis of Cellulose: Mechanisms of Enzymatic and Acid Catalysis, Ed.: Brown, Jr., R.D. and Jurasek, L. Advances in Chemistry Series, Washington, D.C., 1979, vol.181, p. 55.
- 5) Gessler, K.; Krauss, N.; Steiner, T.; Betzel, A. S.; Saenger, W.; J.Am.Chem.Soc., 1995, 117, 11397.
- 6) Sakaki, T.; Shibata, M.; Miki, T.; Hirose, H.; Hayashi, N. Bioresource Technology, 1996, 58, 197.
- 7) Sakaki, T.; Shibata, M.; Miki, T.; Hirose, H. Energy & Fuels, 1996, 10, 684.
- 8) Kabyemela, B.M.; Adschiri, T.; Malaluan, R.M.; Arai, K. Ind. Eng. Chem. Res. 1997, 36, 2025.
- 9) Kabyemela, B.M.; Takigawa, M.; Adschiri, T.; Malaluan, R.M.; Arai, K. Ind. Eng. Chem. Res. 1998, 37, 357.
- 10) Sakanishi, K., Ikeyama, N., Sakaki, T., Shibata, M., Miki, T., Ind.Eng.Chem.Res. in submission.

Table 1 Hydrothermal decomposition of chitin by a fixed bed flow reactor

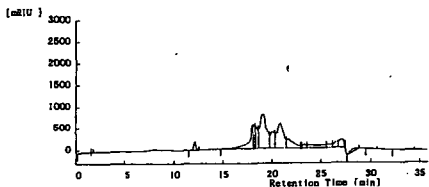
Salt bath temp.(°C)	Reaction press.(MPa)	WS Yield (wt%)	WI yield (wt%)	Recovery (%)
350	7.0	24.0	64.9	89.0
350	18.0	29.6	63.3	92.9
400	25.0	35.5	44.7	80.2



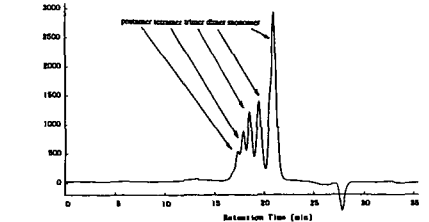
(d)



(c)



(b)



(a)

Fig. 1 HPLC profiles of the WS fractions produced under variable conditions

(a) standard chitin oligomers (b) 300 °C in water (c) 350 °C in water (d) 300 °C in 5%CH₃COOH aq.

Table 2 Effect of acid addition on the hydrothermal decomposition of chitin by a batch tube reactor¹⁾

Additives (-)	Salt bath temp.(°C)	Reaction temp.(°C)	Yields (wt%)			
			WS	MS	MI	Gas
water	300	285	11.4	1.2	75.6	11.8
bamboo acid 100%	300	279	22.0	0.0	75.8	2.2
bamboo acid 100%	350	323	21.1	1.0	73.1	4.8
acetic acid 5 %	300	287	55.5	3.6	52.9	-
acetic acid 10 %	300	286	73.7	1.8	39.7	-
formic acid 10 %	300	288	76.3	0.4	29.2	-

1) reaction time 60 sec after the preheating at 250 °C for 3 min
chitin 0.5 g + solvent 3.0 g for water and bamboo acid,
chitin 0.4 g + solvent 2.4 g for acetic acid and formic acid solutions

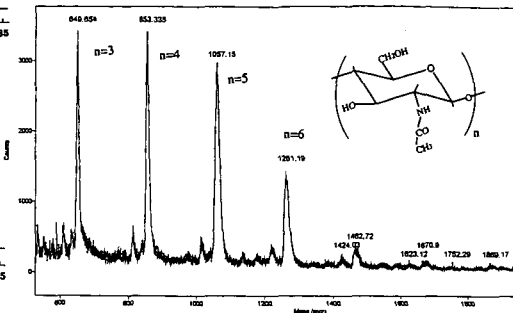


Fig. 2 TOF-MS profile of the WS fraction produced at 300 °C in water

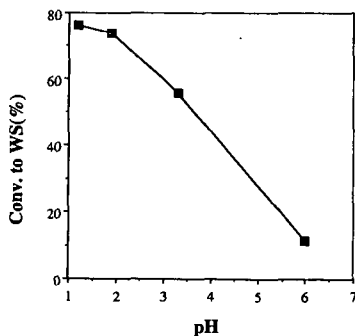


Fig. 3 Effect of pH on the conversion of chitin to WS

[pH; 10% formic acid 1.2
10% acetic acid 1.9
5% acetic acid 3.3
H₂O ca. 6]

KINETICS OF DEUTERIUM EXCHANGE OF RESORCINOL IN D₂O AT HIGH PRESSURE AND HIGH TEMPERATURE

Clement R. Yonker, Shi Bai, and Bruce J. Palmer, Environmental and Energy Sciences Division, Pacific Northwest National Laboratory, Richland WA, 99352

KEYWORDS: High Pressure NMR, Deuterium Exchange

ABSTRACT

The exchange kinetics of deuteration of resorcinol in pure D₂O were studied using a flow-through capillary tubular reactor with *on-line*, proton and deuterium NMR detection at high temperatures and high pressure. The temperatures of these measurements covered a range up to 450°C at a pressure of 400 bar. The hydrogen/deuterium (H/D) exchange in resorcinol (1,3-dihydroxybenzene) under these extreme conditions was easily detected by both proton and deuterium NMR as a function of resorcinol residence time in the capillary tubular reactor, which also served as the high pressure NMR cell. The qualitative NMR results indicate that H/D exchange in resorcinol is observed at 200°C. The kinetics of H/D exchange in resorcinol and the activation energies were extracted from the experimental ¹H and ²H NMR data.

INTRODUCTION

In subcritical (superheated) and supercritical water the hydrothermal oxidation of many organic compounds are enhanced due to the increased reactivity of the substrate and the enhanced solubility of non-polar organic compounds at these high temperatures. The increased reactivity of organic compounds in superheated water has been recognized for its potential in the destruction of toxic and organic wastes via oxidation.^{1,2}

Hydrogen/deuterium (H/D) exchange of some extremely weak organic acids in supercritical water has been investigated.^{3,4} Yao and Evilia³ estimated the equilibrium constant for the acid-base reaction of H/D exchange of benzene with OD⁻ to be three orders of magnitude higher at 400°C than at 25°C. Qualitatively, for substituted benzene compounds (fluorobenzene, 1,2-diphenylhydrazine, and nitrobenzene), the hydrogen in the ortho position was found to be slightly more acidic than those in the para or meta positions when reacted under basic conditions in D₂O at 400°C.³ However, difficulties were encountered when attempting to obtain quantitative chemical kinetic data for these reactions due to the large experimental error in determining temperature, pressure, and heating time when using a batch reactor.

While, NMR has not been widely used for *in situ* investigations of reactions in supercritical water, it has been used to monitor batch reaction products after quenching. The use of NMR detection for the *in situ* study of chemical kinetics generally requires that the NMR data acquisition time for a spectrum be much shorter than the reaction half-life.⁵ An experimental effort using a high pressure, high temperature flow-through capillary tubular reactor with *on-line* NMR detection for the investigation of H/D exchange of resorcinol in superheated and supercritical water will be discussed. The pseudo-first order rate constant for H/D exchange was determined by the disappearance of the α -hydrogens in resorcinol for the first time under these extreme conditions using this micro-volume ¹H NMR technique. In a similar manner, the product of the H/D exchange reaction was monitored *on-line* by ²H NMR. The rates for the resorcinol hydrogen/deuterium exchange reaction and the difference in the reactivity of the α and β hydrogens on resorcinol will be described.

EXPERIMENTAL

Resorcinol (Aldrich Chemical Company, Inc.) was used without further purification. To deoxygenate the solution, D₂O (Cambridge Isotope Laboratories) was boiled for 5 minutes under dry nitrogen and a 20% (w/w) resorcinol-D₂O solution was prepared and purged using dry nitrogen for 10 minutes.

Flow-through Capillary Tubular Reactor

The capillary tubular reactor set-up includes a high pressure syringe pump (ISCO 260D), a tubular piston separator (HIP), a fused silica capillary NMR cell (180 μ m i.d. by 360 μ m o.d., Polymicro Technologies, Inc), and back pressure regulators (Upchurch Scientific). In practice, the resorcinol-D₂O solution was loaded into one side of the piston separator and the other side was filled with water and connected to the syringe pump. The fused silica capillary was bent in a U shape and placed in a 10-mm glass NMR tube so that the bent end did not extend below the bottom edge of the NMR sensitive region along the z-axis. One end of the capillary tube was connected to the solution outlet of the piston separator and the other end of the capillary was connected to the back pressure regulators. When the high pressure syringe pump was operated in a constant flow rate mode, the sample pressure was controlled by the back pressure regulators. Five back pressure regulators (~80 bar each) were used in series so that the sample pressure was maintained between 380 to 400 bar depending on the flow rate.

The detection volume (V) within the NMR sensitive region was estimated from the inner diameter (180 \pm 6 μ m) of the capillary tubular reactor and twice the length of the NMR receiving coil (3.90cm). The volume of the NMR detection region was estimated to be $\sim 9.8 \times 10^{-6}$ ml (0.98

μl). Therefore, the reactor residence time (t_R) may be calculated from the mass flow rate (f) and the solution density (ρ) using equation 1,

$$t_R = V \cdot \rho / f \quad (1)$$

Since the accuracy of the reactor residence time depends on flow rate control and fluid density in the reactor, a system calibration was performed at room temperature and a pressure of 400 bar by collecting and weighing the water eluted from the capillary at specific flow rates over a set time interval. A step profile is assumed for the temperature contour in the reactor region and the density is determined from the Steam Tables⁶. This assumption allows a qualitative determination of the reaction rate under these extreme conditions.

NMR Measurements

All NMR data were obtained on a Varian UnityPlus 300 NMR spectrometer operating at 299.3 and 46.13 MHz for proton and deuterium detection, respectively. A high temperature, high resolution, broad band 10-mm NMR probe (Doty Scientific, Inc.) produces a line width at half-height of 8-10 Hz for proton and 4-8 Hz for deuterium in the resorcinol-D₂O solution in the capillary NMR cell at room temperature. Because of the probe design, there is a region where the tubular reactor temperature is not well controlled. This pre-heated area, before the NMR detection region, could contribute to an overestimation of the deuterated product and an underestimation of the reactant conversion rate. We anticipate solving this problem in future NMR investigations, through redesign of the probe's heated region.

In a typical experiment, the resorcinol-D₂O solution is moving through the capillary high pressure NMR cell⁷ under a constant flow rate at constant temperature and pressure. Concurrent with solution flow, a NMR experiment is running coadding transients until a satisfactory spectrum with an adequate signal to noise ratio is obtained. Since the capillary tubular reactor is an integral part of the NMR capillary cell, a steady state concentration is established in the reactor at constant flow during the experiment. The sample temperature was changed with each flow rate at a constant pressure and the peak integral was used in both the proton and deuterium data analysis.

RESULTS AND DISCUSSION

Proton NMR

The reaction of substituted benzene in basic solutions of D₂O has been discussed by Yao and Evilia.³ The H/D exchange mechanism for resorcinol in pure D₂O is facilitated by the presence of electron-withdrawing groups on the aromatic ring. This activated aromatic ring is deuterated by an electrophilic substitution mechanism, which increases the ease of deuteration under these experimental conditions and eliminates the need of either an acid or base to catalyze the reaction.^{5,8} Resorcinol is an ortho/para director in electrophilic substitution reactions.⁹ Therefore, H/D substitution would be facilitated for the α -hydrogens and not for the β -hydrogen. The α -hydrogen peak area decreased as a function of increasing temperature and reactor residence time. From the H/D substitution reaction rates the pseudo-first order kinetics could be determined for resorcinol under these extreme conditions. The NMR experimental results demonstrate the positional selectivity of the electrophilic substitution during H/D exchange due to the molecular structural information obtained from this technique.

The β -hydrogen in resorcinol can serve as an internal molecular indicator relating to the stability of the molecule to thermolysis reactions under these conditions. Qualitatively, the peak area of the β -hydrogen decreases with increasing reactor residence time, but shows little temperature dependence. Thermolysis of resorcinol at 460°C and 254 bar was reported to produce conversions of ~10%, for residence times of 1 - 7 seconds at 0.01M solution concentration.¹⁰ The NMR results demonstrate the occurrence of a parallel thermolysis reaction of resorcinol under these temperatures and reactor residence times. The thermolysis products could not be identified as they were below the detection limits of the NMR.

Deuterium NMR

At a reaction temperature of 200 °C, the deuterium NMR spectrum shows a new peak with a chemical shift of ~7.2 ppm. The chemical shift difference between this new peak and that of D₂O at 200 °C is ~3.0 ppm, which is the same as the chemical shift difference between the α -hydrogens and water in the ¹H NMR measurement at the same temperature. Therefore, this resonance was assigned to resorcinol deuterated at the α -positions. This qualitative observation demonstrated that H/D exchange did indeed occur for the resorcinol-D₂O solution at 200°C at very long reactor residence times. The intensity of the α -deuterated resorcinol peak increases as a function of temperature and reactor residence time. A pseudo-first order rate constant can be determined from the rate of appearance of the α -deuterium peak and compared with that determined from the ¹H NMR measurements under similar experimental conditions. A β -deuterium peak is not observed under the experimental conditions investigated.

ACKNOWLEDGMENT

Work at the Pacific Northwest National Laboratory (PNNL) was supported by the Office of Energy Research, Office of Basic Energy Sciences, Chemical Sciences Division of the U. S. Departments of Energy, under Contract DE-AC076RLO 1830.

REFERENCES

- (1) Yang, H. H.; Eckert, C. A. *Ind. Eng. Chem. Res.*, **1988**, *27*, 2009-2014.
- (2) Webley, P. A.; Tester, J. W.; Holgate, H. R. *Ind. Eng. Chem. Res.*, **1991**, *30*, 1745- 1754.
- (3) Yao, J.; Evilia, R. F. *J. Am. Chem. Soc.*, **1994**, *116*, 11229-11233.
- (4) Kuhlman, B.; Arnett, M.; Siskin, M. *J. Org. Chem.*, **1994**, *59*, 3098-3101.
- (5) Grimaldi, J.; Baldo, J.; McMurray, C.; Sykes, B. D. *J. Am. Chem. Soc.*, **1972**, *94*, 7641-7645.
- (6) Haar, L.; Gallagher, J. S.; Kell, G. S.; NBS/NRC Steam Tables, Hemisphere Publishing Corp., New York, 1984.
- (7) Yonker, C. R.; Zemanian, T. S.; Wallen, S. L.; Linehan, J. C.; Franz, J. A. *J. Magn. Reson., Ser A*, **1995**, *113*, 102-107.
- (8) Maksić, Z. B.; Kovačević, B.; Kovaček, D. *J. Phys. Chem. A*, **1997**, *101*, 7446-7453.
- (9) Morrison, R. T.; Boyd, R. N. *Organic Chemistry*, 3rd Ed., Allyn and Bacon, Inc., Boston, **1973**, p. 340.
- (10) Martino, C. J.; Savage, P. E. *Ind. Eng. Chem. Res.*, **1997**, *36*, 1385-1390.

HYDROGEN STABLE ISOTOPE RATIOS OF KEROGEN, BITUMEN, OIL, AND WATER IN HYDROUS PYROLYSIS

A. Schimmelmann¹, M. D. Lewan², and R. P. Wintsch¹

¹ Department of Geological Sciences, Indiana University, 1005 East 10th Street,
Bloomington, IN 47405-1403

² U. S. Geological Survey, Box 25046, MS 977, Denver Federal Center,
Denver, CO 80225

INTRODUCTION

Diverse isotopic evidence has been mounting in favor of an active role of water in the chemical transformation of kerogen to bitumen, oil, and gas, and also as an agent promoting hydrogen isotopic exchange with organic hydrogen (e.g., Koepp, 1978; Schoell, 1981; Hoering, 1984; Stalker et al., 1998). At low temperatures, water-hydrogen exchanges quickly with isotopically labile organic hydrogen most of which is bound to organic nitrogen, sulfur, and oxygen (NSO-functional groups; Koepp, 1978; Schoell, 1981). In contrast, most carbon-bound hydrogen does not exchange with water at neutral pH, low temperature, and in the absence of a catalyst, thus conserving the D/H ratios of *n*-alkanes at temperatures well above 150°C (Hoering, 1984; Koepp, 1978). Some aromatic hydrogen and few alkyl hydrogen sites adjacent to branching and carbonyl positions may exchange with water-hydrogen at temperatures as low as 100°C (Alexander et al., 1982; Werstik and Ju, 1989), especially at low pH via carbonium ion mechanisms. At higher temperatures, extensive exchange between water-derived hydrogen and organic hydrogen is attributed to the quenching of free organic radical sites (Hoering, 1984; Lewan, 1997; Stalker et al., 1998). Thermodynamic calculations indicate that reactions of water with alkyl free radicals are highly favorable under experimental and natural maturation conditions (Lewan, 1997, p. 3714-3715).

The determination of meaningful D/H ratios in organic substrates needs to take into account the isotopically labile organic hydrogen that perpetually exchanges with ambient moisture. Only the low concentration of labile NSO-linked hydrogen in oil and bitumen warrants the use of δD of total organic hydrogen. In contrast, kerogens of low to moderate thermal maturity are more hydrophilic because they contain abundant NSO-functional groups that often contain labile hydrogen. In this study we control the isotopic composition of labile hydrogen in kerogen by dual equilibration with isotopic standard water vapors at 115°C, followed by a mass balance calculation to arrive at the isotopic composition of non-labile hydrogen in kerogen (Schimmelmann, 1991). To avoid semantic confusion about different types of exchangeable hydrogen, this study operationally defines "labile organic hydrogen" as the fraction of organic hydrogen that readily exchanges with water vapor at 115°C.

EXPERIMENTAL

We used four thermally immature source rocks that encompass different types of kerogen: Type-I (Mahogany Shale of the Eocene Green River Fm. in Utah), type-II (Clegg Creek Member of the Devonian-Mississippian New Albany Shale in Indiana), type-IIS (Senonian Ghareb Limestone from Jordan), and type-III (Paleocene lignite from Calvert Bluff Fm. of the Wilcox Gp. in Texas).

Hydrous pyrolyses were performed in stainless steel pipe reactors (pipe length 15.1cm, o.d. 1.9cm, internal volume ca. 25.5mL) that were loaded with 5.5 to 10g of rock chips (diameter 2mm to 7mm). The rock was submerged in 10 to 11ml of 0.093 molar aqueous ammonium chloride solution under nitrogen. Three isotopically different aqueous phases were

used with initial δD values of -110, +290, or +1260 per mil. After hydrous pyrolysis and cooling to room temperature, expelled oil or wax on the water surface was collected separately from the water phase. Bitumen was Soxhlet-extracted from dried and powdered rock. Kerogen was prepared by demineralization of bitumen-extracted powdered rock. The isotopic equilibration of aliquots of kerogen at 115°C in isotopic standard water vapors, the conversion of water and organic hydrogen to elemental hydrogen for mass-spectrometric analysis, and the calculation of δD values of non-labile hydrogen in kerogen were described by Schimmelmann (1991). We are aware that water will also continuously exchange with hydrogen in clay minerals and with exchangeable (labile) organic hydrogen.

RESULTS

Waters with strong initial D-enrichment transfer deuterium to organic phases over time, whereas water with an initial δD value of -110 per mil receives organic deuterium. In effect, the directions of isotopic shifts for organic hydrogen in kerogen, bitumen, and oil are opposite to the respective shifts observed for water, depending on the starting δD value of water. Our isotopic choices for water as the dominant hydrogen pool determine the directions of isotopic exchange for all minor, organic hydrogen pools. The converging patterns of isotopic changes of waters and the associated type-II kerogen, bitumen, and oil from 330°C hydrous pyrolysis experiments are shown in Figure 1.

Our D/H data permit a mass balance approach to estimate the fraction of organic hydrogen in kerogen, bitumen, and oil that is derived from water in hydrous pyrolysis experiments. Our calculations are based on hydrous pyrolysis experiments with starting δD values for water of -110 and + 1260 per mil. We cannot discriminate between added hydrogen and hydrogen that was exchanged at temperatures above 115°C, but the calculations are not affected by the presence of labile hydrogen in kerogen. Details of underlying assumptions and algorithms are presented elsewhere (Schimmelmann et al., in review). The percentage P (Table 1) reflects the estimated abundance of water-derived hydrogen in bitumen and oil, and in non-labile organic hydrogen in Kerogen. The isotopic influence of water-hydrogen on type-II kerogen and associated bitumen and oil from New Albany Shale increases over time at 330°C, and with increasing temperature over 72 hours (Table 1a). The four types of source rocks used in this study differ in their content of potentially reactive and exchangeable hydrogen, and therefore in their P values and in their ability to shift δD values of water (Table 1b).

DISCUSSION

Many chemical and physical processes affecting the hydrogen isotopic balance between reactants and phases occur simultaneously and continuously during hydrous pyrolysis of immature source rocks in contact with water. Some bitumen is already present in immature source rocks prior to hydrous pyrolysis, but significant amounts are generated from the kerogen with increasing temperature, along with low-molecular weight compounds (Lewan, 1997). With increasing temperature, the water-saturated bitumen partially decomposes into an immiscible hydrophobic oil that is expelled from the rock (Lewan, 1997). Our D/H data represent time-series of snapshots of this dynamic system of water, kerogen, bitumen, and oil.

Our P values in Table 1b show that hydrogen in type-I kerogen and its associated bitumen and expelled wax is the most isotopically conservative, i.e. with the lowest P values, whereas hydrogen is least isotopically conservative in type-IIS kerogen and its associated bitumen and expelled oil. The decrease in P values in the order of kerogen-types IIS > II \approx III > I can be interpreted in terms of basic chemical structural differences. The strongly aliphatic

type-I kerogen (Tissot and Welte, 1984; Horsfield et al., 1994) has a large isotopically conservative pool of hydrogen in its mostly *n*-alkyl linkages, and can thus be expected to generate the smallest number of free radicals during hydrous pyrolysis and to express the smallest *P* values for kerogen, bitumen, and oil. Type-II kerogen is expected to contain a more branching molecular carbon structure, with larger propensity toward generation of free radical sites and consequently larger *P* values. A similar increase in *P* in type-III kerogen may be the result of a larger abundance of oxygen in lignite, which favors the formation of free radicals. Type-IIS kerogen would form even more free radicals under the same thermal conditions because it contains labile S-S and C-S bonds with low activation energy (Tomic et al., 1995; Lewan, 1998).

CONCLUSIONS

Immature source rocks containing different types of kerogen were heated in hydrous pyrolysis experiments. D/H ratios were monitored in isolated kerogen, extracted bitumen, expelled oil, and ambient water. The isotopic transfer of hydrogen between water and organic hydrogen increases with higher temperature and longer duration of hydrous pyrolysis, via exchange and/or addition, resulting in a convergence of δD values of water and of organic hydrogen. Isotopic mass-balance calculations suggest that, depending on temperature, time, and source rock type, between 35 and 75% of carbon-bound hydrogen is ultimately derived from water-hydrogen. Organic hydrogen in kerogen, bitumen and oil/wax from source rocks containing different types of kerogen rank from least to most isotopically conservative in the order IIS < II \approx III < I, which is consistent with models of chemical reactivity in kerogens through maturation.

The prospect of water-hydrogen becoming available to maturing organic matter may pleasantly revise estimates of oil and gas potentials in sedimentary basins, but its potential D/H isotopic implications may force isotope geochemists to rethink their interpretation of D/H ratios in maturing fossil fuels and associated formation waters. The unresolved controversy about substituting long geologic time in natural maturation with higher temperature in artificial maturation, however, advises to caution when extrapolating our specific isotopic findings from hydrous pyrolysis to D/H ratios in fossil fuels.

ACKNOWLEDGEMENTS

Acknowledgement is made to the donors of The Petroleum Research Fund, administered by the American Chemical Society, for support of this research with grant #31203-AC2, to the U.S. Geological Survey under Energy Resources Project 51564, and to NATO Collaborative Research Programme grant 971381.

REFERENCES

- Alexander, R., Kagi, R. I., and Larcher, A. V., 1982, Clay catalysis of aromatic hydrogen-exchange reactions, *Geochim. Cosmochim. Acta* 46: 219-222.
- Hoering, T. C., 1984, Thermal reactions of kerogen with added water, heavy water and pure organic substances, *Org. Geochem.* 5: 267-278.
- Horsfield, B., Curry, D. J., Bohacs, K., Litke, R., Rullkötter, J., Schenk, H. J., Radke, M., Schaefer, R. G., Carroll, A. R., Isaksen, G., and Witte, E. G., 1994, Organic geochemistry of freshwater and alkaline lacustrine sediments in the Green River Formation of the Washakie Basin, Wyoming, U.S.A., *Org. Geochem.* 22: 415-440.
- Koepp, M., 1978, D/H isotope exchange reaction between petroleum and water: A contributory determinant for D/H-isotope ratios in crude oils? In *Short papers of the Fourth International Conference, Geochronology, Cosmochronology, Isotope Geology.* (ed R.

- E. Zartman), *USGS Open-File Report 78-701*: 221-222. Reston VA, US Geological Survey.
- Lewan, M. D., 1997, Experiments on the role of water in petroleum formation, *Geochim. Cosmochim. Acta* **61**: 3691-3723.
- Lewan, M. D., 1998, Sulphur-radical control on petroleum formation rates, *Nature* **391**: 164-166.
- Schimmelmann, A., 1991, Determination of the concentration and stable isotopic composition of non-exchangeable hydrogen in organic matter, *Anal. Chem.* **63**: 2456-2459.
- Schimmelmann, A., Lewan, M. D., and Wintsch, R. P., (in review), D/H isotope ratios of kerogen, bitumen, oil, and water in hydrous pyrolysis of source rocks containing kerogen types-I, -II, -IIS, and -III, submitted to *Geochim. Cosmochim. Acta*.
- Schoell, M., 1981, D/H-Isotopenverhältnisse in organischen Substanzen, Erdölen und Erdgasen. *BMFT Forschungsbericht T 81-204*, 1-79, Bundesanstalt für Geowissenschaften und Rohstoffe, Hannover, Germany.
- Stalker, L., Larter, S. R., and Farrimond, P., 1998, Biomarker binding into kerogens: evidence from hydrous pyrolysis using heavy water (D₂O), *Org. Geochem.* **28**: 239-253.
- Tissot, B. P., and Welte, D. H., 1984, *Petroleum Formation and Occurrence*. Springer-Verlag.
- Tomic, J., Behar, F., Vandembroucke, M., and Tang, Y., 1995, Artificial maturation of Monterey kerogen (Type II-S) in a closed system and comparison with Type II kerogen: implications on the fate of sulfur, *Org. Geochem.* **23**: 647-660.
- Werstiuk, N. H., and Ju, C., 1989, Protium-deuterium exchange of benzo-substituted heterocycles in neutral D₂O at elevated temperatures, *Can. J. Chem.* **67**: 812-815.

Table 1. Calculated percentage (*P*) of the amount of water-derived hydrogen in the total hydrogen of bitumen and oil, and in the non-labile hydrogen of kerogen, after hydrous pyrolysis experiments in waters with starting δD values of -110 and +1260 per mil. The $\Delta\delta D$ of water is the difference between the final δD values and the starting δD values in water, in per mil.

Hydrous Pyrolysis Experimental Conditions			Kerogen	Bitumen	Oil	$\Delta\delta D$ of Water (per mil)	
Kerogen Type	Temp. (°C)	Time (h)	<i>P</i> (%)	<i>P</i> (%)	<i>P</i> (%)	[starting δD values:]	
						[-110]	[+1260]
a) variations in temperature and time							
II	310	72	47.1	53.1	36.1	10	-115
II	330	12	42.6	48.3	33.9	9	-82
II	330	36	56.6	58.4	43.3	8	-91
II	330	72	61.7	61.9	50.3	11	-104
II	330	144	66.0	70.2	57.7	9	-111
II	350	72	74.5	73.1	58.9	14	-140
b) variations in source rock							
I	330	72	44.4	34.9	39.6	4	-152
II	330	72	61.7	61.9	50.3	11	-104
IIS	330	72	69.7	69.9	68.4	15	-186
III	330	72	69.5	56.9	44.6	22	-262

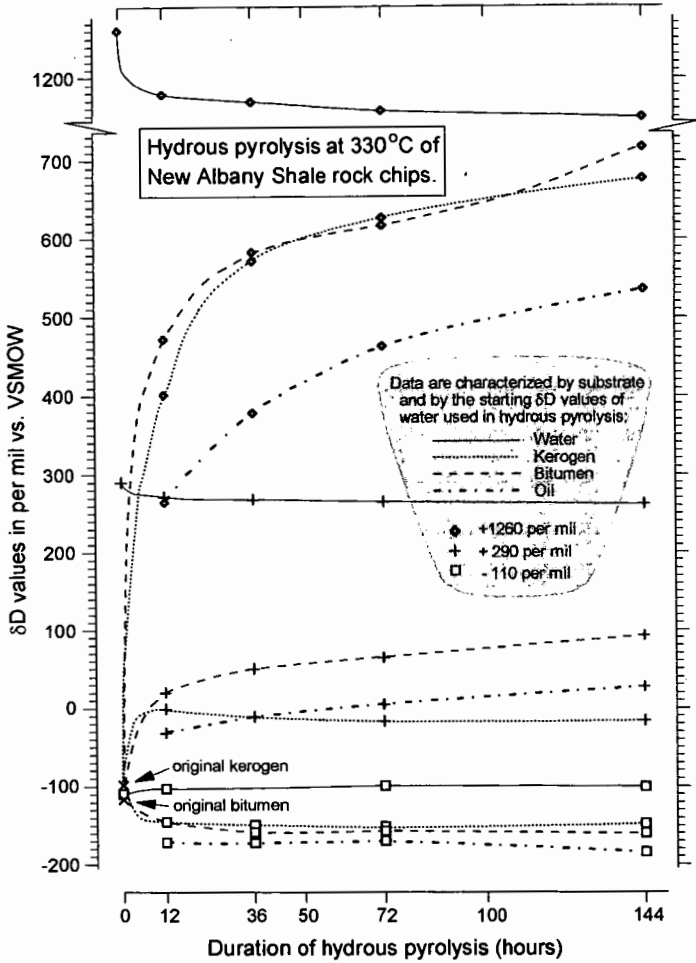


Fig. 1: D/H results from water, kerogen (non-labile hydrogen), bitumen, and oil from hydrous pyrolysis experiments, at 330°C of New Albany Shale. Three isotopically different waters were used, resulting in distinctly converging isotopic shifts of water and organic phases over time for each type of water used, due to isotopic hydrogen transfer between inorganic and organic hydrogen. Connecting lines are drawn to guide the eye. No oil was available before hydrous pyrolysis.

BASE-CATALYZED REACTIONS IN NEAR-CRITICAL WATER FOR ENVIRONMENTALLY BENIGN CHEMICAL PROCESSING

Roger Gläser, James S. Brown, Shane A. Nolen, Charles L. Liotta, and Charles A. Eckert
Schools of Chemical Engineering and Chemistry, and Specialty Separations Center
Georgia Institute of Technology, Atlanta, GA 30332-0100

INTRODUCTION

Water has recently attracted much interest as an environmentally benign solvent for organic syntheses [1,2]. While many of the previous studies have been devoted to water near ambient conditions, it exhibits more favorable characteristics as a medium for organic reactions when it is closer to its critical point (near-critical water) but still in the liquid state. First, the solubility of organic substances in water increases considerably with increasing temperature due to a decrease in dielectric constant. For liquid water at 250 °C the dielectric constant is comparable to that of ambient acetone [3]. Conversely to acetone, product separation from the solvent can occur simply by phase separation upon returning to ambient conditions. Secondly, the ionization constant of near-critical water is several orders of magnitude higher than that of ambient water, thus providing a source of hydronium and hydroxide ions, which can act as catalytically active species in chemical conversions. As shown in previous studies in our group [4,5] acid catalyzed reactions, such as Friedel-Crafts alkylations, can be successfully accomplished in near-critical water with less or even without added catalyst. Thirdly, while reactions in supercritical water have mainly been applied in chemical reactions to break up bonds, e.g., for waste destruction by supercritical water oxidation (SCWO) [6,7], the milder temperature regime of hot liquid water allows for bond formation, i.e., the synthesis of organic compounds.

In this study we aimed at scouting the opportunities to perform organic syntheses in near-critical water that are usually conducted in the presence of base. Based on earlier work by *Katritzky, Siskin et al.* [8], aldol condensations have been chosen as first examples because the reactants are not subject to immediate hydrolysis, and different products can be formed. In the classical preparation methods the selectivity for the products is determined, e.g., by the reaction temperature and by the pH during the work-up procedure. Selectivity for those products might therefore give insight into the effect of water as the reaction medium on product distribution. The aldol condensation of phenylacetaldehyde has been studied in further detail, including different reaction times, reactant concentrations, and in the presence of added acid and base. The scope of this type of reaction has also been explored for some condensations between different reactants. Other synthetically important C-C bond formation reactions involve hydrolyzable compounds, such as esters, and as examples the Dieckmann condensation and typical malonic ester syntheses have been included in the present study to encompass the scope of reactions accessible in near-critical water.

EXPERIMENTAL SECTION

The reactions have been carried out in the batch mode using Titanium vessels (rated to 1 kbar at 500 °C) with an inner volume of 3 ml. After loading, these reactors have been placed in a preheated aluminum block where they reached the desired reaction temperature within ca. 5 min. After stopping the reaction by quenching the reactors in a room temperature water bath, the reactor contents were dissolved in acetone and diluted to a known volume. For determination of product distribution versus time several vessels were loaded in the same manner and have been quenched at different reaction periods. Product analysis was achieved via temperature-programmed capillary GC equipped with an FID or an MS detector and product distribution are given in terms of mole fractions.

All chemicals were ACS grade (Aldrich) and were used as received. Water to be used as reaction solvent was HPLC grade (Aldrich) and was used without further purification. As shown in previous experiments, both deoxygenation of the water and loading under nitrogen atmosphere did not afford a change in the obtained product of more than experimental accuracy.

In a typical run at 275 °C a reactor is loaded at ambient conditions with 1.8 ml liquid reactant/water mixture with a molar ratio of 1/47. Accounting for the expansion of the water with increasing temperature the reactor at 275 °C contains 2.6 ml liquid phase and a small gas phase.

RESULTS AND DISCUSSION

Aldol condensations

The aldol condensation of *n*-butyraldehyde is industrially carried out in the presence of caustic sodium to produce 2-ethyl-2-hexenal. This is later hydrogenated to 2-ethylhexanol which is esterified with phthalic acid to give the plasticizer dioctylphthalate (DOP) [9]. If *n*-butyraldehyde is reacted for 15 hrs at 275 °C in water, essentially complete conversion is obtained without the addition of any catalyst. The main product is, like in the conventional synthesis, 2-ethylhexanal (selectivity 85 %). Some 2-butyl-2-butanone is also formed by double

bond isomerization of the former. Other byproducts with selectivities < 2 % are the dialdol isomerization product, triethylnaphthalene and cis/trans isomers of the formed olefins.

As already pointed out by *Katritzky et al.* [10] phenylacetaldehyde (PAA) is a highly reactive compound and a reaction scheme (Figure 2) has been provided by these authors. The distribution of some key intermediates for the conversion of PAA in water at 275 °C as a function of reaction time is shown in Figure 1. From this Figure it can be clearly seen that products **1** and **2** formed by two aldol reaction steps and subsequent double bond isomerization are intermediate products in the formation of 1,3,5-triphenylbenzene as proposed by the reaction scheme. In addition to the main reaction products observed by *Katritzky et al.* [10] we have also found 2-phenylnaphthalene which can be formed by ring closure of the aldol reaction and subsequent dehydration and isomerization. The presence of small amounts of 2-phenyldihydronaphthalene provides further evidence for the formation of 2-phenylnaphthalene. 2-Phenylnaphthalene is the major reaction product when PAA is converted in the presence of hydrochloric acid (Table 1) and otherwise constant reaction conditions. With added NaOH as a base, however, 1,3-diphenylpropane is the main reaction product and no 2-phenylnaphthalene is observed. Table 1 also shows the influence of the PAA concentration: While higher dilution of the reactant does not afford a considerable change in the product distribution, a higher reactant concentration leads to a lower conversion and lower mole fractions of products formed in subsequent reactions.

Ketones are less reactive in aldol-type reactions than aldehydes. Although acetone is readily converted in near-critical water to mainly mesityloxide, 1-phenyl-2-butanone (PBO) does not undergo any reaction at 275 °C after 24 hrs, and a conversion of only about 15 % is reached in the presence of added NaOH ($n_{\text{PBO}}/n_{\text{NaOH}} = 1/0.5$). Nearly 50 % conversion of PBO is obtained without further addition of base, when it is reacted with benzaldehyde as a more active carbonyl compound. Table 2 summarizes the main products resulting from aldol type C-C bond formations in the conversions of acetone and PBO with benzaldehyde. In accordance with the results reported by *Katritzky, et al.* [11] benzaldehyde alone undergoes primarily Cannizzaro reaction and disproportionation in an overall low conversion (< 5 %) to yield benzoic acid, benzylalcohol, and toluene, respectively.

Dieckmann condensation

Many base catalyzed involve the conversion of hydrolyzable compounds, such as esters in the Claisen condensation [12]. To test whether such reactions can be carried out in near-critical water at 275 °C the Dieckmann condensation of adipic acid and its dimethyl and diethyl ester has been attempted without any added catalyst. Both esters undergo hydrolysis to the monoester and adipic acid, respectively, and, the diethyl ester hydrolyzes slower than the methyl derivative, as expected. It should be noted, however, that even after 16 hrs at 275 °C this hydrolysis is not complete, leaving about a third of the overall adipic acid at the mono- or the diester. Besides hydrolysis the main products were cyclopentanone and benzoic acid. Cyclopentanone is the expected product, if the base-catalyzed ring closure is followed by decarboxylation, which is facilitated at the elevated temperature. More cyclopentanone is formed when the ester hydrolysis is less pronounced, i.e., with diethyl adipate as reactant. With adipic acid the formation of benzoic acid is strongly favored over the formation of cyclopentanone, but the cyclopentanone yield is comparable to the one achieved with the esters. The overall yield of cyclopentanone in all cases is, however, comparably low (< 2 %).

Knoevenagel condensation

The condensation of a carbonyl compound with a malonic ester is a useful tool in the synthesis of substituted organic acids, often referred to as "malonic ester syntheses" [12]. By this method cinnamic acid can be obtained from the conversion of a malonic acid ester with benzaldehyde followed by hydrolysis and decarboxylation. With malonic acid as the reactant, water as the solvent and in the absence of added base, the main product of the conversion is styrene as well as the products arising from self reaction of benzaldehyde (Table 3). Although the desired C-C bond formation has occurred, decarboxylation apparently is the strongly favored reaction under these reaction conditions. In addition to an overall higher conversion than with malonic acid, the use of disodium malonate instead of malonic acid resulted predominantly in an increased formation of benzylalcohol most probably due to the reduction of benzaldehyde, accompanied by the production of carbon dioxide. 2-Methyl-1-propenylbenzene and isobutyric acid were the major products in the conversion of benzaldehyde with dimethyl malonate in near-critical water. The formation of these products involve a series of condensation, hydrolysis, and decarboxylation reactions.

The conversion of benzylaldehyde with diphenylmethane in water at 275 °C did not result in the formation of any detectable condensation product. Presumably the ions from the dissociation of water can neither deprotonate diphenylmethane, nor activate the benzaldehyde carbonyl group to an extent sufficient to bring about the desired reaction.

CONCLUSIONS

Near-critical water is a promising and environmentally benign reaction medium for a number of synthetically important conversions that are conventionally carried out in the presence of base. Due to the high ionization of water these conversions may be accomplished without further addition of base, especially in the when reactive carbonyl compounds and substrates with sufficiently high C-H acidity are involved.

It has been shown that C-C bond formations can be brought about in near-critical water in syntheses that involve hydrolyzable compounds like esters. Decarboxylation, which was indicated to be a limiting factor in these reactions, might be reduced by pressurizing the reaction vessels with carbon dioxide and lowering the reaction temperature. At lower temperature the solubility of the organic reactants might, however, also be considerably reduced. Therefore, more detailed information on the phase behavior of organic substances relevant to chemical synthesis is needed. Investigations are currently underway in our laboratory.

Although the spectrum of prospective reactants might be limited to those thermally stable at temperatures up to ca. 300 °C, the lower cost of the reactants and the solvent, the ease of carrying out the reaction and product separation as well as the opportunity to reduce, if not completely avoid the addition of a catalyst render near-critical water an profitable alternative to many less favorable solvents currently used in chemical processes.

ACKNOWLEDGEMENTS

The authors gratefully acknowledge generous financial support by the U.S. NSF and the U.S. EPA. R.G. thanks the German Research Association (Deutsche Forschungsgemeinschaft) for a research stipend.

REFERENCES

- [1] A. Lubineau, J. Augé and Y. Queneau, *Synthesis*, 741-760 (1994).
- [2] C.-J. Li, *Chem. Rev.* **93**, 2023-2035 (1993).
- [3] M. Siskin and A.R. Katritzky, *Science* **254**, 231-237 (1991).
- [4] K. Chandler, F. Deng, A.K. Dillow, C.L. Liotta, and C.A. Eckert, *Ind. Eng. Chem. Res.* **36**, 5175-5179 (1997).
- [5] K. Chandler, C.L. Liotta, C.A. Eckert and D. Schiraldi, *AIChE J.* **44**, 2080-2087 (1998).
- [6] R.W. Shaw, T.B. Brill, A.A. Clifford, C.A. Eckert and E.U. Franck, *Chem. Eng. News* **69**, 23-39 (1991).
- [7] P.E. Savage, S. Gopalan, T.I. Mizan, C.I. Martino and E.E. Brock, *AIChE J.* **41**, 1723-1778 (1995).
- [8] A.R. Katritzky, M. Siskin et al., series of 18 papers in *Energy & Fuels* **4**, 475-584 (1990).
- [9] K. Weissermel, and H.-J. Arpe: "Industrial Organic Chemistry", 3rd ed., Verlag Chemie, Weinheim, New York (1997).
- [10] A.R. Katritzky, F.J. Luxem and M. Siskin, *Energy & Fuels* **4**, 514-517 (1990).
- [11] A.R. Katritzky, M. Balasubramanian and M. Siskin, *Energy & Fuels* **4**, 499-505 (1990).
- [12] J. March: "Advanced Organic Chemistry, Reactions, Mechanisms, and Structure", J. Wiley & Sons, New York, Chichester, Brisbane, Toronto, Singapore (1985).

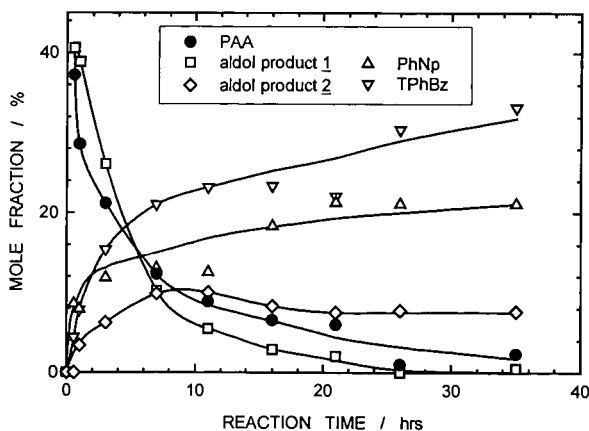


Figure 1: Distribution of major products as a function of reaction time for the conversion of phenylacetaldehyde (PAA) in near-critical water at 275 °C ($n_{\text{PAA}}/n_{\text{H}_2\text{O}} = 1/50$); PhNp: 2-phenylnaphthalene, TPhBz: 1,3,5-triphenylbenzene, aldol product 1 and 2: see Figure 2.

ABIOTIC SYNTHESIS OF ORGANIC COMPOUNDS IN HYDROTHERMAL SYSTEMS:
DEHYDRATION REACTIONS BY SMECTITE CATALYSTS. P.A. O'Day, L.B. Williams,
J.R. Holloway, Arizona State Univ., Tempe, AZ, 85287-1404, and J.R. Delaney, Univ. of
Washington, Seattle, WA 98195

Since the discovery of a diverse, hydrothermally-supported biota at seafloor vents 20 years ago, mid-ocean ridge hydrothermal systems have been postulated as sites in which the abiotic synthesis of simple organic molecules might occur as precursors to the origin of life [1]. Previous work has focused on the role of sulfide catalysts in promoting carbon reduction and hydrocarbon synthesis, primarily by Fischer-Tropsch-type pathways [e. g., 2-3]. Clay minerals and zeolites have also been considered as templates for abiotic synthesis [e.g., 4]. The thermodynamics of a variety of dehydration reactions as a function of temperature and pressure were examined by Shock [5], but few studies have examined specific mechanistic pathways for organic synthesis by mineral catalysts under seafloor hydrothermal conditions.

In a previous study [6], we proposed that formation of C₁-C₄ alcohols may be possible metastable reaction products from seafloor diking events that generate elevated concentrations of CO₂ + H₂. Alcohol formation may be catalyzed by phase separation and reaction with newly precipitated sulfide surfaces in the optimum temperature range of 200-300°C at sub-seafloor pressures (200-500 bars). Solubility of C₁-C₄ alcohols increases with decreasing temperature, allowing for subsequent aqueous reactions with mineral surfaces. Dehydration reactions among short-chain alcohols in the presence of a strong Brønsted-acid catalyst have been shown to produce C₂-C₅ alkenes and C₆-C₈ aromatic compounds [7]. One proposed reaction mechanism is the formation of surface methoxy intermediates from methanol adsorbed at acidic oxygen sites, followed by dehydration and formation of C-C double bonds [8]. Calculations (using SUPCRT92) show that overall methanol dehydration reactions are thermodynamically favored at hydrothermal temperatures (100-375°C) and pressures (100-500 bars) in aqueous solution, and are generally more favored with decreasing temperature. Smectite or other sheet silicates with exchangeable interlayer sites would serve as effective sorbents of alcohols and as strong Brønsted-acid catalysts at low to circum-neutral pH. Recent discovery of significant amounts of smectite within sulfide edifices recovered from MOR vents, in which sulfide minerals are mixed within clay pods, suggests the possibility of natural catalysis by this alcohol-initiated pathway. Results from laboratory experiments of alcohol reaction with smectite under hydrothermal conditions will be discussed.

[1] J. B. Corliss, J. A. Baross, S. E. Hoffman, *Earth. Ocean. Acta* **SP**, 55 (1981).

[2] G. Wächtershäuser, *Prog. Biophys. Molec. Biol.* **58**, 82 (1992).

[3] M. J. Russell, R. M. Daniel, A. J. Hall, J. A. Sherringham, *J. Mol. Evol.* **39**, 231 (1994).

[4] A. G. Cairns-Smith, *Genetic Takeover and the Mineral Origins of Life*. Cambridge University Press (1982).

[5] E. L. Shock, *Geochim. Cosmochim. Acta* **57**, 3341 (1993).

[6] P. A. O'Day, J. R. Delaney, M. D. Lilley, J. R. Holloway, *EOS* **78**, F774 (1997).

[7] C. D. Chang, A. J. Silvestri, *J. Catal.* **47**, 249 (1977).

[8] W. W. Kaeding, S. A. Butter, *J. Catal.* **61**, 155 (1980).

ROLE OF WATER IN PREBIOTIC NITROGEN CYCLES

J. A. Brandes, N. Z. Boctor, G. D. Cody, R. M. Hazen, and H. S. Yoder, Jr.

Geophysical Laboratory, Carnegie Institution of Washington, 5251 Broad Branch Rd,
NW Washington, DC 20015-1305

Nitrogen, prebiotic, aqueous chemistry

INTRODUCTION

Hydrothermal systems have been hypothesized as locations for the genesis of life. However, few experiments have been conducted that examine the interplay of biologically important compounds with minerals associated with these systems. One element generally neglected in the study of prebiotic chemistry is nitrogen. Several key questions in the study of the early Earth's nitrogen cycle are: How and under what conditions was reduced nitrogen formed? How was this reduced nitrogen incorporated into organic compounds, and what were the important parameters controlling the stability of these nitrogen containing organic compounds? A series of high pressure-hydrothermal reactions were undertaken to investigate these questions.

EXPERIMENTAL

Experiments were undertaken using a sealed gold tube (Kullerud & Yoder 1959) method. Samples were placed inside prewashed, combusted 99.95% pure Au gold tubes (10mm x 2 mm), followed by freezing and sealing of both ends by arc-welding. The sealed capsules were incubated at known temperature and pressure by use of an internally heated gas pressure device (Yoder 1950). After incubation, samples were frozen in liquid N₂, opened and extracted. Sample analysis for inorganic nitrogen was done by spectrophotometric methods (Strickland and Parsons, 1972), analysis for amino acids was done by ion-exchange HPLC followed by OPAH post-derivatization, and other organic compounds were analyzed by routine GC-MS techniques.

RESULTS AND DISCUSSION

The results for nitrogen gas reduction are shown in Figures 1 & 2. The amount of nitrogen reduction was significantly affected by the amount of water present in the system, with little observable N₂ reduction under hydrothermal conditions in the presence of excess water. This is hypothesized to occur because of the preferential binding of O to the catalytic FeO surface, preventing the binding of N₂ gas.

The role of water in the reductive amination of pyruvic acid, considered an essential step in early biochemical cycles, was investigated. The results (Fig. 3) indicate that the reaction only takes place in high yield at water:pyruvic ratios of 100:1 or greater. Finally, the stability of amino acids in hydrothermal systems was investigated. Our initial results indicate that certain common hydrothermal minerals have the ability to extend the stability of amino acids by many orders of magnitude.

REFERENCES

- Kullerud, G., & Yoder, H. S., Pyrite stability in the Fe-S system *Econ. Geol.*, 54, 534-550, (1959)
- Yoder, H. S. High-low quartz inversion up to 10,000 bars. *Trans. Amer. Geophys. Union*, 31, 821-835, (1950)
- Strickland, J. D. H., & Parsons, T. R., *A Practical Handbook of Seawater Analysis Fish. Res. Bd of Canada*, (1972)

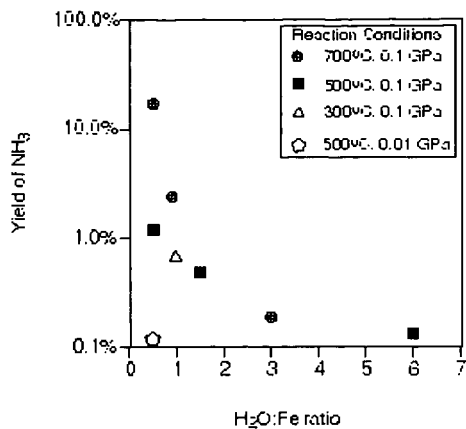


Figure 1. Production of ammonia from N₂ in the Fe:H₂O system

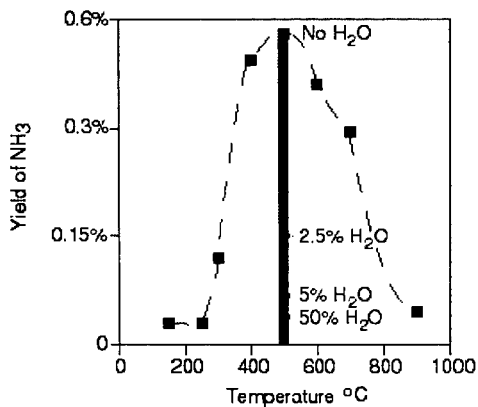


Figure 2. Production of ammonia from N₂ in the Fe₂O₃:H₂CO₂ system

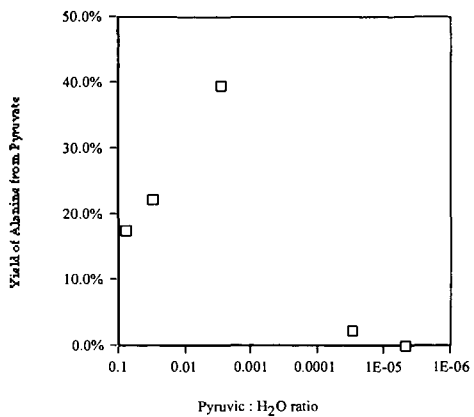


Figure 3. Effect of dilution upon reductive amination of pyruvate to form alanine

A PHYSICAL ORGANIC CHEMIST LOOKS AT HYDROUS PYROLYSIS

John W. Larsen

Department of Chemistry
Lehigh University
Bethlehem, Pennsylvania 18015

Keywords: hydrous pyrolysis, kerogen, water

INTRODUCTION. The invention and development of the hydrous pyrolysis technique by Mike Lewan is an important organic geochemical development and a fascinating reaction system.¹ This paper is a consideration of the reactions between kerogens and water which are a key part of hydrous pyrolysis and is based entirely on data from the literature. We begin with a consideration of the nature of water under hydrous pyrolysis conditions. A special concern here will be the question of contact between water and kerogen. The kerogens are three-dimensionally cross-linked-macromolecular systems and as such do not dissolve in water or any other solvent, but solvents can dissolve in the kerogen.² Another concern here is the possible mechanisms by which water and kerogens might react.

The solution of pentane or other light hydrocarbons in water is an exothermic process.³ These insoluble organic molecules have favorable interactions with water. Their insolubility is due to an enormously unfavorable entropy of solution, the familiar hydrophobic effect.³ As water is heated, its three dimensional hydrogen bonded structure becomes increasingly disarrayed and the entropy driven hydrophobic effect diminishes. The interactions which are responsible for the favorable enthalpy of solution remain so that as water is heated it increasingly becomes a non-polar solvent. This can be seen most easily by looking at the temperature dependence of water's cohesive energy density or its square root, the solubility parameter. These can be calculated as a function of temperature from the data in the Landolt Bornstein Tabellen⁴ and equation 1 where δ is the solubility parameter, ΔE_{vap} and ΔH_{vap} are respectively the energy and enthalpy of vaporization, and V_{mole} is the molar volume. Following Regular Solution Theory and its empirical thermodynamically illegitimate extensions, a liquid having the same δ as a polymer will be the best swelling solvent for it.⁵ As the two δ values (liquid and polymer) diverge, the sorption of the liquid by the polymer will decrease. The δ value for water decreases from 24 cal^{1/2}cm^{-3/2} at temperature to 7.4 cal^{1/2}cm^{-3/2} at 360°C, just below the critical temperature. At 350°C, the temperature used in hydrous pyrolysis, the solubility parameter is 9.1 cal^{1/2}cm^{-3/2}. The solubility for Type I kerogen is approximately 9.75 cal^{1/2}cm^{-3/2} and it is expected that the water will dissolve in and have access to all portions of the kerogen under hydrous pyrolysis conditions. It should also swell the kerogen to whatever extent is permitted by the structure of the surrounding rock.

Equation 1

$$\delta = \left(\frac{\Delta E_{vap}}{V_{mole}} \right)^{1/2} = \left(\frac{\Delta H_{vap} - RT}{V_{mole}} \right)^{1/2}$$

While water probably is soluble in kerogen under hydrous pyrolysis conditions, the situation under geological maturation conditions is not as clear. The oil window occurs at much lower temperatures, temperatures at which the solubility parameter for water is so high as to effectively preclude its dissolution in the kerogen at 200°C, the solubility parameter for water is 19 cal^{1/2}cm^{-3/2}. Only if the kerogen is inhomogeneous on the molecular level might water gain access to polar regions. This "first order" consideration of the solubility of water in Type I kerogen raises a concern about using hydrous pyrolysis as a model for geological kerogen maturation. Type II kerogen will probably be similar to Type I.

If temperature were the only variable, the situation would be simple, but we also need to consider pressure effects and salt effects. Lithostatic pressures between 800 bar and 1000 bar are commonly encountered during kerogen maturation.⁶ These pressures and the temperatures encountered in petroleum kitchens can have significant effects on the solubility of organic molecules in water.⁷ This can be seen most easily in Figure 1 which shows the effect of temperature and pressure on the miscibility of water and 4-methylpiperdine.⁷ The addition of salt

can complicate the situation enormously as shown in Figure 2. The situation is sufficiently complicated so that I am unwilling to reach a conclusion as to the solubility of water in kerogen under the conditions existing in petroleum kitchens. This is an important point for understanding not only what is going on in hydrous pyrolysis, but also its use to model kerogen maturation.

The next concern is the mechanisms by which the kerogens and water react. There are three strong indications that this reaction does not occur by radical pathways. As pointed out by Dave Ross, at 330°C β -scission of an alkyl radical is 300 times faster than hydrogen abstraction from water so olefin formation will greatly exceed saturates formation.⁸ Formation of large amounts of olefin in hydrous pyrolysis has not to my knowledge been reported and olefins are rare components of crude oils.⁶ Lewan has carried out hydrous pyrolysis in the presence of added H₂ and did not observe any significant change in the product distribution.¹ The bond in water at 119.1 kcal/mole is much stronger than the bond in H₂ at 104.2 kcal/mole.⁸ A radical that can abstract H from water will abstract H from H₂ much more rapidly so a significant change in the product distribution is expected when hydrogen is added to the hydrous pyrolysis system if it is undergoing a radical reaction with water. The only thing which might affect this would be inaccessibility of hydrogen to the reacting centers and this seems unlikely. Finally, there has been one study of pure compounds under hydrous pyrolysis conditions using simulated oil field brine.¹⁰ n-Hexadecane cracked to give alkanes and olefins in reactions that were inhibited by a radical hydrogen donor. These results are best explained using radical reactions. There was no evidence of hydrogen abstraction from or oxidation by water. These three lines of evidence lead to the conclusion that the reactions between kerogen and water are not occurring by a radical process.

Direct reaction between water and some functional groups is possible, but it is hard to envision hydrocarbon formation from kerogens based solely on water-kerogen reactions of the type so thoroughly studied by Siskin and Katritsky.¹¹ Both Ross and Helgeson et al have argued for involvement of mineral matter in reactions between organics and water.^{12,13} Ross argued for the possibility of a mineral matter catalyzed oxidation of hydrocarbons by water and Helgeson et al argued that in oil reservoirs, hydrocarbons, water, minerals, carboxylic acids and CO₂ had reached thermodynamic equilibrium. In both cases, mineral matter is involved in the oxidation of hydrocarbons by water. This is shown most directly using the scheme below taken directly from a paper by Dave Ross. In it, a hydrocarbon is cleaved and oxidized to CO₂ by a metal oxide, for example an iron oxide which is reduced in the process. In the second step of the reaction, the reduced metal oxide is reoxidized by water generating a pair of hydrogen atoms which are added to an organic molecule. The net reaction is the oxidation of the organic material, kerogen, by water catalyzed by mineral matter. The thermodynamics of this are favorable as long as the end products are carboxylic acids or carbon dioxide. The thermodynamics are not favorable for the formation of intermediate carbon oxidation states such as alcohols or aldehydes. There is some evidence for this chemistry occurring. Eglinton studied the hydrous pyrolysis of several immature kerogens and measured, among other things, the formation of carboxylic acids.¹⁴ The addition of limonite to Kimmeridge kerogen tripled the amount of carboxylic acids formed. The limonite was not altered (XRD analysis). It seems that limonite catalyzes carboxylate formation from Kimmeridge kerogen during hydrous pyrolysis. This is in general agreement with Ross's scheme and Helgeson et al observations.

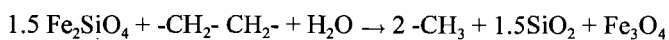
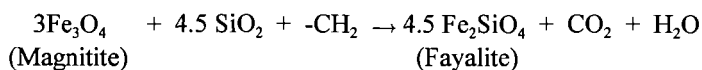
The hydrous pyrolysis reaction system is intriguing both physically and chemically. It is an excellent entree to the chemistry responsible for kerogen maturation and has the advantage that it can be studied in our lifetimes. It is a major step forward and worthy of very careful scrutiny.

ACKNOWLEDGMENTS: Acknowledgment is made to the Donors of the Petroleum Research Fund, administered by the American Chemical Society, for the partial support of this research. I would like to thank Drs. Raymond Michels and Patrick Landais and the CNRS for three wonderful months in Nancy during which time many of the ideas in this paper were initially developed.

REFERENCES

1. Lewan, M. *Geochim. Cosmochim Acta* **1997**, *61*, 3691-3723 and references therein.
2. Larsen, J. W.; Li, S. *Organic Geochem* **1997**, *26*, 305-309.
3. Tanford, C. *The Hydrophobic Effect: Formation of Micelles and Biological Membranes* Krieger Publishing Co., Malabar, FL: **1991**
4. Landolt-Bornstein Tabellen, Band IV, 4 Teil, Springer-Verlag, Berlin **1967**, pp. 426-439.
5. Hildebrand, J. H.; Prausnitz, J. M.; Scott, R. L. *Regular and Related Solutions* Van Nostrand Reinhold Co., New York: **1970**.
6. Hunt, J. M. *Petroleum Geochemistry and Geology* W. H. Freeman and Co., New York: **1996**.
7. Schneider, G. M. *Water. A Comprehensive Treatise, Vol. 2*, F. Franks, Ed., Plenum Press, New York, **1973** Cp. 6.
8. Ross, D. S. *Prepr. Pap. Am. Chem. Soc. Fuel Div.* **1992** 1555-1566.
9. Lide, D. R. Ed., *CRC Handbook of Chemistry and Physics* 72nd Ed., **1991**.
10. Weres, O.; Newton, A. S.; Tsao, L. *Org. Geochem.* **1988**, *12*, 433-444.
11. Katritzky, A. R.; Allin, S. M.; Siskin, M. *Acci. Chem. Res.* **1996**, *29*, 399-406.
12. Ross, D. S., *4th Intl. Symp. On Hydrothermal Reactions*, Nancy, France, **1992**.
13. Helgeson, H. C.; Knox, A. M.; Owens, C. E.; Shock, E.L. *Geochim Cosmochim. Acta*, **1993**, *57*, 3295-3339.
14. Eglinton, T. I.; Curtis, C. D.; Rowland, S. J. *Mineral Mag.* **1987**, *51*, 495-503

Scheme 1 (from reference 12)



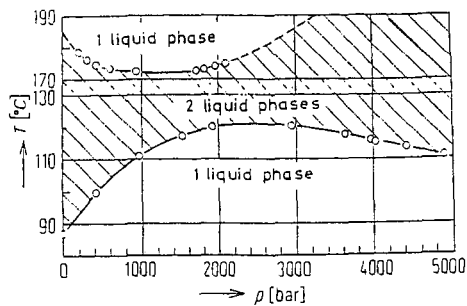


Fig. 1. Pressure influence on liquid-liquid immiscibility in the system 4-methylpiperidine-H₂O for $\chi = \text{const.} \approx \chi_c^{\text{loc}}$ at 1 bar (from ref. 7).

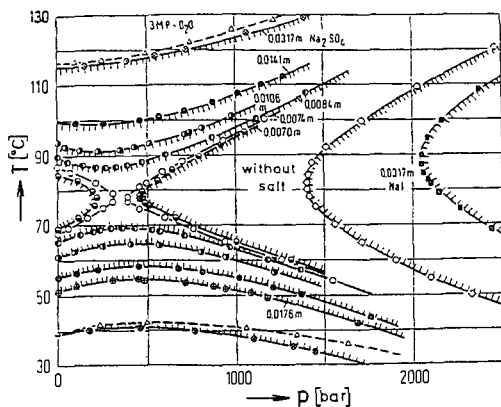


Fig. 2. Salt and pressure effects on liquid-liquid immiscibility in the system 3-methylpyridine-H₂O wt.% water/wt% 3-methylpyridine = const. = 7/3; (from ref. 7).

PROCESSES LEADING TO INCREASE OF ALKYL CHAIN LENGTHS UNDER HYDROUS PYROLYSIS CONDITIONS

Tanja Barth and Birthe G. Hansen
Department of Chemistry, University of Bergen,
Allégaten 41, N-5007 Bergen, Norway

KEYWORDS:

Hydrous pyrolysis, polymerisation, short-chain carboxylic acids

INTRODUCTION

In the last decades, various kinds of pyrolysis procedures have been used to simulating petroleum generation from source rocks or kerogen, and the effect of water on the saturated hydrocarbon yields has been a matter of debate. Pyrolysis processes tend to give a larger proportion of both unsaturated compounds and polar compounds than in natural petroleum, where the aliphatic hydrocarbon fraction is normally the major constituent. Confined system pyrolysis with excess water present during pyrolysis results in a more hydrocarbon-rich product with a composition more similar to natural petroleum than products from unconfined and dry pyrolysis (Lewan, 1997). Confined pyrolysis in gold tubes, with a compressed gas phase and some excess water produced in the initial reactions, also give a high proportion of aliphatic products (Michels *et al.*, 1995).

The generally accepted model for hydrocarbon generation assumes that a given quantity of aliphatic chains is present in the polymeric kerogen material, and is released in the thermal cracking of the polymer. In this model, water functions as a hydrogen donor and increases the amount of saturated products after an initial cracking step. In confined systems with less water, other constituents, including hydrogen gas produced during pyrolysis, may function in a similar way. However, both models imply that the total amount of aliphatic compounds possible to generate is limited by the amount of alkyl units initially incorporated in the starting material.

However, pyrolysis experiments with simple compounds show that polymerisation type reactions producing liquid phase products also occur. Investigations on the thermal stability of organic acids in formation waters (Andresen *et al.*, *in press*) and gases in hydrothermal systems (Berndt *et al.*, 1996) show the generation of larger hydrocarbon molecules from small reactants. To explain such observations, polymerisation reactions of gaseous molecules with water involved in the reaction seem the most relevant pathway.

In this presentation, observations of alkyl chain generation in "classical" hydrous pyrolysis of simple compounds will be shown to reproduce the series of homologous organic acids found in waters in the vicinity of oil, and also contribute to the long-chain hydrocarbon compounds that are found in the petroleum phases. The possibility of a Fischer-Tropsch mechanism for the polymerisation step will be discussed.

EXPERIMENTAL

Hydrous pyrolysis of simple organic compounds has been performed in stainless steel autoclaves. In one series of experiments, formic acid (HCOOH) is used as the organic reactant. The gaseous, aqueous and extractable products have been analysed for an experimental design on the experimental conditions, varying the parameters in the following range: *Reactors*: Parr 71 ml(=L), SS tubes 10 ml (S); *Temperatures*: 300-380 °C; *Head-space to liquid volume ratios(subcritical)*: 0.1-0.9; *Water/formic acid ratio*: 0 - 9; *Presence of mineral phase (goethite)*: present/absent; *Oil phase (cyclohexane)*: present/absent. All experiments have had a duration of 72 hours. After the experiment, quantitative analyses were made of the generated gas phase for hydrocarbon gases including hydrogen and carbon monoxide in some cases, the aqueous phase was analysed for content of dissolved organic compounds and the oil phase products were extracted, quantified gravimetrically and analysed by GC.

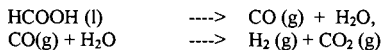
For comparison, the results from similar experiments are given for a Kimmeridge source rock.

RESULTS AND DISCUSSION

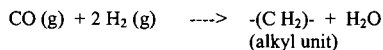
Products with increased alkyl chain length were consistently found both in the gas phase and aqueous products. In the experiments using the small reactors, wax profiles were observed in the extractable organic fraction (Figure 1). Selected experimental results are summarised in Table 1.

The results confirm observations from previous experiments with acetate cracking in gold tubes, which gave generation of a wide spectrum of longer-chain products, including C₃-C₆ hydrocarbon gases and C₇+ hydrocarbons with chain lengths up to C₃₂ (Andresen *et al.*, *in press*). Considerable levels of carbon monoxide was also found in the gas phase, while hydrogen was not analysed.

In the new experiments with formic acid (HCOOH) as the starting material, polymerisation reactions is the only possibility for generation alkyl chains. Formic acid rapidly decomposes and reacts with water upon heating:



and the products can polymerise by a surface catalysed Fischer-Tropsch mechanism:



Carboxylic acids are a well-known product from such reactions. The distribution of homologues expected from this mechanism correspond to the distribution generally observed in oil-field waters, with an exponential reduction of concentration relative to acetic acid with increasing carbon number. This distribution has also been observed in all hydrous pyrolysis experiments performed at this laboratory, and it seems to be

completely independent of the type of organic starting material (single compounds, biomass or sedimentary organic material).

As shown by the results given in Table 1, there is a considerable effect from variations in the reaction conditions with regards to the product composition. The choice of reactor is one major factor. n-Alkanes in the wax range, as shown in the chromatogram in Figure 1, were found in higher than trace amounts only in the experiments using the small stainless steel reactors. This can be caused either by differences in the catalytic activity of the reactor surfaces, or by the relatively higher loading in the small reactors, which will give higher concentrations of reactive gas phase species. At present it is not clear what is the limiting factor for the alkane formation.

REFERENCES

- Andresen, B., T.Barth, I.Johansen and K. Vagle (1998) Thermal stability of aqueous acetate *Organic Geochemistry*
- Barth, T., Borgund A.E. and Hopland A.L. (1989) Generation of organic compounds by hydrous pyrolysis of a Kimmeridge Oil shale - bulk results and activation energy calculations. *Organic Geochemistry*, **14**, 69-76.
- Berndt, M.E., Allen, D.E. and Seyfried, W.E. (1996) Reduction of olivine at 300 degrees C and 500 bar. *Geology*, **24**, 351-354
- Lewan, M.D. Experiments on the role of water in petroleum formation. *Geochimica et Cosmochimica Acta*, **61**, 3691-3723.
- Michels, R., Landais, P., Torkelson, B.E. and Philp, R.P. (1995) Effects of effluents and water pressure on oil generation during confined pyrolysis and high-pressure pyrolysis. *Geochimica et Cosmochimica Acta*, **59**, 1589-1604.

Table 1. Composition of products from selected pyrolyses

Reaction conditions	Gas phase (% of initial C)				Aqueous acids (mM)			HC chains ?	
	CO ₂	CO	CH ₄	H ₂	C ₁	C ₂	C ₃		
Formic acid									
S/330 /-w	Not measured				0.75	17.10	4.92	C ₇ -C ₂₅	
S/330 /-w,+min.	Not measured				0.60	10.28	2.34	C ₈ -C ₂₈	
S/300 /-w (Fig.1)	Not measured				3.03	3.34	0.63	C ₈ -C ₃₁	
S/380 /-w	Not measured				0.50	3.39	1.91	C ₉ -C ₃₂	
S/380 /+w,+C	Not measured					3.30	7.26	1.18	
S/380 /+w, C ₁₄ -C ₃₂	Not measured				2.96	3.93	0.89	C ₁₉ -C ₃₁	
L/330 /+w,+min.	46.5	n.m.	0.18	n.m.	0.82	0.76	0.56	-/trace	
L/380 /+w,+C		43.8	n.m.	0.28	n.m.	6.28	1.21	0.10	
/trace									
L/380 /+w,+min.+C	70.4	n.m.	0.07	n.m.	0.51	0.50	0.004	-/trace	
L/380 /+w	18.6	n.m.	0.02	n.m.	0.49	0.12	0.09	-/trace	
L/330 /+w	23.6	0.76	0.02	n.m.	0.98	0.09	0.05	-/trace	
L/330 /+w,+min	16.3	0.26	0.02	n.m.	0.58	0.74	0.15	-/trace	
Kimmeridge source rock -standard hydrous pyrolysis (Barth et al. 1989)									
L/300 to >C ₂₉		4.8	n.m.	0.4	0.06	tr	13.15	2.45	up
L/330		7.8	n.m.	1.3	1.84	tr	14.26	2.71	
L/350 C ₁₀ -C ₃₀		10.4	n.m.	1.5	1.75	tr	12.38	2.80	

n.m.: Not measured

-: Below detection level

Figure 1.

Gas chromatogram of the alkane profile from experiment 3, Table 1.

Column: HP-5, 25m; Temperature program: 40°C*1 min, 6°C/min to 290°C *5 min., FID detector.

IMPORTANCE OF THE POLARS AS INTERACTION MEDIUM WITH WATER DURING HYDROUS PYROLYSIS OF WOODFORD SHALE.

V. Burkle¹, R. Michels¹, E. Langlois¹, P. Landais¹ and O. Brevart²

¹ UMR7566/CREGU Universite Henri Poincare BP239 54506 Vandoeuvre les Nancy, France

² Elf Exploration Production CSTJF 64018 Pau, France

Keywords: hydrous pyrolysis, shale, petroleum generation

INTRODUCTION

The thermal degradation of kerogen leads to the formation of a complex system in which gases, water, free hydrocarbons, polars and the residual kerogen are in close contact. The simulation of the formation of the bitumen wetted kerogen during artificial maturation allows to study the close interactions between the various phases formed. Previous studies have compared the influence of the reaction medium on the generation of hydrocarbons in hydrous pyrolysis conditions (where water is added to the sample) and confined pyrolysis (no water is added to the sample)^{1,2}. These experiments could account for the effect of an external phase on the thermal evolution of type II kerogen. Other studies, (using a combination of pyrolysis and selective extractions) have focused on the role of internal media (free hydrocarbons, polars, residual kerogen) in the maturation processes and interactions with water during the maturation of type III organic matter^{3,4}. The comparison between the two types of studies allows to precise the respective role of the organic reactants versus water in the chemical control of the organic system.

Although the role of liquid water is capital in hydrous pyrolysis, the role of the organic phases generated, the interactions between themselves and their interactions with water need still to be clarified. The following study aims to describe the reactivity of the organic system and its interactions with water in relation to the generation of hydrocarbons during hydrous pyrolysis of Woodford shale.

EXPERIMENTAL

The sample used is Woodford shale (WD26; 22%TOC; HI=401mgHC/gTOC, Tmax=427°C), collected in the Anadarko basin, Oklahoma. Powdered shale aliquots (10g) were loaded in stainless steel reactors (30cm³ internal volume) pyrolyzed in the presence of 100 weight% water at temperatures between 260°C and 365°C for 3 days (temperature measurements were performed through an internal thermocouple in contact with the sample). Several maturation series were performed: 1) a reference series, called HP 2) a series called HPEC in which a same shale aliquot was treated the following way: pyrolysis at temperature T1, subsequent chloroform extraction; pyrolysis of the extracted sample at T2, subsequent chloroform extraction. This process was performed until 365°C. 3) a series called HPEP in which a same shale aliquot was treated the same way as for the HPEC series, but the extracting solvent was pentane.

In the HPEC and HPEP series, the same shale aliquot was repyrolyzed several times. Therefore, the pyrolysis time-temperature pair was compensated by TTI calculations in order to obtain maturation series that have reached TTI values identical to the reference series. However, for convenience, maturation scales are indicated in temperature and not in TTI, as far as the effective pyrolysis temperatures are not much different for all the series.

The samples were extracted either by hot chloroform or pentane for 45 minutes. No distinction was made between the expelled phase and the bitumen.

In order to quantify the polars yields and for further analysis of the solid residue, the samples of the HPEP series were also extracted by chloroform.

The asphaltenes were precipitated in hot heptane for 15 minutes and filtered. The maltene fraction was fractionned on alumina and silica micro-columns in resins, aromatics and saturates. All fractions were quantified.

PyGCMS was performed on chloroform extracted residues with a Pyroprobe CDS2000 connected to a HP5980 Series II Plus gas chromatograph coupled with a HP5972A mass spectrometer. The GC was equipped with a 60m DB-5 ms column initially held at 0°C for 5 min, then heated to 300°C at 5°C/min and held at 300°C for 15min.

RESULTS

Figure 1 shows the polars and aliphatics cumulated yields obtained for each series as well as the non cumulated values for the HPEC series. The yields obtained with the experimental procedures used have different meanings and therefore, some values must be mathematically cumulated in order to allow comparisons. The data for the reference series are always cumulative values, as far as the reactor is loaded with a new shale aliquot at each pyrolysis step, and no mathematical treatment needs to be done. For the HPEP series, the resins yields have been cumulated and added to the non cumulated asphaltenes yields of each experiment (asphaltene are not removed from the sample at each pyrolysis step).

Up to $T=300^{\circ}\text{C}$, Figure 1 shows similar values for the polars yields of the reference and the cumulated HPEP series. The cumulated HPEC series on the contrary are far stronger at $T>300^{\circ}\text{C}$. The secondary cracking of the polars during hydrous pyrolysis can be estimated from these data. The values for the reference series decrease at $T>300^{\circ}\text{C}$, while the polars generation potential of the kerogen is not totally exhausted (there is a difference of about 55mg/g of rock between the reference series and the cumulated HPEC series at 330°C). Therefore, it seems that the « real » maximum bitumen generation occurs at 350°C and not 300°C as shown by the maximum non cumulated yield of the HPEC series (occurring at 350°C) and the flattening of the HPEC cumulated curve. However, additional experiments at 310°C would be necessary in order to confirm this aspect. The removal of the hydrocarbons and part of the resins by pentane extraction does not modify the polars yields in the $260\text{-}300^{\circ}\text{C}$ range as shown by Figure 1.

Figure 1 also shows the aliphatics yields for the reference series and the cumulated values for the HPEC-HPEP series as well as the non cumulated values for the HPEC series. At $T>330^{\circ}\text{C}$, the cumulated aliphatic yields are far higher for the HPEC series than for the others. In addition, the non cumulative aliphatic yield for the HPEC series decreases, indicating that the kerogen alone is not able to generate additional hydrocarbons. The HPEP series shows always the lowest yields, even when cumulated.

As for the polars, the maximum aliphatic yield observed at 330°C is only apparent. The HPEC series shows that the kerogen is able to generate hydrocarbons up to 350°C . The low values for the HPEP series indicate that the removal of the maltenes has a deleterious effect on the capacity of the kerogen+asphaltene assemblage to generate hydrocarbons.

It is difficult to estimate the secondary cracking of the aliphatics as far as 1) the reference series includes the aliphatics generated by the kerogen and the polars, while the HPEC series includes only the generation from the kerogen 2) the generation of aliphatics from the kerogen+asphaltene assemblage is modified by the removal of the maltenes.

Table I and Figure II are respectively the Rock-Eval data and the PyGCMS chromatograms of the chloroform extracted samples. Despite the different pyrolysis conditions, these data are identical for all maturation series. This shows that the kerogen itself is not much influenced by the removal of either the polars+hydrocarbons or the maltenes.

DISCUSSION AND CONCLUSION

The use of the successive extraction-maturation series (HPEC and HPEP series) allows to investigate the role of the bitumen as well as the maltenes on the maturation of kerogen in hydrous conditions. The removal of the bitumen or the maltenes at each maturation step does not influence the generation of the polars from kerogen. It seems therefore that the polars and the hydrocarbons do not have a great influence on the initial thermal breakdown of Woodford kerogen in hydrous pyrolysis. As far as Lewan⁵ reached similar conclusions through his anhydrous versus hydrous pyrolysis conditions, it may be concluded that neither the polars+hydrocarbons nor water influence the initial thermal breakdown of the kerogen. This may support the idea that this stage resembles a « depolymerization » process⁶.

The situation is somewhat different when the generation of aliphatic hydrocarbons is considered. The removal of the bitumen (HPEC series) at each maturation step does not influence the aliphatic generation from the kerogen. However, the data show that the aliphatic generation from the kerogen is almost exhausted at $T \geq 350^\circ\text{C}$. On the contrary, the aliphatic yield is strongly lowered in the HPEP series (removal of the maltenes) whatever the temperature: the kerogen+asphaltenes assemblage yields less aliphatics than the kerogen alone (HPEC). This might be surprising as far as the polars content of the system decreases. However, the decrease in polars is not counterparted by the generation of C_{15} aliphatics. For Mahakam coal^{4,5}, such behavior has been attributed to crosslink reactions between the asphaltenes and the kerogen in the absence of the maltenes. However, the effect must be less important for Woodford kerogen in the conditions described here, as far as the Rock-Eval Tmax and the pyGCMS chromatograms are not modified (these parameters were strongly influenced in the experiments using Mahakam coal^{4,5}).

These results suggest that the presence of liquid water is not the only necessary condition to allow the generation of aliphatics from the type II kerogen+asphaltenes assemblage. Indeed, water and the maltenes need to be present together in order to allow good conditions for aliphatics generation. As far as the kerogen alone yields higher amounts than the kerogen+asphaltenes assemblage, it is suggested that the maltenes in addition to water avoid the crosslink reactions of the asphaltenes with the kerogen during maturation

ACKNOWLEDGEMENTS The authors wish to thank Elf EP for financial support and M. D. Lewan for providing the Woodford samples.

REFERENCES

- 1 Michels R., Landais P., Philp R. P., and Torkelson B. E. (1994) *Energy Fuels*, 8, 741-754.
- 2 Michels R., Landais P., Torkelson B.E. and Philp R.P. (1995) *Geochim. Cosmochim. Acta*, 59, 1589-1604.
- 3 Mansuy L. and Landais P. (1995) *Energy Fuels*, 9, 809-821.
- 4 Mansuy L., Landais P. and Ruau O (1995) *Energy Fuels*, 9, 691-703.
- 5 Lewan M. D. (1998) *Geochim. Cosmochim. Acta*, 61, 3691-3723
- 6 Larsen J. W. and Li S. (1997). *Energy Fuels*, 11, 897-901

TABLE I Rock-Eval data on raw Woodford Shale and on pyrolyzed samples HP. Hydrous pyrolysis reference series. HPEC successive pyrolysis- chloroform extraction series. HPEP successive pyrolysis- pentane extraction series. All samples chloroform extracted prior to Rock-Eval pyrolysis.

Pyrolysis Temperature ($^\circ\text{C}$)	HP		HPEC		HPEP	
	Tmax ($^\circ\text{C}$)	HI mgHC/gC	Tmax ($^\circ\text{C}$)	HI mgHC/gC	Tmax ($^\circ\text{C}$)	HI mgHC/gC
Raw Woodford Shale	427	401				
278	440	349	438	390	438	371
298	442	305	441	319	442	287
329	453	126	453	109	454	101
346	461	57	468	38	466	50
358	554	21	540	19	-	-

FIGURE 1 Polars and C₁₅⁺ aliphatics yields for the HP, HPEC and HPEP series. Cumulated and non cumulated values as indicated. The reference series (HP) values are intrinsic cumulative data as far as a new shale aliquot is loaded in the reactor at each pyrolysis temperature.

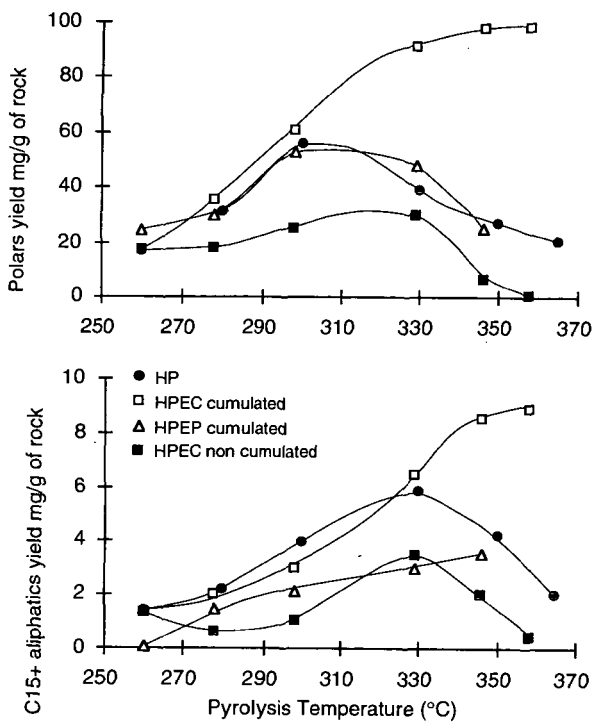
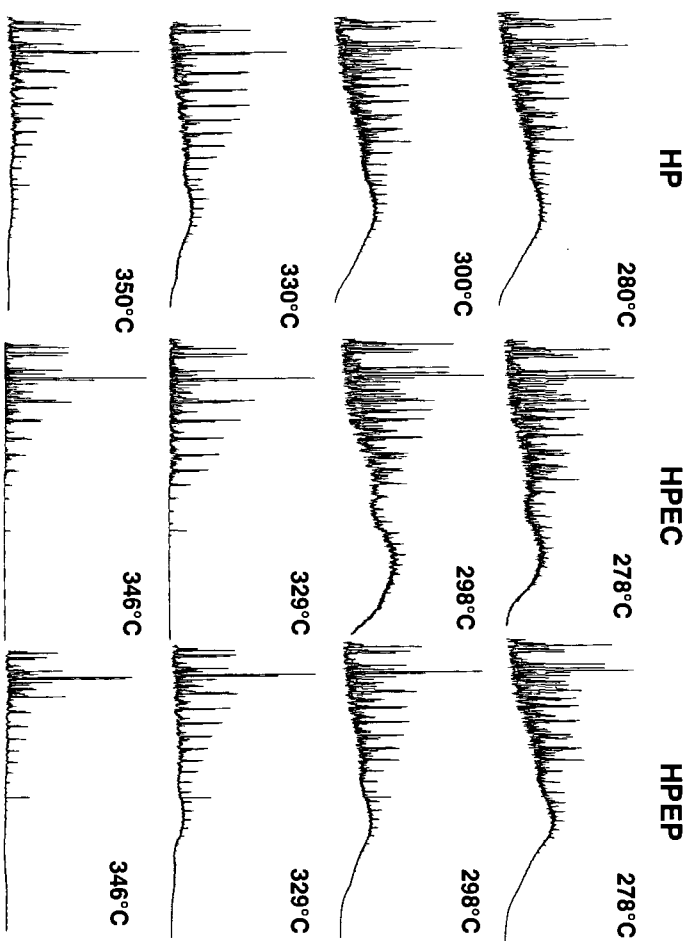


FIGURE 2 PyGCMS chromatograms of the chloroform extracted residue for each pyrolysis series



COMPETITION BETWEEN THE ORGANIC MATTER AND WATER IN THE HYDROGEN TRANSFER REACTIONS DURING ARTIFICIAL MATURATION.

R. Michels¹, V. Burkle¹, L. Mansuy¹, E. Langlois¹, P. Landais¹ and O. Brevart².

¹ UMR7566/CREGU UHP BP239 54506 Vandoeuvre les Nancy, France

² Elf Exploration Production CSTJF 64018 Pau, France

Keywords: artificial maturation, coal, kerogen

INTRODUCTION

The quantity, quality and timing of oil generation from source rock is directly dependant upon the type of organic present in the sediment. Type II are considered as oil prone, while type III is rather considered as gas prone, although some coals are sources of economic oil fields. The initial nature of the kerogen being significantly different in type II and III kerogens, it is important to study the similarities or differences of the chemical reactions taking place in both during maturation. Water is considered as an important parameter in the generation of hydrocarbons and is suspected to act as a source of hydrogen. However, coals are known to contain significant amounts of hydronaphthalenics able to efficiently provide hydrogen to organic reactions. Also, type III kerogens are richer in aromatics than type II kerogens and undergo more readily aromatization reactions which provide abundant hydrogen to the surrounding medium.

The following experiments compare the role of the free hydrocarbons, polars and water in the maturation and oil generation capabilities of type II kerogen (Woodford) and type III coal (Mahakam). The aim of the study is to identify the interactions between organic moieties (residual kerogen, polars, free hydrocarbons) and of these moieties with water. It is suspected that the dominant hydrogen sources and transfer mechanisms are different depending on the availability of specific hydrogen sources and on the stages of maturation of each kerogen type.

EXPERIMENTAL AND ANALYTICAL

The samples used are Woodford kerogen (Devonian Type II, Anadarko basin, Oklahoma, USA; T_{max}=422°C, HI=534mgHC/gOC) and Mahakam coal (Tertiary Type III, Mahakam delta, Kalimantan, Indonesia; T_{max}=418°C HI=258mgHC/OC). Experiments were performed by confined pyrolysis¹ (250-370°C, 24 and 72 hours, 700 bars). The experiments using successive pyrolysis of a same sample aliquot were adjusted to the reference series using temperatures adjusted by Time Temperature Index calculations². Several experimental series were performed: 1) standard pyrolysis (CP) in which the gold cell is loaded with fresh sample at each maturation stage 2) EC series in which a unique sample aliquot is isothermally heated from 250 to 370°C and chloroform extracted (removal of the bitumen) after each pyrolysis step. 3) EP series using the same procedure as for the previous series, but chloroform is replaced by pentane (removal of the free hydrocarbons and part of the resins after each pyrolysis step). 4) these series were also performed in the presence of 100 weight percent water (ECO and EPO series).

Hot chloroform and pentane extraction were performed on powdered samples during 45 minutes. For the CPEP series, the aliquots of the residual solid obtained after pentane extraction were extracted by chloroform for the quantitation of the asphaltenes. In such experiments, pentane yields values must be cumulated in order to be comparable to the CP and CPEC series, while the values for asphaltenes are not (they are intrinsic cumulative values as far as they remain in the reactor at each maturation step). Therefore, the cumulative pentane extraction yields are summed with the asphaltenes yields obtained at each temperature in order to obtain the cumulative bitumen yields. The residual kerogen (chloroform extracted) were analyzed by Rock-Eval pyrolysis and Py-GCMS (Pyroprobe CDS2000 connected to a HP5980 Series II Plus gas chromatograph coupled with a HP5972A mass spectrometer. The GC was equipped with a 60m DB-5 ms column initially held at 0°C for 5 min, then heated to 300°C at 5°C/min and held at 300°C for 15min).

RESULTS AND DISCUSSION

Figure 1 compares the effect of the removal of the bitumen, of the absence of the resins+free hydrocarbons and of the presence of water on the capacity of the residual kerogen (EC-ECO series) and kerogen+asphaltenes assemblage (EP-EPO series) to generate bitumen. General trends of the behavior for both kerogens appear: the cumulative bitumen yields for the EC and ECO series give values close to the maximum bitumen yield of the reference series. The removal of the resins+free hydrocarbons (EP series) lead to a deficit in the generation of bitumen. However, the effects are stronger for the coal than for the type II kerogen.

The addition of water to the sample in the chloroform extracted series (ECO experiments) does not change much the results for type II kerogen, while the effect is stronger for type III. In the pentane extraction series, the addition of water (EPO series) clearly improves the yields for both kerogens.

The removal of specific organic phases and the addition of water can also be followed through the analyses obtained on the residual kerogen. T_{max} values increase faster with maturation in the EC and EP series (Figure 2). The removal of the resins+hydrocarbons has strongest effect on the coal. For type II kerogen, the fastest T_{max} increase occurs in the EC series. In general, the extraction of the bitumen (EC) or resins+hydrocarbons (EP) has a smoother effect on the type II kerogen than on type III.

The addition of water retards the increase of T_{max} with maturation. With Mahakam coal, the effect is clear in the ECO series while the strongest retardation is noticed with the EPO series. For type II kerogen, the ECO is not much different from the EC series, while the EPO series shows the strongest effect (as for the coal).

The impact of the extractions on the structure of the residual kerogen were followed by PyGCMS (Figure III). For type III, the removal of the bitumen (EC series) or of the resins+hydrocarbons (EP series) leads to the destruction of the hydrocarbon potential (no free hydrocarbons are generated to counter part the loss of hydrocarbons in the coal). The presence of water in the ECO series allows a better preservation of the hydrocarbon potential of the coal. The effect is much stronger in the EPO series (kerogen+asphaltenes assemblage). This potential is also well preserved in the reference series.

For type II kerogen, the removal of the bitumen (EC series) leads to a PyGCMS chromatograms containing less aliphatics than the reference. For the EP series the results are fairly similar to the reference. The addition of water (comparison of the EC and EP chromatograms with the ECO and EPO series) has not much effect on the Py-GCMS chromatograms.

DISCUSSION AND CONCLUSION

In both types of kerogen, the removal of the bitumen does influence the yields, but the effects are rather limited. On the contrary, the removal of the resins+free hydrocarbons strongly decreases the bitumen yields, especially for the coal. The thermostability of the kerogen (T_{max} in the EC series) and the kerogen+asphaltenes (EP series) increases faster than for the reference series. This effect is related to an increasing aromaticity of the residue and a loss of the aliphatic potential of the sample (as followed by Py-GCMS and Mansuy et al.). This effect is however far stronger for the coal than for type II kerogen. These experiments show that the resins+hydrocarbons play a crucial role in the generation of hydrocarbons from kerogen. The kerogen+asphaltenes assemblage needs the presence of the resins+hydrocarbons in order to generate the bitumen. The presence of the resins+hydrocarbons avoids the crosslink of the kerogen+asphaltenes during maturation, which leads to the loss of the hydrocarbons potential in the kerogen^{2,3}

For the coal, the addition of water improves the yields in presence of the kerogen alone (ECO series) and in the presence of the asphaltenes (EPO). At the same moment, the thermostability of the residue (Table I) increases later in the maturation profile while the hydrocarbons potential in the kerogen is better preserved, especially in the EPO series (Figure III). For type II kerogen, water does not modify the behavior of the kerogen alone (EC and ECO series). A clear improvement is however noticed on the bitumen yields in the EPO series. Water also retards the increase of the Rock-Eval T_{max} with maturation (the effect is moderate in the ECO series for type II kerogen, but significant for the EPO series). The PyGCMS chromatograms are however not very conclusive concerning the preservation of the aliphatic potential in the residual kerogen

These data suggest that in the kerogen and especially in the kerogen+asphaltenes assemblage, chemical functions allowing the interaction with water are present. These interactions allow a better preservation of the oil potential in the kerogen and improve the generation of the bitumen from the kerogen+asphaltenes assemblage. It must however be noticed that the addition of water to the kerogen+asphaltenes (EP and EPO series) never totally restores the generation capability of the kerogen (either reference series or EC+ECO series). Therefore, it can be concluded that the full capacity of the organic matter to generate the bitumen needs the presence of the resins, the free hydrocarbons and water. In the reference series, these conditions are reached as far as the sample generates all of these ingredients during confined pyrolysis. The kerogen alone, as shown by the EC and ECO series behave fairly closely to the reference series. This shows that the crucial chemical interactions leading to good conditions of the generation of bitumen avoid crosslink reactions between the asphaltenes and the kerogen and allows a good preservation of the hydrocarbons potential.

The close contact between the kerogen, the asphaltenes, the resins, the hydrocarbons and water are therefore responsible for proper generation of bitumen. Specific oxidation of the polars by water during hydrous pyrolysis could be evidenced on Woodford Shale⁴. These results strongly suggest that water preferentially interacts with the polars (through oxidation-reduction reactions) during maturation. The fact that the addition of water in the EPO series never completely restores the generation capabilities as seen in the reference series suggests that other compounds are acting in the chemical network.

A closer analysis of the polars and kerogen from Mahakam coal (for which the removal of the resins+hydrocarbons has the most drastic effect) lead to identify the presence of significant amounts of hydronaphthalenics. These compounds are known to be very effective in the radical hydrogen transfer reactions during the pyrolysis of coal. Also, the strong abundance of naphthalenes in the aromatics generated by the coal during maturation is a good marker of hydronaphthalenic precursors. The removal of the polars by pentane extraction would remove this source of hydrogen and contribute to the destruction of the hydrocarbon potential in the kerogen by crosslink reactions.

Therefore, two types of hydrogen transfer reactions can be considered prior to aromatization reactions (which occur later in the maturation profile): 1) the polars+water interactions through oxidation-reduction reactions 2) the radical hydrogen transfer between hydronaphthalenics and the organic system.

Both systems are certainly active during maturation and are in competition, one taking advantage of the other depending on the composition of the medium. This composition is dependant either on the maturation stage (as in the reference series) or on the modifications induced by the chemical treatment during the EC, EP, ECO and EPO series.

ACKNOWLEDGEMENTS The authors wish to thank Elf EP for financial support, TOTAL and M. D. Lewan for providing the Mahakam and Woodford samples respectively.

REFERENCES

- 1 Landais P., Michels R. and Poty B. (1989) J. of Anal. and Appl. pyrolysis, 16, 103-115.
- 2 Mansuy L. and Landais P. (1995) Energy Fuels, 9, 809-821.
- 3 Mansuy L., Landais P. and Ruau O (1995) Energy Fuels, 9, 691-703.
- 4 Michels R., Langlois E., Ruau O., Mansuy L., Elie M., and Landais P. (1996). Energy Fuels, 10, 39-48.

TABLES AND FIGURES

TABLE 1: ROCK-EVAL Tmax (°C) for the chloroform extracted residual kerogen obtained after confined pyrolysis of Woodford kerogen and Mahakam coal. CP: reference series EC: chloroform extracted series EP: pentane extracted series ECO: chloroform extracted series with addition of water EPO: pentane extracted series with addition of water.

	WOODFORD KEROGEN					MAHAKAM COAL				
	CP	EC	ECO	EP	EPO	CP	EC	ECO	EP	EPO
Raw	422					418				
260	-	440	440	439	439	-	-	-	-	-
278	432	444	-	441	441	437	439	437	437	437
300	436	449	450	445	445	444	446	445	455	449
323	-	-	-	-	-	451	463	455	544	453
330	445	461	456	455	456	454	538	486	553	455
346	-	564	550	540	464	-	-	-	-	-
350	496	-	560	-	-	457	564	542	574	521
358	-	580	-	560	553	-	-	-	-	-
365	521	-	-	-	-	514	582	556	579	531
375	-	580	585	573	569	561	-	-	-	-
400	541	-	-	-	-	579	-	-	-	-

FIGURE 1: Bitumen yields obtained after confined pyrolysis of Mahakam coal and Woodford kerogen. Pyrolysis series as in Table I. The yields are cumulative for the EC, EP, ECO and EPO series. The yields are not cumulated for the reference series (CP), however, they are intrinsic cumulative values (see text).

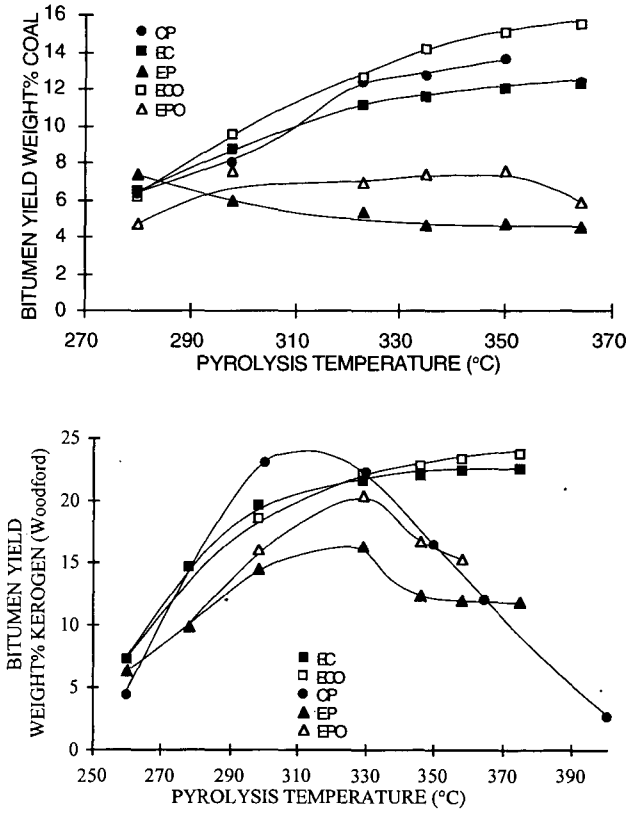
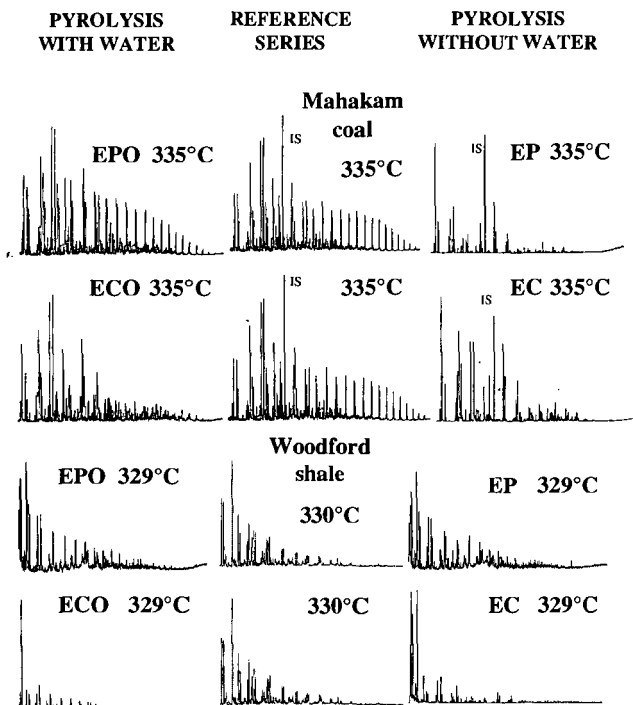


FIGURE II: PyGCMS chromatograms of the chloroform extracted kerogens obtained after confined pyrolysis at 335°C (Mahakam coal) and 330°C (Woodford kerogen). EC, EP, ECO, EPO as in text. IS: internal standard



THE EFFECT OF SUPERCRITICAL WATER ON VITRINITE REFLECTANCE AS OBSERVED IN CONTACT METAMORPHISM AND PYROLYSIS EXPERIMENTS

Charles E. Barker and M.D. Lewan, U.S. Geological Survey, Box 25046, Denver, Colorado, USA.

Introduction

Natural thermal maturation of sedimentary organic matter (SOM), which includes both coal and dispersed organic matter, increases with heating. In particular, dike contact metamorphic zones are widely studied because within the narrow sampling range near the dike, SOM composition changes little along a well-exposed sample plane while thermal maturation increases markedly as temperature increases from ambient to as high as 700°C (Bostick, 1979; Clayton and Bostick, 1986; Bishop and Abbott, 1994; Galushkin, 1997, and Barker et al., 1998; among others). These studies indicate contact metamorphism typically increases thermal maturity as measured by vitrinite reflectance, Rock-Eval parameters, as well as affecting SOM, petroleum and biomarker compositions. In this study, mean vitrinite reflectance in oil (mean or maximum parameter both annotated as R_0 for this general discussion) is used because it is widely reported in dike studies as an index of heating relative to petroleum generation (i.e., the thermal maturation process). R_0 is a physical measure of the degree of aromaticity in the SOM. During thermal maturation, the degree of aromaticity in vitrinite increases with the continuing condensation of aromatic clusters (van Krevelen, 1981; Wilson, 1987).

Given the change in host-rock temperature from ambient to those produced by contact with a magma, a surprising aspect of these studies is that R_0 does not always continue to increase as a dike is closely approached. Next to some dikes R_0 increase is retarded or R_0 may even decrease. This is true whether R_0 is measured next to dikes as discussed above or next to sills as well as whether maximum or random reflectance of vitrinite is measured (Raymond and Murchison, 1989). Fluid inclusion evidence indicates that the zone of retarded or reduced R_0 roughly corresponds to a zone where water vapor or supercritical-water phases evolve during contact metamorphism by the dike (Barker, 1995). In particular, the limited range of physical and chemical conditions that lead to the evolution of supercritical fluids may explain the retarded or reduced R_0 found near dikes. The development of water vapor is thought less important because it typically forms during contact metamorphism (Jaeger, 1959; Delaney, 1982; 1987) at the shallow to moderate crustal depths prevalent in sedimentary basins and its effects should be widely expressed next to dikes. Although there are other possible causes of retarded or reduced R_0 near dike contacts, the purpose of this paper is to investigate the effect of supercritical water on thermal maturation by hydrous pyrolysis experiments.

Contact Metamorphism

The sample selected for hydrous pyrolysis study is a bituminous coal (mean random $R_0 = 0.6\%$), taken from a site not locally affected by contact metamorphism even though from an area where a mid-Cretaceous age dike swarm intrudes the Upper Jurassic-Lower Cretaceous Strzelecki Group, western onshore Gippsland Basin, Victoria, Australia. This sample was collected about 50 meters below the surface in the State coal mine near Wonthaggi, Victoria. The Strzelecki Group banded coals contain mostly normal vitrinite (i.e., not suppressible by the definition of Barker et al., 1996). Thermal history reconstruction suggests that at the time of dike swarm intrusion the host rock was at a temperature of 100-135°C while fracture-bound fluid inclusions in the host rocks next to thin dikes (< 3.4 m thick) suggest temperature increases to at least 450°C at the dike contact (Fig. 1). Burial history reconstruction indicates that when intrusion occurred the host rocks were near two km depth and at about 20 MPa pressure using a fresh water hydrostatic gradient (Barker et al., 1998). Fresh water boils at about 300°C at this depth. The critical point of fresh water is near 374°C, 22 MPa. Thus, the temperature and pressure near the dike contact, along with the low to moderate salinity fluids (Barker, 1995) are conditions close to those required for the development of water vapor or supercritical fluids (Roedder, 1984; Bodnar and Vityk, 1994).

Pyrolysis Experiments

The development of supercritical fluids next to these dikes was simulated by heating aliquots of the Strzelecki Group coal in closed-system experiments using pyrolysis techniques developed by Lewan (1993) and a small stainless steel reactor described by Barker et al. (1996). The initial series of pyrolysis experiments was held at temperatures of 300°C, 330°C, 365°C and 380°C for 72 hours. The 380°C experiment was then run again for 24 hours. Experiments at 365°C or lower temperature were designed to keep liquid water in contact with the sample. Experiments at 380°C introduced supercritical water to the sample.

These experiments showed an increase in vitrinite reflectance as long as pyrolysis temperatures were held to subcritical liquid-water conditions. The runs at 380°C, with supercritical-water conditions in contact with the sample, showed a reduced R_0 (Fig. 2). Increasing time from 24 to 72 hours at 380°C produced a further reduction in R_0 .

Discussion

During contact metamorphism R_0 increase sometimes is retarded or even reduced close to the dike contact, even though fluid inclusion homogenization data indicates that temperatures were still increasing. Fluid inclusion evidence also indicates that the evolution of water vapor or supercritical

water in the rock pores roughly corresponds to the zone where R_0 is retarded or reduced. This relationship infers that the generation of water vapor or supercritical water near the dike contact may change vitrinite evolution reactions. The limited range of conditions in sedimentary basins that allow supercritical fluids to exist may explain why a retarded or reduced R_0 is not always observed near dikes. Because water vapor and supercritical water have a limited range of occurrence in sedimentary basins, there may be other causes of retarded or reduced R_0 next to dikes. Some of these causes are hydrothermal overpressuring next to the dike, catalytic effects, advection, convection, groundwater flow across the dike, and the presence of suppressible SOM.

The physical and chemical basis for a retarded R_0 with increasing temperature remains speculative. For example, is it that condensation reactions in SOM are inhibited causing a retardation of R_0 or is condensation destroyed causing a reduction of R_0 . What is known is that within the zone of retarded or reduced R_0 , molecular disorder is increasing (Khavari-Khorasani et al., 1990); and the fraction of aromatic carbon increases and then may fluctuate (Barker, 1995). Further, as the dike is approached, ^{13}C CP MAS nuclear magnetic resonance (NMR) data suggest that phenol and carbonyl contents initially decrease but that there is slight increase in phenol and carbonyl content in the zone of retarded R_0 (Barker, 1995). Along with these changes, the total organic carbon (TOC) content is lowered (Degens, 1965; Barker, 1995). The loss in TOC as the dike is approached is partially attributable to petroleum generation and migration as shown by a corresponding decrease in Rock-Eval hydrogen index (HI) and S_1 (Fig. 3). Next to some dikes, HI and the oxygen index (OI) may both stop decreasing or start to increase in the zone where R_0 increase is retarded. This change in HI and OI may be caused by the addition of phenol and carbonyl radicals to the residual SOM. These geochemical data suggest that in the presence of water vapor or supercritical water, hydrogen and oxygen are being introduced into the coal during reactions like those observed in liquid-water pyrolysis experiments (Stalker et al., 1994; Lewan, 1997).

A fraction of the TOC, however, also appears to directly react with the pore water and is in part mobilized as CO_2 (Lewan, 1992; Price, 1994). Given the exceptional solubility of SOM in supercritical fluids, SOM may be directly dissolved in the supercritical water (Lewan, 1993). The strong loss of TOC indicates the presence of a supercritical fluid rather than a vapor phase. SOM is thought to have a far lower solubility in a water vapor. A mesh-like porous structure observed in the Strzelecki Group vitrinite after supercritical pyrolysis also may be a reflection of a selective dissolution process.

Conclusions

1. The evidence suggests several reaction mechanisms producing a reduction or a retardation of condensation in SOM caused by the development of water vapor or supercritical water: a) After high temperature condensation reactions, the substitution of oxygen- and hydrogen-bearing radicals destroy aromatic carbon bonds in the highly condensed SOM; b) further condensation of the SOM may be retarded by the early reaction of phenolic and carbonyl radicals with the aromatic carbon clusters in a less mature vitrinite; and c) simultaneous thermal maturation and dissolution of the condensed structures at the surface of the vitrinite leaving residual SOM with a retarded aromaticity.
2. Experimental, geochemical and petrographic evidence indicate direct SOM reactions with water are a major factor during contact metamorphism near the dike contact.
3. The atypical occurrence of retarded R_0 near dike contacts is attributed to the limited range of physical conditions and pore-water chemistry under which supercritical water can exist in sedimentary basins.
4. Because water vapor and supercritical fluids have a limited range of occurrence, there may be other causes of retarded or reduced R_0 next to dikes in sedimentary basins.

References

- Barker, C.E., 1995, Physical and chemical conditions of organic metamorphism next to selected dikes, Victoria, Australia. Ph.D. thesis, University of Adelaide, 293 p. + appendices.
- Barker, C.E. and Pawlewicz, M.J., 1994. Calculation of vitrinite reflectance from thermal histories and peak temperature: a comparison of methods, in P.K. Mukhopadhyay and W.G. Dow (Editors), Vitrinite Reflectance as a Maturity Parameter. Am. Chem. Soc. Symp. Series no. 570, p. 216-229.
- Barker, C.E., Lewan, M.D., and Pawlewicz, M.J., 1996, A simple hydrous pyrolysis technique to detect suppressed vitrinite reflectance: Abstracts and Program, The Soc. for Org. Petrol., v. 13, p. 36-38.
- Barker, C.E., Bone, Y. and Lewan, M.D., 1998, Fluid inclusion and vitrinite reflectance geothermometry compared to heat flow models of maximum paleotemperature next to dikes, western onshore Gippsland Basin, Australia: International J. Coal Geol., v. 37, p. 73-113.
- Bishop, A.N. and Abbott, G.D., 1994, Vitrinite reflectance and molecular geochemistry of Jurassic sediments: the influence of heating by Tertiary dykes (northwest Scotland): Org. Geochem., v. 22, p. 165-177.
- Bodnar, R.J. and Vityk, M.O., 1994, Interpretation of microthermometric data for $\text{H}_2\text{O-NaCl}$ fluid inclusions, in De Vito, B. and Frezzotti, M.L., eds., Fluid Inclusions in Minerals: methods and applications: Short Course, International Mineralogical Association Working Group "Inclusions in Minerals", p. 117-130.
- Bostick, N.H., 1979, Microscopic measurement of the level of catagenesis of solid organic matter in sedimentary rocks to aid exploration for petroleum and to determine former burial temperatures--a review, in Scholle, P. A., and Schluger, P. R., eds., Aspects of Diagenesis: Society of Economic Paleontologists and Mineralogists Special Publication, No. 26, p. 17-44.

- Clayton, J.L., and Bostick, N.H., 1986, Temperature effects on kerogen and molecular and isotopic composition of organic matter in Pierre Shale near an igneous dike: *Org. Geochem.*, v. 10, p. 135-143.
- Degens, E.T., 1965, *Geochemistry of Sediments-A Brief Survey*: Prentice-Hall, New Jersey, 346 p.
- Delaney, P.T., 1982, Rapid intrusion of magma into wet rock: groundwater flow due to pore pressure increases: *J. Geophysical Research*, v. 87, p. 7739-7756.
- Delaney, P.T., 1987, Heat transfer during emplacement and cooling of mafic dykes. In: H.C. Halls and W.F. Fahrig (Editors), *Mafic Dyke Swarms*. Geol. Assoc. of Canada Special Paper 34, pp. 31-46.
- Galushkin, Y.I., 1997, Thermal effects of igneous intrusions of maturity of organic matter: A possible mechanism of intrusion: *Org. Geochem.* v. 26, p. 645-658.
- Khavari-Khorasani, G.K., Murchison, D.G. and Raymond, A.C., 1990, Molecular disordering in natural cokes approaching dyke and sill contacts: *Fuel*, v. 69, p. 1037-1045.
- Jaeger, J.C., 1959, Temperatures outside a cooling intrusive sheet: *Rev. of Geophysics*, v.2, p. 443-466.
- Lewan, M.D., 1992, Water as a source of hydrogen and oxygen in petroleum formation by hydrous pyrolysis: *Am. Chem. Soc., Division of fuel Chemistry*, preprints, vol. 37, no. 4, p. 1643-1649.
- Lewan, M.D., 1993, Laboratory simulation of petroleum formation: hydrous pyrolysis, in, M.H. Engel and S.A. Macko (Editors), *Organic Geochemistry*. Plenum Press, New York, p. 419-442.
- Lewan, M.D., 1997, Experiments on the role of water in petroleum formation: *Geochim. Cosmochim. Acta*, v. 61, p. 3691-3723.
- Price, L. C., 1994, Metamorphic free-for-all. *Nature*, v. 370, p. 253-254.
- Raymond, A.C. and Murchison, D.G., 1989, Organic maturation and its timing in a Carboniferous sequence in the central Midland Valley of Scotland: comparisons with northern England: *Fuel*, v. 68, p. 328-334.
- Roedder, E., 1984, *Fluid Inclusions: Min. Soc. Am., Reviews in Mineralogy*, v. 12, 644p.
- Stalker, L., Farrimond, P. and Larter, S.R., 1994, Water as an oxygen source for the production of oxygenated compounds (including CO₂ precursors) during kerogen maturation: *Org. Geochem.* v. 22, p. 477-486.
- van Krevelen, D.W., 1981, *Coal*: Elsevier, Amsterdam, 514 p.
- Wilson, M.A., 1987, *NMR Techniques and Applications in Geochemistry and Soil Chemistry*: Pergamon Press, Oxford, 353 p.

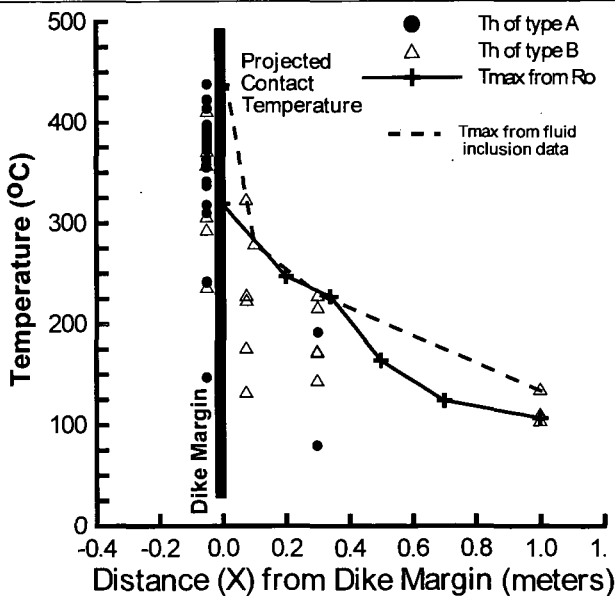


Figure 1. Measurements and calculated maximum host rock temperatures reached next to the 0.6 m thick San Remo-1 dike, western onshore Gippsland Basin, Australia. Figure from Barker (1995). T_h = homogenization temperature of a fluid inclusion. Type A and B refer to types of fracture-bound fluid inclusions. Projected contact temperature is estimated from fluid inclusion measurements on a host rock xenolith partially imbedded in the dike. T_{max} from R_o refers to a temperature estimate made using the hydrothermal geothermometer of Barker and Pawlewicz (1994). A reassessment of the position of the xenolith sample used to determine the projected contact temperature indicates it was taken a few centimeters from the dike contact rather than 20 cm away as reported by Barker (1995).

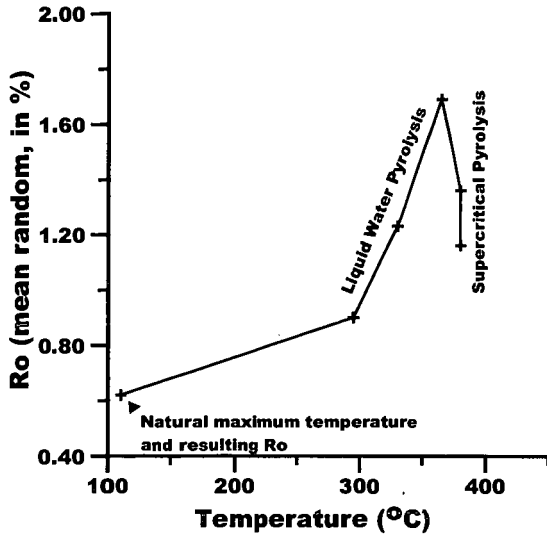


Figure 2. Vitrinite reflectance of Strzelecki Group coal after natural diagenesis, liquid water and supercritical water pyrolysis.

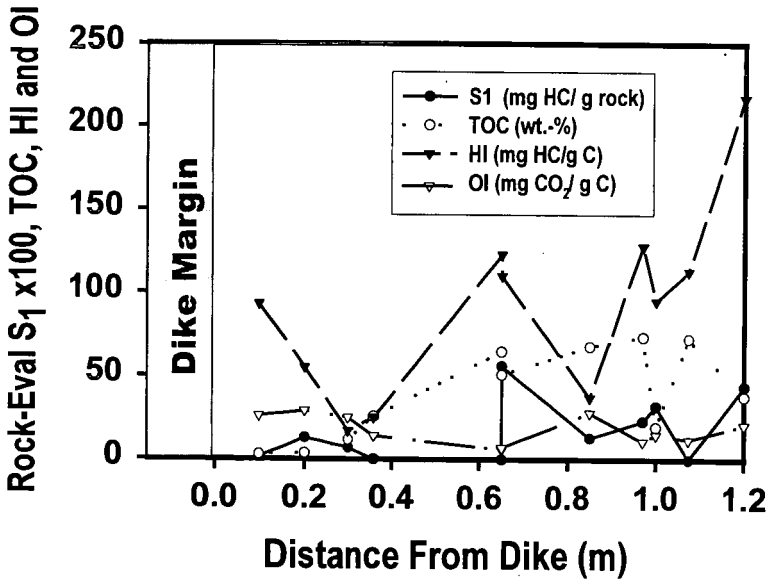


Figure 3. Rock-Eval pyrolysis assay results from coaly rocks in the Strzelecki Group next to the San Remo-1 dike, western onshore Gippsland basin, Australia. Data from Barker (1995)

THERMODYNAMIC CONSTRAINTS ON THE GENERATION AND MATURATION OF PETROLEUM IN SEDIMENTARY BASINS

Harold C. Helgeson, Laurent Richard, William F. McKenzie, and Denis L. Norton
 Department of Geology and Geophysics
 University of California
 Berkeley, CA 94720

KEYWORDS: Hydrolytic disproportionation, oxidation of kerogen, chemical evolution of petroleum

ABSTRACT

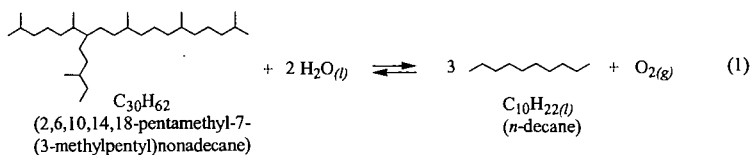
Preliminary Gibbs free energy minimization calculations indicate that high molecular weight compounds in kerogen may be in metastable equilibrium with hydrocarbon species in petroleum during the incongruent partial melting process responsible for the generation and maturation of petroleum, which is accompanied by progressive oxidation of kerogen with increasing depth of burial. It appears that H₂O plays a crucial role in the process, which may be driven by escape from the system of methane as the ultimate product of the irreversible hydrolytic disproportionation of the light paraffins.¹

INTRODUCTION

Although the overall process responsible for the generation of bitumen from kerogen and the chemical evolution of high molecular weight compounds in bitumen to the lower molecular weight species that predominate in petroleum is irreversible (Tissot and Welte, 1984; Béhar *et al.*, 1992; Helgeson *et al.*, 1993; Planche, 1996), thermodynamic calculations indicate that metastable equilibrium states probably prevail among liquid hydrocarbon species with carbon numbers $\geq 6-15$ and carbon-bearing aqueous species such as CO₂ and CH₃COOH at the oil-water interface (Helgeson *et al.*, 1993). In addition, it appears from the results of recent calculations that mature kerogen may be in metastable equilibrium with maturing crude oil in hydrocarbon source rocks. Thermodynamic calculations lead to the conclusion that the maturation process may be driven by the extent to which methane escapes from the system as the ultimate product of the irreversible hydrolytic disproportionation of hydrocarbons with carbon numbers $\leq 6-15$. The large chemical affinities of these reactions are an attractive energy source for thermophilic microbes, which may then mediate the maturation process if the system is open at the hydrocarbon-water interface (Helgeson *et al.*, 1993).² It follows that irreversible hydrolytic disproportionation reactions among the light hydrocarbons should perturb to the right reversible reactions representing hydrolytic reduction of the higher molecular weight compounds to form lighter species.

HYDROLYTIC OXIDATION/REDUCTION AND DISPROPORTIONATION REACTIONS

To illustrate the hydrolytic oxidation/reduction process in a maturing source rock, reversible reaction of the highly branched isoprenoid liquid species corresponding to 2,6,10,14,18-pentamethyl-7-(3-methylpentyl)nonadecane (C₃₀H₆₂) in kerogen or bitumen to form a light paraffin species such as liquid decane (C₁₀H_{22(l)}) in petroleum can be described in terms of the overall reaction represented by

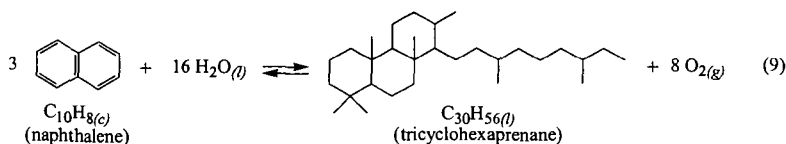
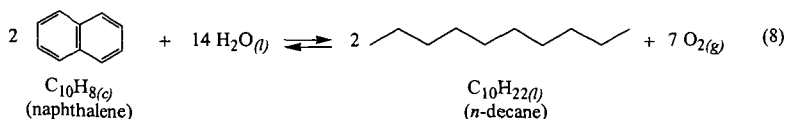
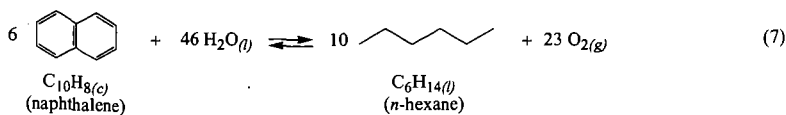


¹ The term hydrolytic disproportionation refers to reaction of a given hydrocarbon with H₂O to form a lighter hydrocarbon and oxidized carbon-bearing species.

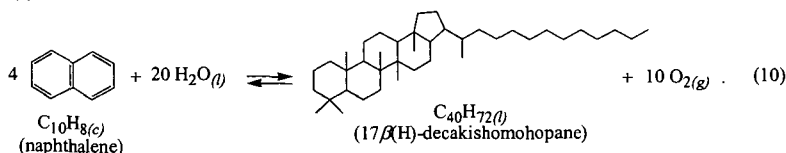
² The chemical affinity of the *r*th irreversible reaction (*A_r*) can be expressed as $A_r = 2.303RT \log(K_r / Q_r)$, where *A_r* stands for the chemical affinity of the *r*th reaction, *R* refers to the gas constant, *K_r* represents the equilibrium constant for the reaction, and *Q_r* designates the activity quotient for the subscripted reaction, which is given by

$$Q_r = \prod_i a_i^{\hat{n}_{i,r}}$$

where *a_i* denotes the activity of the *i*th species in the system and $\hat{n}_{i,r}$ stands for the reaction coefficient of the *i*th species in the *r*th reaction, which is positive for products and negative for reactants. Although *K_r* is computed from the standard molal thermodynamic properties of the species in the reaction, *Q_r* is evaluated from compositional data. Hence, if $Q_r = K_r$, *A_r* = 0 and the reaction is reversible. Otherwise, $A_r d\xi_r > 0$ where ξ_r stands for the progress variable for the *r*th reaction.



and



The logarithmic analogs of the law of mass action for these reactions can be written for unit activity of crystalline naphthalene as

$$\log a_{\text{C}_6\text{H}_{14}(l)} = (\log K_{(7)} - 23 \log f_{\text{O}_2(a)}) / 10 \quad (11)$$

$$\log a_{\text{C}_{10}\text{H}_{22}(l)} = (\log K_{(8)} - 7 \log f_{\text{O}_2(a)}) / 2 \quad (12)$$

$$\log a_{\text{C}_{30}\text{H}_{56}(l)} = \log K_{(9)} - 8 \log f_{\text{O}_2(a)} \quad (13)$$

and

$$\log a_{\text{C}_{40}\text{H}_{72}(l)} = \log K_{(10)} - 10 \log f_{\text{O}_2(a)} \quad (14)$$

where $K_{(7)}$, $K_{(8)}$, $K_{(9)}$, and $K_{(10)}$ stand for the equilibrium constants for the subscripted reactions. Equations (10)-(14) represent the curves shown in Fig. 2, where it can be seen that the curves in each of the four diagrams cross each other over narrow temperature intervals at log activity values which are slightly below zero. It follows that the liquid hydrocarbons represented by these curves can coexist with appreciable concentrations in a single liquid phase in metastable equilibrium with crystalline naphthalene at the temperatures and fugacities of oxygen corresponding to those of the curve-crossings in Fig. 2. A $\log f_{\text{O}_2(a)}$ - temperature profile consistent with this observation is depicted in Fig. 3, where it can be compared with the profile in the hydrocarbon reservoirs of the Texas Gulf Coast (Helgeson *et al.*, 1993). It can be seen in Fig. 3 that the two curves are separated by only 2 log units or $\sim 10^\circ\text{C}$.

Calculated changes in speciation are depicted in Fig. 4 for maturation of the hypothetical hydrocarbon liquid represented by the curve-crossings in Fig. 2 and the upper temperature - $\log f_{\text{O}_2(a)}$ profile in Fig. 3. The curves shown in this figure were generated from Eqns. (11)-(14) and the relation $\sum_i X_i = 1$ (where X_i stands for the mole fraction of the i th species in the liquid) assuming in a first approximation ideal mixing of the four hydrocarbon species in the hypothetical liquid.³ It can be deduced from Fig. 4 that increasing burial of naphthalene in kerogen coexisting with this liquid along the upper temperature - $\log f_{\text{O}_2(a)}$ profile in Fig. 3 would be accompanied by "maturation" of the liquid from ~ 90 mole percent tricyclohexaprenane ($\text{C}_{30}\text{H}_{56}(l)$) and 17 β (H)-decakishomohopane ($\text{C}_{40}\text{H}_{72}(l)$) at low temperatures to ~ 80 mole percent *n*-hexane ($\text{C}_6\text{H}_{14}(l)$) and *n*-decane ($\text{C}_{10}\text{H}_{22}(l)$) at 125°C . Preliminary calculations indicate that similar, but much more complex behavior can be expected in actual bitumen and

³ The mole fraction of the i th hydrocarbon species (X_i) in bitumen or petroleum is related to its activity (a_i) by $X_i = a_i / \lambda_i$

where λ_i stands for the rational activity coefficient of the subscripted species, which is unity in the case of ideal mixing.

petroleum during burial of hydrocarbon source rocks along profiles like those depicted in Fig. 1. Although the incongruent partial melting of kerogen in source rocks may not occur to an appreciable extent at low temperatures, the metastable equilibrium calculations represented by the curves shown in Figs. 2, 3, and 4 indicate that the incongruent partial melting of kerogen species and the maturation process are simultaneous interrelated processes.

CONCLUSIONS

The fact that the curves in each of the diagrams in Fig. 2 cross each other over narrow temperature ranges is a consequence of the actuality that hydrocarbon species are members of closely related homologous series. However, the observation that they cross each other at log activities corresponding to appreciable concentrations at geologically reasonable values of $\log f_{O_2(a)}$ and temperature is a manifestation of the physical, chemical, and thermodynamic reality of metastable equilibrium states among many (but not all) hydrocarbon species in kerogen, bitumen and petroleum in the Earth. Under these circumstances, if hundreds of curves were drawn in Fig. 2 representing reversible hydrolytic reduction reactions for the multitude of hydrocarbon species found in bitumen and petroleum, all of them would be expected to cross in approximately the same narrow temperature - $\log f_{O_2(a)}$ interval shown in Fig. 3. A similar result would be expected for metastable equilibrium among these species in the liquid phase and other hydrocarbon compounds in kerogen. Gibbs free energy minimization calculations are currently being carried out to explore the extent to which these metastable equilibrium states may obtain in hydrocarbon source rocks. Preliminary results of these calculations indicate that oxidized kerogen may coexist in metastable equilibrium with crude oil in source rocks during progressive burial and maturation of the oil. Furthermore, the maturation process may persist at temperatures in excess of 200°C. Because the composition and speciation of both the kerogen and maturing oil generated in the Gibbs free energy minimization calculations are consistent with geologic reality, it appears that the process is not controlled by chemical kinetics, but instead by the thermal gradient, rate of burial, availability of H₂O, and the degree to which methane can escape from the system.

ACKNOWLEDGEMENTS

The research described above was supported by the United States Department of Energy (DOE Grant DE-FG03-85ER-13419) and the National Science Foundation (NSF Grants EAR 8606052, EAR 9117395, and EAR 9613753), together with funds received from the donors of the Petroleum Research Fund, administered by the American Chemical Society (ACS-PRF Grants 23026-AC2, 26237-AC2, and 28550-AC2), and the Committee on Research at the University of California, Berkeley. Support was also contributed in the form of a postdoctoral grant to Laurent Richard by Elf Aquitaine Production. We are indebted to Leigh Price, Jan Amend, Christine Owens, Allen Young, and Everett Shock for helpful discussions during this research.

REFERENCES

- Béhar, F.; Kressmann, S.; Rudkiewicz, J.-L.; Vandenbroucke, M. *Org. Geochem.* **1992**, *19*, 173.
- Helgeson, H.C.; Knox, A.M.; Owens, C.E.; Shock, E.L. *Geochim. Cosmochim. Acta* **1993**, *57*, 3295.
- Helgeson, H.C.; Owens, C.E.; Knox, A.M.; Richard, L. *Geochim. Cosmochim. Acta* **1998**, *62*, 985.
- Planche, H. *Geochim. Cosmochim. Acta* **1996**, *60*, 447.
- Richard, L.; Helgeson, H.C. *Geochim. Cosmochim. Acta* **1998** (in press).
- Tissot, B.P.; Welte, D.H. *Petroleum Formation and Occurrence*; Springer-Verlag: Berlin, 1984.

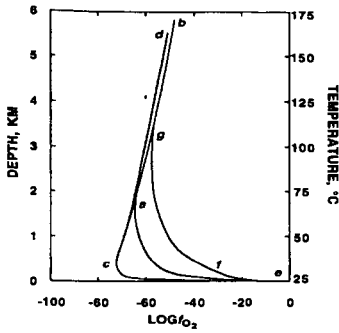


Fig.1 Temperature - $\log f_{O_{2(l)}}$ - depth profiles in hydrocarbon source rocks and reservoirs (see text). The profiles were generated for a nominal temperature gradient of 25°C/km. Curves *ea* and *ec* represent idealized profiles drawn to connect curves *ab* and *cd* at *a* and *c*, respectively, with atmospheric $f_{O_{2(a)}}$ at 25°C. Curve *efg* is a hypothetical profile representing more oxidized conditions at greater depths than those along *ea* and *ec*. Curves *cab* and *cad* are consistent with the temperature - $\log f_{O_{2(l)}}$ profiles in hydrocarbon reservoirs calculated by Helgeson *et al.* (1993).

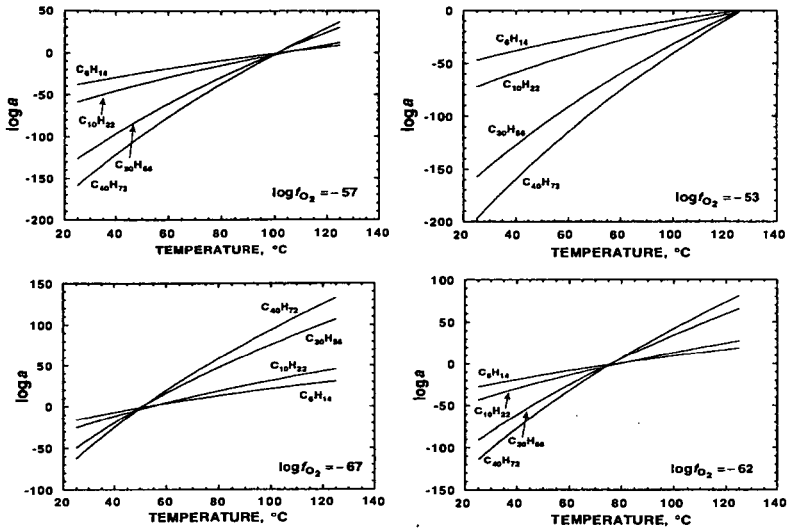


Fig.2 Graphic representation of Eqns. (11) - (14) as a function of temperature at constant pressure and $\log f_{O_{2(l)}}$ (see text).

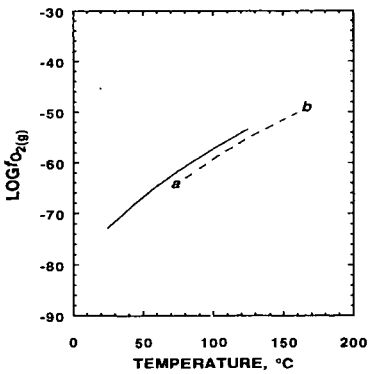


Fig. 3 Temperature - $\log f_{O_{2(l)}}$ profile consistent with the curve-crossings in Fig. 2 (upper curve) and profile *ab* in hydrocarbon reservoirs in the Texas Gulf Coast taken from Helgeson *et al.* (1993).

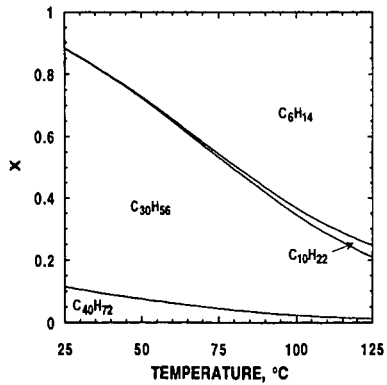


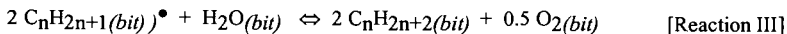
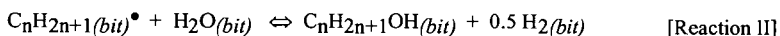
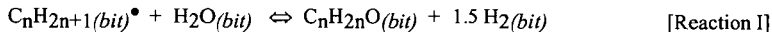
Fig. 4 Mole fraction (*X*) - temperature maturation diagram for the hypothetical hydrocarbon liquid represented by the upper curve in Fig. 3 coexisting with naphthalene in kerogen (see text).

THEMODYNAMICS OF REACTIONS INVOLVING H₂O AND HYDROCARBON RADICALS BETWEEN 27 AND 374°C

Michael D. Lewan
U. S. Geological Survey
Box 25046, MS 977
Denver Federal Center
Denver, CO 80225

Hydrous pyrolysis experiments at temperatures between 300 and 360°C for 72 hours have shown that H₂O is a source of oxygen and hydrogen in the generation of oil from petroleum source rocks. Oxygen mass-balance calculations indicate that the only source of the calculated excess oxygen in the form of CO₂ is H₂O (Lewan, 1992; Seewald, 1994). Experiments with D₂O instead of H₂O show that generated hydrocarbons are highly deuterated (Hoering, 1984), which is interpreted as being the result of D₂O-derived deuterium quenching free-radical sites as the organic matter in a petroleum source rock thermally decomposes (Lewan, 1997).

Hydrous pyrolysis experiments are typically conducted with crushed gravel-sized (0.5 to 2.0 cm) source rock, which is heated in contact with liquid H₂O at subcritical temperatures (<374°C). Initially, the maturing source rock gravel is impregnated with polar-rich bitumen that partially decomposes with increasing thermal stress to yield an expelled saturate-rich oil. As demonstrated by Lewan (1997), the reaction of H₂O with the organic matter occurs within the hydrophobic bitumen-impregnated rock and not in the liquid H₂O that surrounds the rock gravel. Therefore, the reaction involves dissolved H₂O in the bitumen of the rock and not aqueous organic species in the surrounding liquid water. It has been proposed that the H₂O dissolved in the bitumen (H₂O_(bit)) of a source rock reacts with free radical sites to generate aldehydes, alcohols, alkanes, hydrogen, or oxygen. The model reactions include the following:

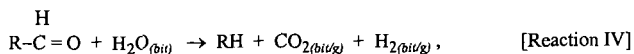


Although it is uncertain whether these model reactions have kinetic energy barriers to overcome, the first concern is whether they are thermodynamically possible within the experimental conditions. Unfortunately, thermodynamic data on alkyl radicals, H₂O, and the proposed products in a bituminous phase are not currently available. However, a first approximation of the thermodynamic feasibility of these model reactions can be obtained by considering the reactions in a gaseous phase for which thermodynamic data are available.

Gibbs free energies for these reactions in the gaseous phase where $n = 2$ were calculated from tabulated standard-state (25°C at 100 kPa) heat capacities given by Benson (1976) and Gurvich et al. (1994) for temperatures between 27 and 374°C. As shown in Figure 1, the resulting Gibbs free energy of reaction between 0 and 400°C at 100 kPa for Reactions I, II, and III are -10.5 to -13.5 kcal/mol, -18.8 to -11.9 kcal/mol, and -27.3 to -17.8 kcal/mol, respectively. These negative values indicate that the model reactions for $n = 2$ are thermodynamically favorable in this temperature range at hydrogen or oxygen fugacities of 100 kPa or less.

Reaction I involves oxygen from a water molecule reacting with an unpaired electron at an alkyl radical site to form an aldehyde and hydrogen. The hydrogen would be available to react with other free radical sites and the aldehyde would react with other water molecules to form a carboxylic acid and through subsequent decarboxylation form CO₂. Each molecule of water that reacts with a free radical site by this reaction,

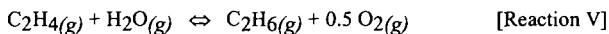
generates three atoms of hydrogen that can terminate or initiate additional free radical sites. A subsequent reaction of the resulting aldehyde with other water molecules yields two additional hydrogen atoms by the reaction



where R is an alkyl or aryl group in macromolecules of the organic matter. The interaction of water with carbonyl groups has been suggested to be responsible for increased CO₂ yields associated with the weathering of coal in water vapor at low temperatures (150°C; Peitt, 1991) and the noncatalytic liquefaction of water-treated coals at 350°C (Song et al., 1994). As a result, reactions I and IV may collectively generate 5 water-derived hydrogen atoms for every water-derived oxygen that reacts with a free radical site.

Alcohols have not been reported in the products of hydrous pyrolysis experiments as prescribed by reaction II. However, Stalker et al. (1994) have reported the generation of phenols from water-derived oxygen in H₂¹⁸O-experiments with kerogen at 300°C after 72 hours. Smith et al. (1989) observed that hydrous pyrolysis of n-octadecanol in the presence of coal completely reacts to form n-alkanes at 330°C after 72 hours. Therefore, it is reasonable to tentatively suggest that alcohols derived from reaction II may be ephemeral intermediates in the formation of alkanes.

Reaction III is the most thermodynamically favorable reaction of the three model reactions. Molecular oxygen generated from this reaction would be highly reactive and prone to generate or terminate other free-radical sites. Eventually, this oxygen would occur as a carbonyl, carboxyl, or CO₂ through a series of subsequent reactions. The significance of the thermodynamic favorability of reaction III is demonstrated by comparing its low Gibbs energy of reaction with that of the thermodynamically unfavorable reaction of H₂O with ethene to form an ethane (Figure 1):



It is not the intent of this discussion to suggest that reactions I, II, and III are specific reactions that occur in petroleum formation, but rather they simply serve to demonstrate that reactions between alkyl free-radical sites and water in gaseous phases are thermodynamically favorable between 27 and 374°C at 100 kPa. A more specific thermodynamic evaluation of the feasibility of these model reactions requires obtaining thermodynamic parameters on H₂O as a dissolved species in bitumen or oil solvents. Once these parameters have been determined, the competition between H₂O_(bit) and H₂(bit) for alkyl free-radical sites can be properly assessed.

REFERENCES CITED

- Benson, S. W., 1976, *Thermochemical Kinetics*, John Wiley & Sons, New York.
- Gurvich, L. V., Iorish, V. S., Yungman, V. S., and Dorofeeva, O. V., 1994, Thermodynamic properties as a function of temperature, in Lide, D. R., ed., *CRC Handbook of Chemistry and Physics*, 75 th Edition, CRC Press, Boca Raton, Section 5, p. 48-71.
- Hoering, T. C., 1984, Thermal reactions of kerogen with added water, heavy water and pure organic substances: *Organic Geochemistry*, v. 5, p. 267-278.
- Lewan, M. D., 1992, Water as a source of hydrogen and oxygen in petroleum formation by hydrous pyrolysis: *ACS, Div. Fuel Chemistry Preprints*, v.37, No. 4, pp. 1643-1649.
- Lewan, M. D., 1997, Experiments on the role of water in petroleum formation: *Geochimica et Cosmochimica Acta*, v. 61, p. 3691-3723.

- Peitt, J. C., 1991, A comprehensive study of the water vapour/coal system: application to the role of water in the weathering of coal: *Fuel*, v. 70, pp. 1053-1058.
- Seewald, J. S., 1994, Evidence for metastable equilibrium between hydrocarbons under hydrothermal conditions: *Nature*, v. 370, p. 285-287.
- Smith, J. W., Batts, B. D., and Gilbert, T. D., 1989, Hydrous pyrolysis of model compounds: *Organic Geochemistry*, v. 14, pp. 365-373.
- Song, C., Saini, A. K., and Schobert, H. H., 1994, Effects of drying and oxidation of Wyodak subbituminous coal on its thermal and catalytic liquefaction. Spectroscopic characterization and product distribution: *Energy & Fuels*, v. 8, pp. 301-312.
- Stalker, L., Farrimond, P., and Larter, S. R., 1994, Water as an oxygen source for the production of oxygenated compounds (including CO₂ presursors) during kerogen maturation: *Organic Geochemistry*, v. 22, nos. 3-5, p. 477-486.

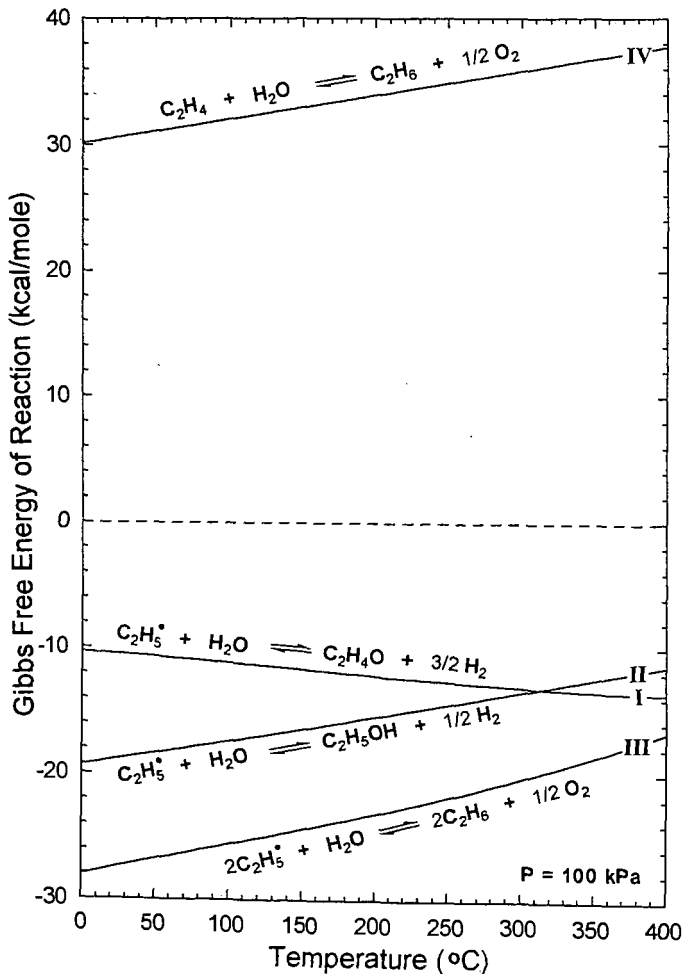


Figure 1. Gibbs free energy of reaction for model reactions I, II, III, and IV for various temperatures at 100 kPa.